Revised Modeling Sediment Dispersion from Cable Burial for Seacoast Reliability Project, Upper Little Bay, New Hampshire

Prepared for: Normandeau Associates, Inc., Bedford, NH
Authors: Craig Swanson[1], Deborah Crowley[2], Daniel Mendelsohn[2], and Nathan Vinhateiro[2]
Date: June 27, 2017
Project Number: 2017-119 (Update to 2014-270)
RPS ASA | 55 Village Square Drive | South Kingstown, RI 02879

[1] Swanson Environmental
[2] RPS

Executive Summary

Public Service of New Hampshire d/b/a Eversource Energy (PSNH) has proposed the construction of an electrical cable system to increase the reliability of the electrical transmission grid in southern New Hampshire. This cable, known as the Seacoast Reliability Project, would cross the Little Bay portion of the Great Bay Estuarine System. The crossing would entail burial of three separate but parallel cables by jet plowing, which is a technique that liquefies the sediment with high pressure water jets and simultaneously allows the cable to be buried at a predetermined depth. The cable sections in the shallow areas near the western and eastern landfalls will be buried by diver. The environmental consultant for the Project, Normandeau Associates, Inc., previously contracted with RPS to supply its modeling capabilities to simulate the jet plowing and diver burial processes along the cable route to determine both the likely suspended sediment concentrations generated in the water column above the cable route and the resulting re-deposition of the sediments in and along the route; the result of that effort was a report *Modeling Sediment Dispersion from Cable Burial for Seacoast Reliability Project, Little Bay, New Hampshire* (Issued 14 December 2015). The modeling study has been updated and expanded based upon new project details and new data. The results of the updated modeling are presented herein.

Two computer models were used in the analysis: BELLAMY, a hydrodynamic model used for predicting the currents in Upper Little Bay, and SSFATE, a sediment dispersion model used for predicting the fate and transport of sediment resuspended by the jet plowing and diver burial operations. BELLAMY is a finite element, two-dimensional, vertically averaged, time stepping circulation model developed at Dartmouth College and previously applied to the Great Bay Estuarine System. The SSFATE (Suspended Sediment FATE) model was utilized to predict the excess suspended sediment concentration and the dispersion of suspended sediment resulting from jetting activities. The model predicts excess concentration, which is defined as the concentration above ambient suspended sediment concentration generated by the seabed activities. Summaries and conclusions for the BELLAMY and SSFATE model results and associated analyses are presented below

BELLAMY Hydrodynamic model output

The BELLAMY model used has previously been applied successfully to the Great Bay Estuary System over the last 15 years. Its use was found entirely appropriate as follows:

- The tides in the GBES are known at mesoscale with a range between 2 and 4 m. This tidal amplitude generates a tidal prism of 64 x 10^6 m^3 and induces high tidal-induced turbulence conducive to energetic mixing in the system.
- A recent measurement program conducted in Upper Little Bay using a bottom mounted Acoustic Doppler Current Profiler (ADCP) showed that the the structure is mostly vertical from maximum flood to slack high but during the higher velocity ebb the bottom friction inhibits the speeds in the deeper layers. This does not invalidate using a vertically averaged modeling approach since the currents in a vertically averaged model somewhat overestimates near bottom currents and overestimates near surface currents, which provides a conservative (higher) current that transports the sediment released by jetting activities.
- The freshwater flow into an estuary can cause stratified salinity conditions and resultant complex currents if sufficiently large. The annual average freshwater flow to the GBES is 32.3 m^3. This means that the flow is less than 2% of the tidal prism and that the GBES is dominated by

tidal flow and the GBES is thus considered a well-mixed system as has been consistently pointed out in the scientific literature for at least the last 35 years.

- An examination of previous salinity measurements in the Little Upper Bay area show very little salinity stratification due to vigorous tidal mixing and relatively low river flow.
- A review of the U.S. Geology Survey gauge data shows that the average flow in the September-October period when the cables will be installed is less than 6.2% of the annual flow thus significantly reducing the effects of river flow even further. The use of average flows in the BELLAMY model overestimates the flow for September-October by a factor thus is highly conservative.
- The USGS daily flow was examined for the 2007-2016 decade showed that high flows due to precipitation events are rare in the September-October period.
- The winds for Pease International Tradeport from the NOAA DS3505 database were examined for the September-October period for the decade 2007-2016. It was found the 88% of the winds were below 5 m/s and that only 0.4% exceed 10 m/s with none of the largest wind events originating from the north or northwest or from the south or southeast, the alignment of Upper Little Bay, thus making it very unlikely that wind-induced effects would be significant.

The use of the BELLAMY model was thus fully justified for this project (and a number of others) to simulate currents in the GBES.

Sediment Dispersion Modeling

The SSFATE sediment dispersion model was successfully applied to simulate the cable installation activities across Upper Little Bay. The analysis was updated to reflect new and/or refined inputs and the modeling study was expanded in order to address the sensitivity of the results to some of the modeling assumptions.

A number of input parameters have been updated since the previous modeling. These include:

- The burial route was updated to reflect the latest plans. The route is primarily the same except for minor revisions to the diver burial route on the eastern shore.
- The use of silt curtains was accounted for in the regions where they will be implemented; this includes the entire western diver burial and approximately 57.5 % of the eastern diver burial route.
- The minimum burial depth for the jet plow installation in waters greater than 10 ft has changed from 8 ft to 5 ft.
- The sediment grain size characteristics have been updated based on refined laboratory analysis. The new information shows that the sediment has more mass in larger sizes than had been assumed in the previous analysis.
- The percent solids have been updated based on laboratory analysis of moisture. This provides a better estimate of the sediment loading to the water column.

Multiple simulations were completed as part of this revised study. These included

- Updated base case of the jet plow
- Sensitivity to Advance Rate (slower and faster) of the jet plow
- Sensitivity to loss rate (lower and higher) for the jet plow
- Sensitivity to tide range (spring vs neap) for the jet plow
- Additional run to evaluate the effects of continued resuspension for the jet plow

- Updated base diver burial simulations

Based on the set of model simulations the following conclusions can be made

- The jet plow installation is anticipated to need approximately 7.1 hours of active sediment disturbing activity to install each cable.
- Each cable is anticipated to be installed with continuous operations without long stoppages; the advance rate modeled and the duration of 7.1 hours is an average rate provided by the installers.
- The sediment plume is temporary, present when construction takes place and dissipates within an hour after construction stops
- The sediment plume follows the currents. Times of weaker currents (neap tide) have a smaller overall footprint but have some contours within the footprint that extend further due to the diminished advection.
- The base case found areas totaling 91.2 ac and 0.2 ac were exposed to a concentration of 10 mg/L or greater for 1 hr, and 2 hrs, respectively, while no areas were exposed to such a concentration for a duration of three hours.
- The base case deposition thickness patterns found the footprint over 0.1 mm extended 67.81 ac due to jet plowing the three cable routes.. Areas with thickness over 5 mm are 0.1 acres.
- The sensitivity runs to advance rate showed that the footprint changed primarily due to the change in exposure to currents due to the different timing relative to tides. Further the region immediately adjacent to the route showed increasing peak concentration with increasing advance rate.
- The sensitivity to loss rate showed that the lower loss rate (15% less than the base) had a more drastic change than the higher loss rate (10% greater than the base). This is expected due to the trend of mass released based on the loss rate.
- An additional model run was simulated that include the effects of continued resuspension. This run showed a footprint of SS excess concentrations that was larger than the base case, though the concentrations were present intermittently and confined to the very bottom of the water column. Much of the area has the potential for continued resuspension due to the relatively strong currents. Resuspension was most pronounced on the first tide following jet plowing and fully dissipated by the third day. The model does not include all processes that would interact with the continued resuspension and serves as a conservative prediction.
- The diver hand jetting takes place intermittently over a longer span of time (4 hours a day between 9-18 days for west and east routes respectively) as compared to the jet plow operations. The intermittent installation is due to operational constraints limited by water depth and currents. The duration of active sediment disturbing activities is 1.7 days for the west route and 3.0 days for the eastern route.
- The diver hand jetting assumes use of silt curtains for the entire west route and 57.5% of the east route.
- The diver concentrations are intermittent and dissipate quickly due to the relatively low mass flux, particularly in regions within the silt curtain.
- The diver hand jetting results in concentration plumes local to the areas of hand jetting and do not extend as far as the jet plow plume.
- The maximum excess SS concentration due to diver burial is 500 mg/L, which will occur over an area of 0.59 ac. Lower concentrations will extend over a greater area, with excess SS of 20 mg/L covering 14.21 acres at some point in time. Concentrations diminish shortly after diver activity

ceases, for example a time history of concentration local to diver activity showed that the signal of excess concentration mimicked the duration of activity with concentrations diminished to zero after 20 minutes.

- The deposition due to diver burial is generally similar to the maximum water column plume footprint but reduced in extent. The higher deposition areas are adjacent to the cable route. A total of 10.79 ac will accrue deposition greater than 0.004 in.
- The current schedule to embed each cable by jet plowing plans for a 5 to 7-day interval between installations. The water column concentration duration analysis shows that the excess concentration will drop to zero within approximately 1 hour following cessation of jet plowing. With continued resuspension enabled the simulation shows excess concentration will drop to zero within 3 days. Thus, there will be no cumulative increases in suspended sediment concentrations because of these installations.
- There will be a cumulative threefold increase in deposition inside the silt curtains, for the three cables averaging 3 inches.

Table of Contents

List of Figures

List of Tables

1 Introduction

Public Service of New Hampshire d/b/a Eversource Energy (PSNH) has proposed the construction of an electrical cable system to increase the reliability of the electrical transmission grid in southern New Hampshire. This cable, known as the Seacoast Reliability Project, would cross the Little Bay portion of the Great Bay Estuarine System (GBES) as shown in Figure 1-1. The crossing would entail burial of three separate but parallel cables primarily by jet plowing, which is a technique that liquefies the sediment with high pressure water jets and simultaneously allows the cable to be buried at a predetermined depth. The cable sections in the shallow areas near the western and eastern landfalls will be buried by diver.

The environmental consultant for the Project, Normandeau Associates, Inc. (Normandeau), contracted with RPS ASA to support the analysis using its model systems to simulate the jet plowing process along the cable route to determine both the likely suspended sediment concentrations generated in the water column above the cable route and the resulting re-deposition of the sediments in and along the route (Swanson et al., 2015b). With the introduction of new data and new project details, that modeling study has been updated and expanded, and is presented herein. Furthermore, additional modeling and analyses have been performed in response to comments on the previous report. A separate document (Eversource Energy, 2017) has been generated with response to comments that refer to sections of this report.

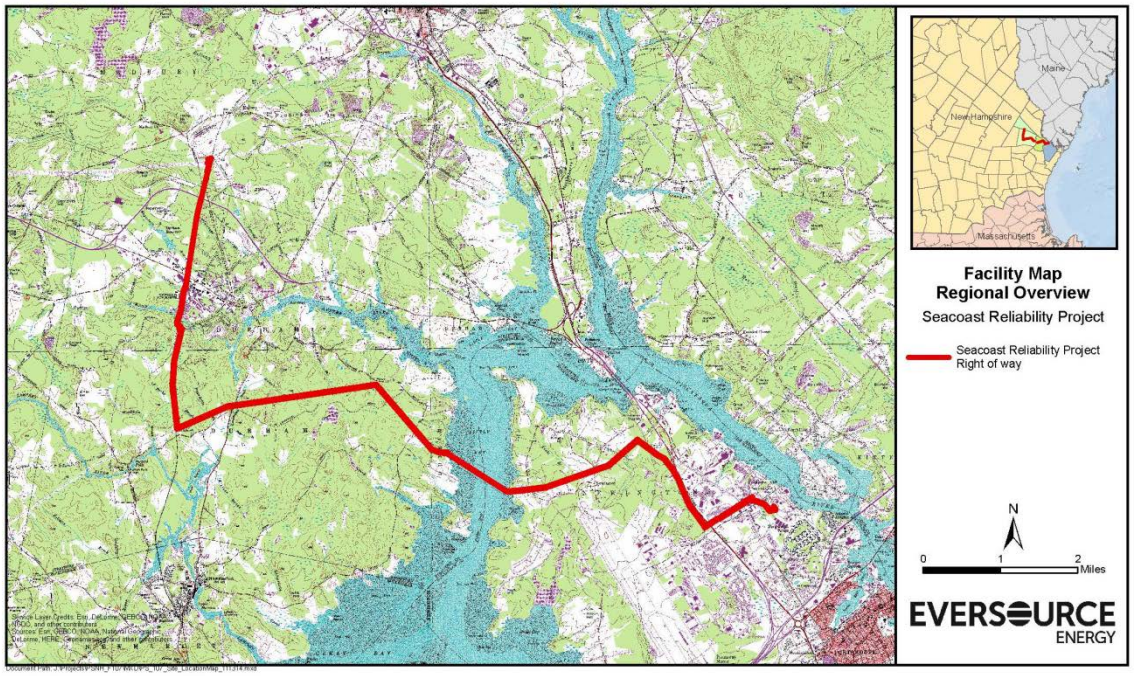

Figure 1-1. Location of the proposed cable route across Little Bay in the Great Bay Estuarine System.
(image from Normandeau Associates).

1.1 Report Structure

This report documents the hydrodynamic and sediment dispersion modeling activities performed to assess the effects from installation of the electrical cable using jet plowing and diver burial. To facilitate comparison to the previous report, the Chapter numbers have been kept the same however include additional sub sections. Specifically, Section 1 introduces the present effort; provides a summary of the changes and development in the project assumptions between the previous and present study; and includes a description of the study area. Section 2 presents the hydrodynamic modeling performed, and Section 3 presents the updated and supplemental sediment dispersion modeling performed. Section 4 consists of conclusions drawn from the study and references are listed in Section 5.

1.2 Summary of Present Work Performed

The previous study included sediment dispersion simulations of the proposed cable installation activities. The present study includes updated simulations of all previously modeled construction components (jet plow, diver jetting) as well as several sensitivity simulations for the jet plow simulation. The 'base case' was rerun with inputs reflecting the changes in the project assumptions and incorporation of new data. The sensitivity runs were simulated to assess the plow advance rate, sediment loss rate, and tidal amplitude (spring/neap). Additionally, a simulation was run that included the effects of continued resuspension. Continued resuspension refers to potential resuspension that may occur after the initial sediment plume settles, so sediments from that activity deposit on the seabed but may become resuspended under specific conditions (e.g. high current velocities); the threshold for resuspension depends on the sediment type. A summary list of the cases run is presented in Table 1-1, the details of which will be described in Section 3.

Table 1-1. Summary of present study model runs.

ID	Activity	Description
1	Jet Plow	Base Case
2	Jet Plow	Sensitivity to Advance Rate - Slow
3	Jet Plow	Sensitivity to Advance Rate -Fast
4	Jet Plow	Sensitivity to Loss Rate -Low
5	Jet Plow	Sensitivity to Loss Rate - High
6	Jet Plow	Sensitivity to Tide
7	Jet Plow	Additional Run with Continued Resuspension
8	Diver	West Diver Burial
9	Diver	East Diver Burial

1.3 Summary Changes between Previous and Present Studies

A description of the changes between the December 2015 study and the present study is provided here and expanded on in later sections. Multiple developments have been made since the previous study including slight changes to the marine crossing route, updated minimum burial depth in the deep portion of the jet plow, additional and improved sediment grain size distribution data, selection of a new installer with updated production rates, and modification of hydrodynamic data. A brief overview of each of those changes and the relevance with respect to sediment dispersion modeling is presented below.

1.3.1 Route & Silt Curtains

Most of the present route will remain the same as that modeled previously except for the hand jetting portion along the path towards the east landing. Figure 1-2 illustrates the center line of the present and previous modeled routes of the hand jetting path toward the eastern landing (the full project includes three lines, one north and one south of the center line). Table 1-2 summarizes the differences in length of hand jetting. The present modeling is in a slightly different location and has a decreased length.

Table 1-2. Summary of east diver burial route distance modeled in previous and present study.

Parameter	Previous East Diver Burial	Present East Diver Burial
Route distance	178 m 583 ft	165 m 541 ft

The proposed construction will utilize silt curtains during diver burial, for the entire west shore portion and for a portion of the east shore portion. The route and silt curtain lengths are summarized in 3 and illustrated in Figure 1-2.

Table 1-3. Summary of east diver burial route distance modeled in previous and present study.

Parameter	West Diver Burial	East Diver Burial
Route length	91.4 m 300 ft	165 m 541 ft
Length with silt curtain	91.4 m 300 ft	95 m 311 ft
Length without silt curtain	0 m 0 ft	70.1 m 230 ft
Percent route within silt curtain	100%	57.50%

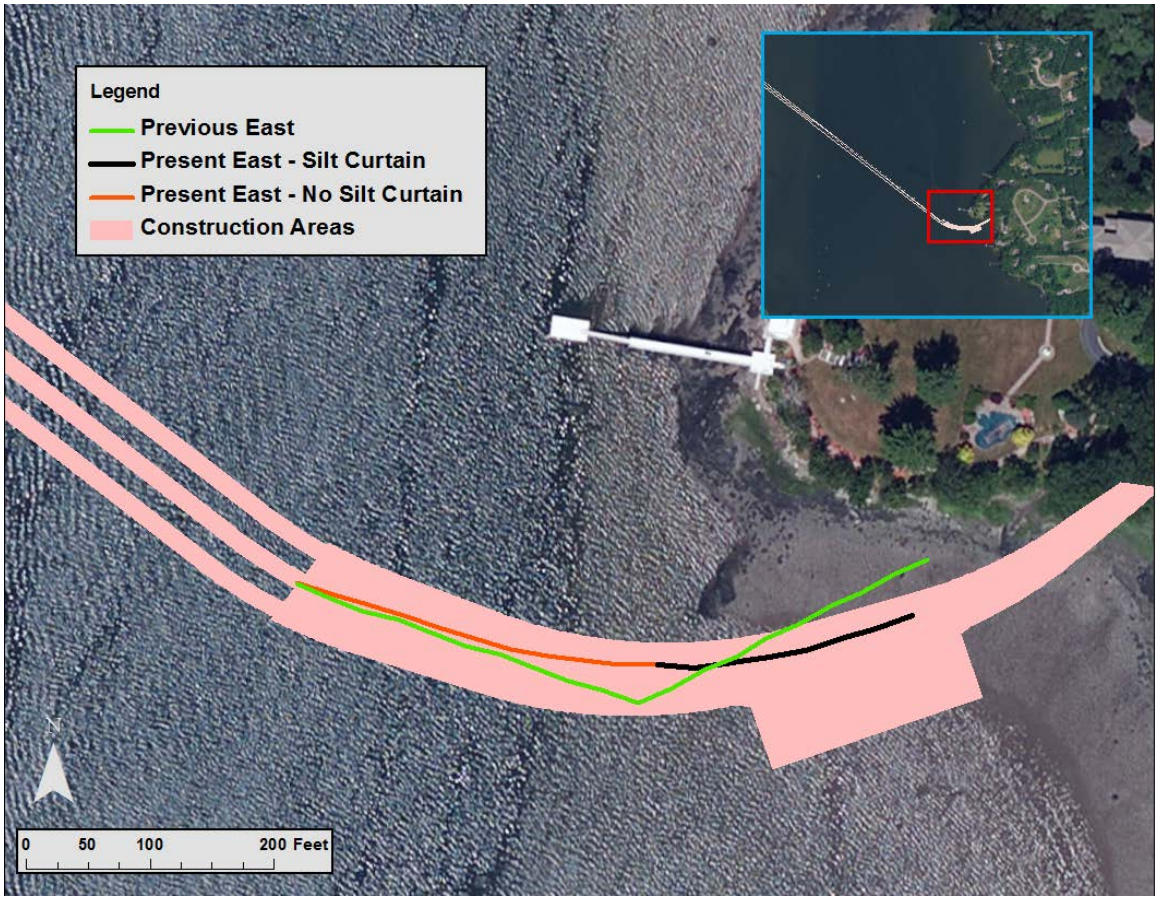

Figure 1-2. Illustration of previous and present diver burial eastern route highlighting the portion that will use silt curtains. Construction areas includes the cable areas and other areas designated for barges/equipment.

1.3.2 Minimum Burial Depth

The minimum burial depth for the cable varies depending on location. The minimum depth of burial for the present proposed installation is the same as the previous proposal except for the jet plow section in the deeper waters which has been decreased from 2.44 m to 1.52 m (8 ft to 5 ft) as shown in Figure 1-3. Eversource engineers have determined that 5 feet of burial would provide adequate protection against potential risk of damage from scour and boating activities. The new minimum burial depth results in a smaller disturbed volume of sediments and therefore less sediment mass introduced to the water column as compared to what was previously modeled.

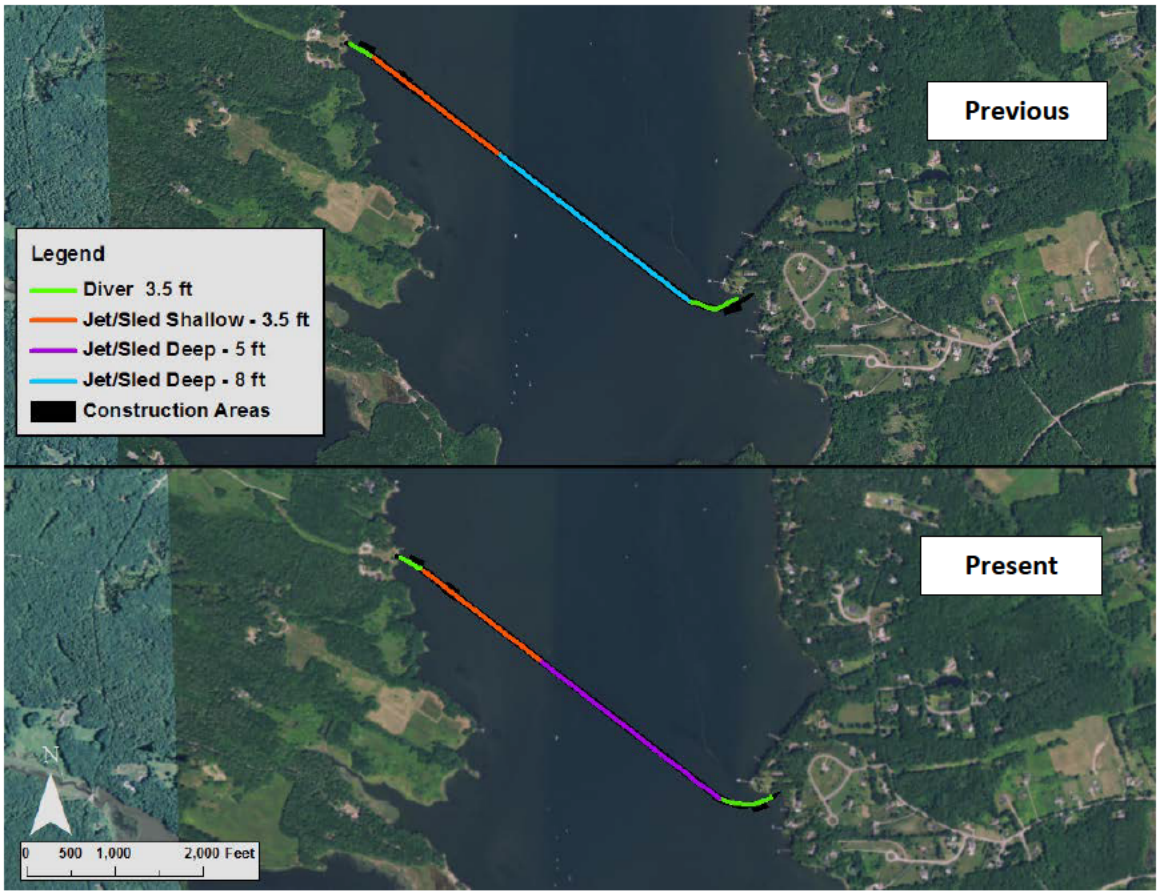

Figure 1-3. Illustration of previous (top) and present (bottom) minimum burial depth. Note that the full project includes three parallel lines but only the center one is shown.

1.3.3 Sediment Characterization

Since the previous report was prepared additional sediment samples were obtained which were analyzed by sieve and hydrometer to determine the grain size distribution; the hydrometer analysis was specifically performed to obtain a better characterization of the fine-grained material (Normandeau Associates 2016 & Normandeau Associates 2017). The samples were taken at stations along the route, like the previous samples, however the additional laboratory analysis provided more detail about the mass distribution of sediment sizes. The new data provided finer resolution of definition of mass in different size ranges. These details were used to first determine the cumulative distribution for each sample and then to determine the amount of mass within the SSFATE model bin ranges; more details on the SSFATE treatment of sediment grain size is provided in Section 3.2. Note that SSFATE classes use descriptive terms that do not necessarily align with other conventional schemes, however are used to describe the progression of fine to coarse material (See Table 3-2).

Figure 1-4 shows the grain size distribution as described by five classes used in the SSFATE sediment dispersion modeling for both the previous modeling and present modeling. In both cases the distributions were determined from analysis of sediment data, however the refined present data allows for more accurate description whereas the previous data used more conservative assumptions. As a point of comparison pie charts of the average of all samples

from both the previous and present sampling are shown in Figure 1-5. Both figures illustrate that the new sampling and analysis shows a much different sediment characterization with a shift to coarser sediments; this shift results in more mass settling out of the water column quickly.

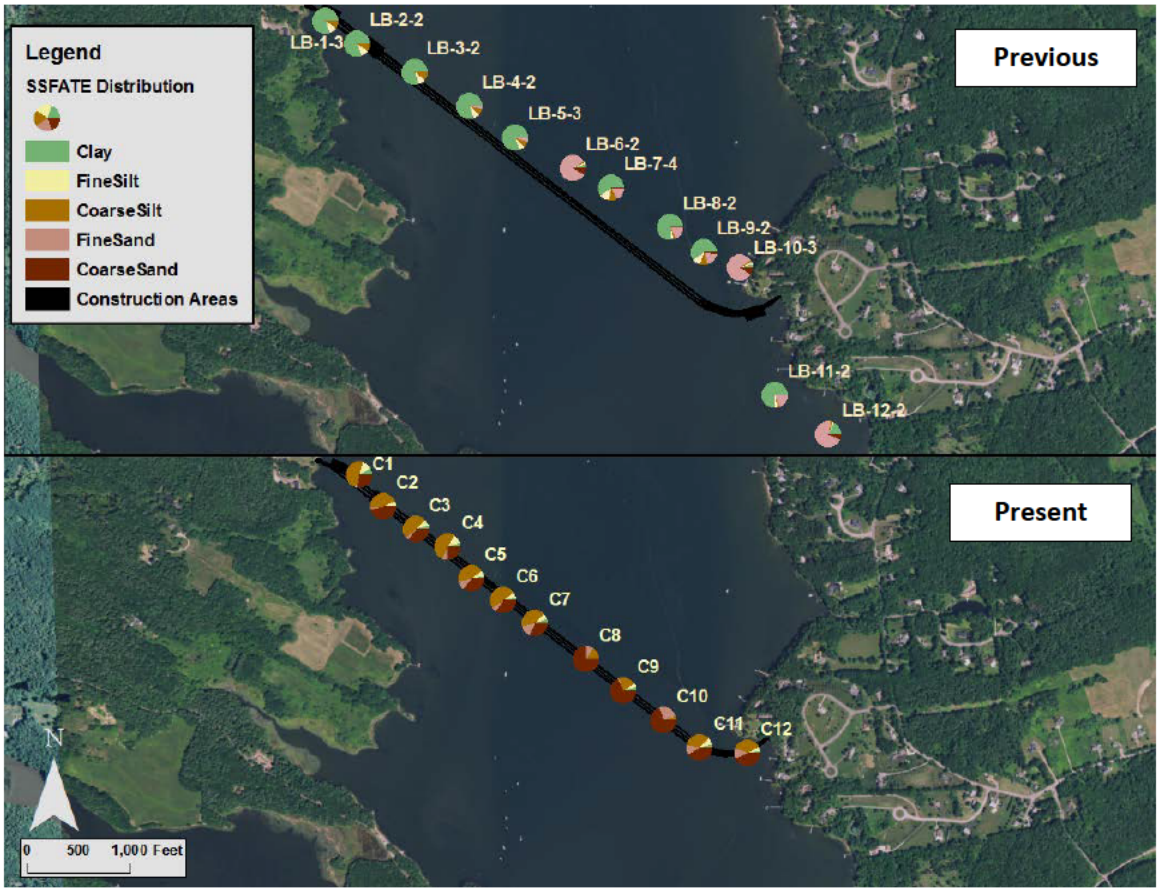

Figure 1-4. Illustration of previous (top) vs. present (bottom) grain size distribution delineated in classes used by the sediment dispersion model.

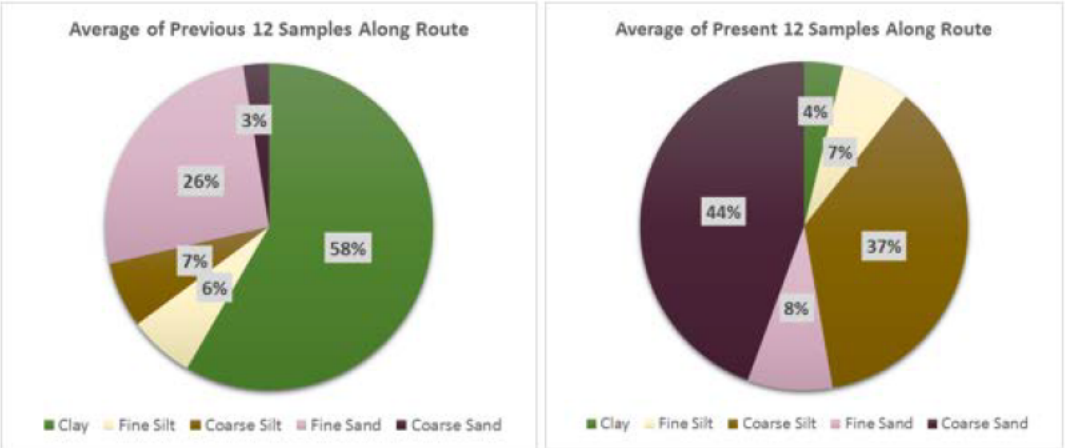

Figure 1-5. Illustration of previous (left) vs. present (right) average grain size distribution from samples along the route.

In addition to grain size, the new refined grain size analysis provided a measure of water content (moisture). These values were used to convert which is expressed as a percentage and is the ratio of the weight of water to the weight of sediment in a sample. The previous modeling did not have access to samples with a measure of water content, and as such it was conservatively assumed that the sediments were 100% solids. This means the entire volume was assumed to be solids, however in reality there would be some fraction of pore water within the total volume of sediment introduced to the water column and thus the mass of sediment introduced to the water column would be less than that calculated based on the assumption of 100% solids. The present modeling has accounted for water content based on moisture property. Figure 1-6 illustrates the previous and present percent solids associated with each sample used to define the sediment loading. As can be seen from this figure the sediment volumes are between 48-67% solids, 55% on average. This refined information allows for a more accurate solid loading to the water column which is significantly reduced from the previous modeling.

Figure 1-6. Illustration of previous (top) and present (bottom) percent solid associated with each sample used.

1.3.4 Installation (Advance Rate)

The present sediment dispersion modeling was performed in a similar nature to the previous modeling with some refinements, including updated values for the advance rate or production rate which is the rate at which installation would take place (e.g. meters per hour). The different construction activities (diver jetting vs jet plow) have different rates where the diver jetting moves at a much slower rate than the jet plow. The installer (LS/Durocher) provided updated estimates of the range of likely average (over the installation timeframe) production rates for the jet plow as summarized in Table 1-4. LS/Durocher confirmed that the previously assumed values for diver jetting remained appropriate (Table 1-4). The production rate, along with start time, dictate the tidal regime during construction (since production rate dictates duration). The base case was modeled for a spring tide (largest tidal range) to capture maximum transport from the source; a sensitivity to tide range is also included as part of this study by modeling during a neap tide (smallest tidal range). Each cable jet plow installation will start on the west coast; due to this fact and the shallow nature of the western waters, the work will begin on a high tide slack water. Due to this operational constraint, it was determined that sensitivity to start time (as described by phase of the tide) was determined to not offer practical insight.

The previous and present advance rate, along with the present sensitivity run advance rates for slower and faster than expected, are summarized in Table 1-4 along with associated duration for construction. An illustration of the operations duration overlaid on a typical spring tide (amplitude and velocity) is presented in Figure 1-7.

If all other parameters remained equal, a change in advance rate changes the mass loading rate to the water column. In this case the increase in expected advance rate from 5.47 ft/min to 10 ft/min would result in an increase in mass flux to the water, however the reduced percent solid (calculated from improved sediment data including moisture content) and reduced cross section in places both serve to reduce the total load and therefore loading rate. Further the advance rate in this application results in activities taking place over a different range of tide stages.

Table 1-4. Summary of previous and present advance rate and duration for jet plow operations.

Parameter	Previous - Expected Average Rate	Present - Expected Average Rate	Present - Slow	Present – Fast	Previous and Present Diver Jetting
Advance Rate	100 m/hr 5.47 ft/min	182.9 m/hr 10 ft/min	91.4 m/hr 5 ft/min	274.3 m/hr 10 ft/min	2.3 m/hr 0.15 ft/min
Duration	13 hours	7.1 hours	14.2 hours	4.7 hours	1.7 days West* 3.0 days East*

*Duration is the total cumulative of the activity and not the calendar span. The diver burial will be intermittent over a longer period.

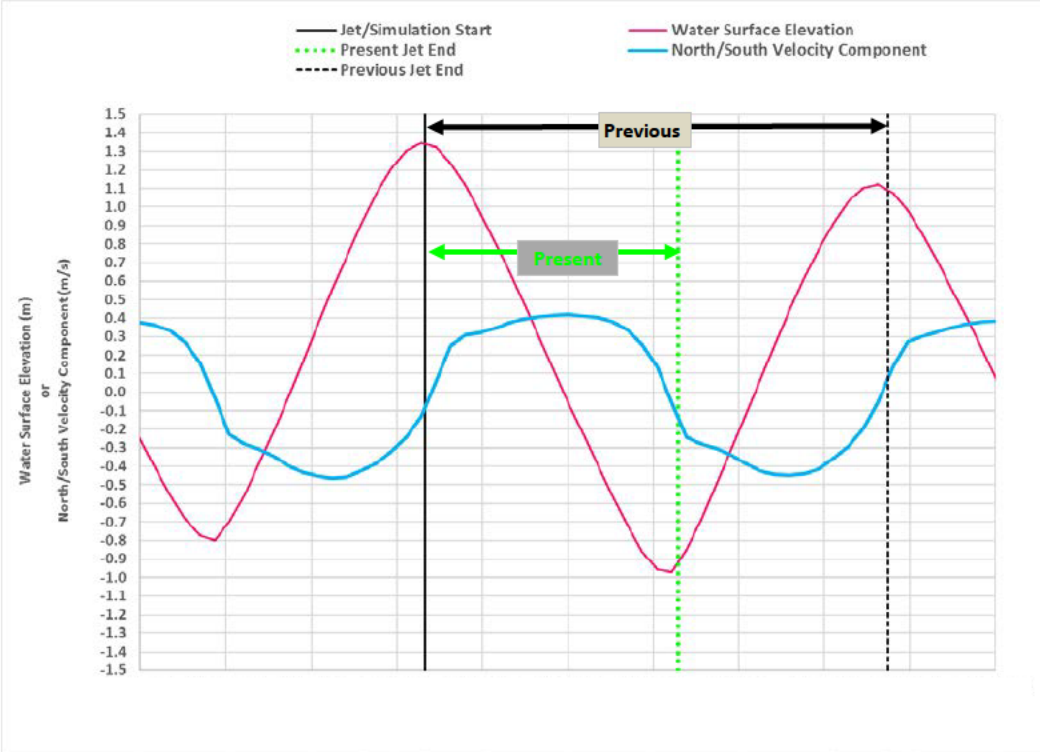

Figure 1-7. Illustration of duration difference between previous and present jet plow operations overlaid on water surface elevation and current velocity time series.

1.3.5 Hydrodynamic Data

The previous study had documented the Bellamy hydrodynamic model application to the study area (Bilgili et al., 2005) that had been used to generate hydrodynamic data input for the sediment dispersion model. During the present modeling, it was realized that a different model output was used in the sediment transport simulations. The output used was from a HYDROMAP (Isaji et al., 2001) model application that had been intended for troubleshooting and comparison. The HYDROMAP model output is very similar to the Bellamy model output. Both models covered the study area domain and generated water surface elevation and current speeds and directions based on similar approaches to input forcing and solution techniques. The HYDROMAP model output had reflected an average tidal amplitude as opposed to a spring tidal amplitude. To demonstrate the impact of the use of the HYDROMAP model and mean tide input the previous sediment dispersion simulation was rerun with the Bellamy model output and a comparison of the maximum time integrated footprint of concentrations was generated (Figure 1-8). The previously reported results (using HYDROMAP) are shown on the left and the rerun (using Bellamy) are shown on the right. These figures show that the shape and extent of the footprints are very similar and confirm that the same results and conclusions hold true regardless of the choice of hydrodynamic input (between HYDROMAP and BELLAMY) to the sediment dispersion model. That said, all runs for the present study were simulated using the Bellamy hydrodynamic model output.

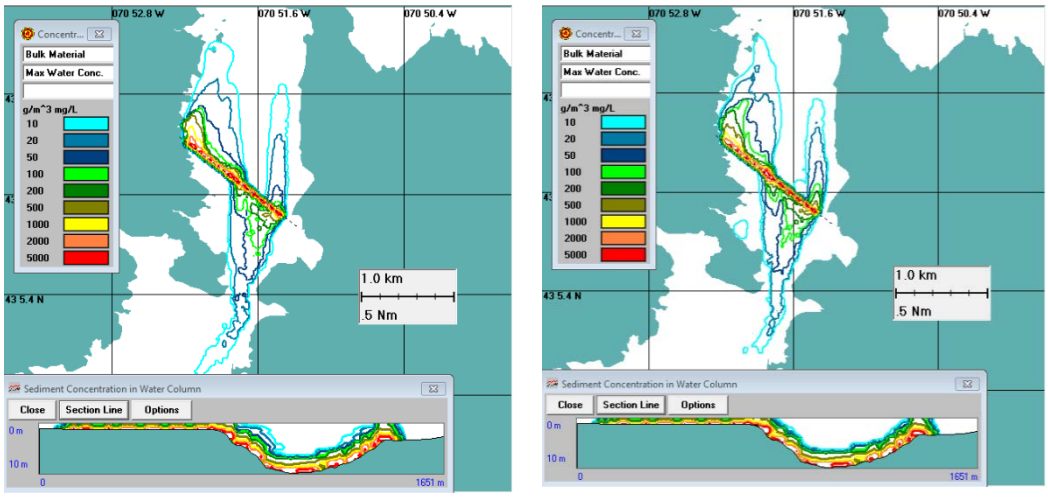

Figure 1-8. Illustration of maximum time integrated concentration footprint using HYDROMAP (left) and Bellamy (right) for previous loading and sediment characterization inputs

1.4 Description of Study Area

The Great Bay Estuary System (GBES) consists of a complex system of drowned river valleys with an area of 2,307 ha at mean high water (Meeker et al., 1998). The GBES, Figure 1-9, consists of the Piscataqua River running from north to south along the border between New Hampshire and Maine. It is intersected by Lower Little Bay at Dover Point about 13 km (8 mi) upstream of its mouth at Massachusetts Bay. Lower Little Bay runs west northwest for 3.5 km (2.2 mi) to Cedar and Fox Points before turning south (as Upper Little Bay) for 3.5 km (2.2 mi) until ultimately connecting to Great Bay at Furber Strait. A series of rivers feed the Piscataqua River, Little Bay and Great Bay as shown in the figure. The main channel depths are on the order of 10-15 m (33 ft – 48 ft) in the lower parts of GBES and 3 m (10 ft) in Great Bay to 10 m (33 ft) in Little Bay (Bilgili et al., 2005). The extensive tidal flats in Little and Great Bays cause almost 50% of these estuarine areas to be exposed at low tide (Bilgili et al, 2005).

Sections 1.1.1 through 1.1.3 discuss the physical processes driving the circulation in the GBES and specifically Upper Little Bay: tides, river flow (salinity), and winds. The discussion includes references to previous studies extending from the 1970s to the 2000s.

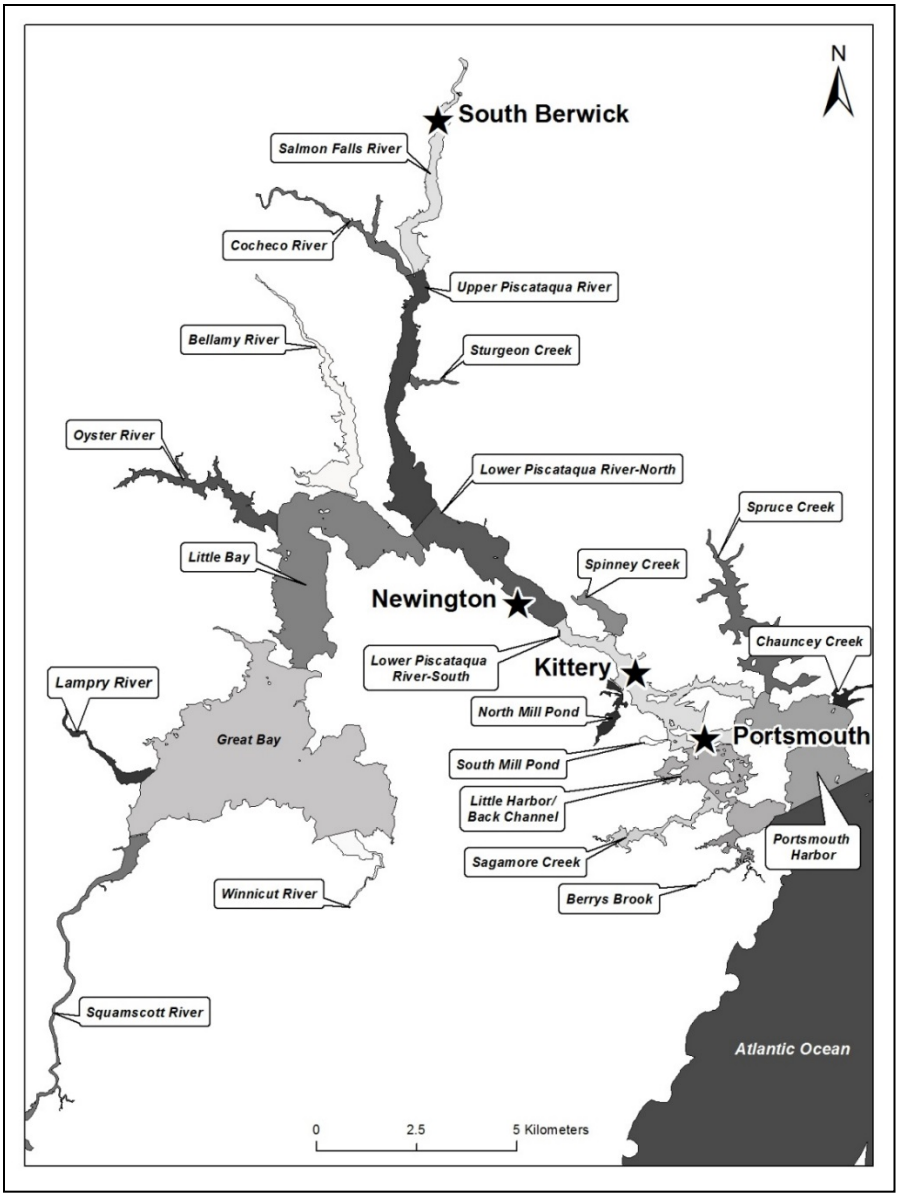

Figure 1-9. Great Bay Estuarine System regions used for previous modeling (Swanson et al., 2015a). Little Bay is located in the central portion of the System.

1.4.1 Tides

The tide in GBES is semidiurnal and consistent with the tide in Massachusetts Bay to which it is connected. The mean tide range at the mouth of the Piscataqua is 2.6 m (8.5 ft), 1.9 m (6.2 ft) at the entrance to Lower Little Bay (Dover Point) and 2.1 m (6.9 ft) at the mouth of the Squamscott River in Great Bay, furthest upstream (Ward and Bub, 2000) so the GBES is considered a mesoscale tidal regime (range between 2 and 4 m [6.6 – 13 ft]). Mesoscale tides are indicative of currents strong enough to generate sufficient turbulence to mix the water column. The tide acts like a progressive wave in the Piscataqua River but as a standing wave in Little and Great Bays. Tidal currents in Little Bay reach a maximum of about 0.5 m/s (1 kt) (Ward and Bub, 2000).

One study in GBES of tidal elevation and currents was conducted in 1975 by Swenson et al. (1977) which consisted of moored current meters and tidal gauges, generating time series, as well as vertical measurements at three stations in transects across various channel locations. One of the transects was near Adams Pt. located about 1.2 km (0.75 mi) south of the proposed cable crossing and a second one was located at Fox Point, where Lower and Upper Little Bay meet approximately 2.3 km (1.4 mi) north of the proposed cable crossing. There were several problems with the study methods. One problem was that the measurement of the vertical structure of currents was performed with a single instrument thus requiring that the boat stay at each location in the transect for 15-20 min so that the entire transect could take up to an hour to acquire; hardly a synoptic measurement in a semidiurnal tidal situation. Another was that the station locations at times diverged from a straight line transect, sometimes by as much as 200 m. Finally the velocity contours shown in the vertical transect sections, which were drawn by hand, were sometimes extrapolated without actual data taken.

Ward and Bub (2000) reported the mean high tide volume of GBES is ~230 x 10^6 m^3 (8.1 x 10^9 ft^3) and the mean tidal prism is ~64 x 10^6 m^3 (2.2 x 10^9 ft^3). Short (1992) reported the total estimated mean freshwater input is 32.3 m^3/s (1,140 cfs) so that the ratio of freshwater input to tidal prism is only approximately 1 to 2%, which defines a well-mixed system due to high tidal-induced turbulence.

1.4.1.1 UNH ADCP Deployment in Upper Little Bay

The University of New Hampshire conducted a field program in Great Bay, led by Prof. Thomas Lippmann, consisting of deployment of eight Acoustic Doppler Current Profilers (ADCPs), one of which was located in the channel of Upper Little Bay about 600 m (2000 ft) south of the proposed cable crossing and 600 m (2000 ft) north of Adams Point. The instrument was bottom mounted in water approximately 17 m (56 ft) below MSL and deployed from 25 August through 29 September 2015. It was configured to record measurements at 0.5 m intervals from near bottom to near surface resulting in the deepest bin located at 1.71 m (5.6 ft) above the bottom and the shallowest bin at 13.21 m (43.34 ft) above the bottom for a total of 24 complete bins. Data for four additional bins were intermittently acquired depending on the stage of the tide. The data were averaged into 5040 10-minute time steps starting at 25 August 2015 17:05 UTC.

The water elevation data as measured by the pressure sensor in the ADCP is shown in Figure 1-10. The spring-neap tide variation is relatively small during this period with maximum spring tides at approximately 31 August, 14 September and 29 September separated by lower amplitude neap tides.

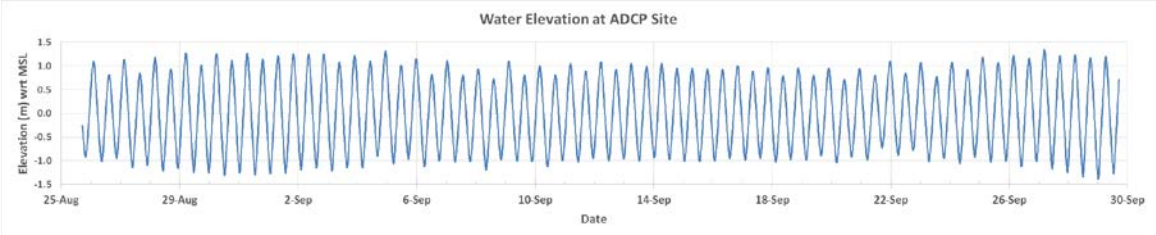

Figure 1-10. Time series of water elevation from ADCP.

Figure 1-11 and Figure 1-12 display the V (north-south) and U (east-west) velocities (at different scales) for the entire period. There is sometimes increasing amplitude with depth above the bottom particularly for higher velocities. The amplitude of the V velocities is significantly larger than the U velocities since the channel orientation is more aligned with the V direction.

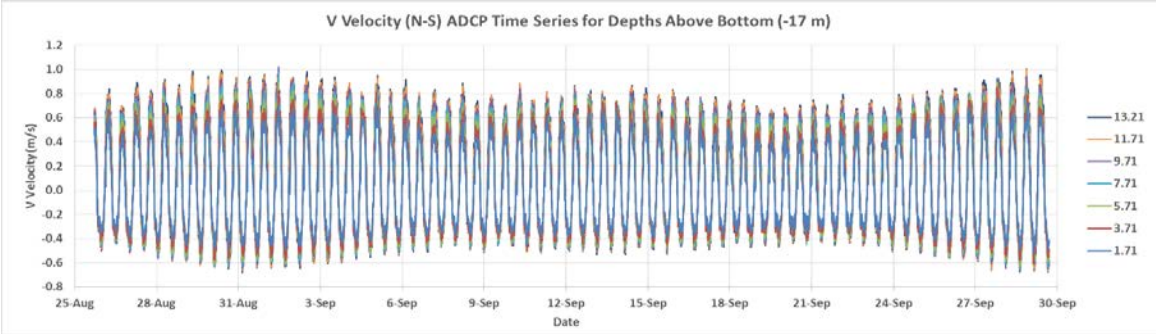

Figure 1-11. Time series of V (north-south) velocities for selected depths from ADCP.

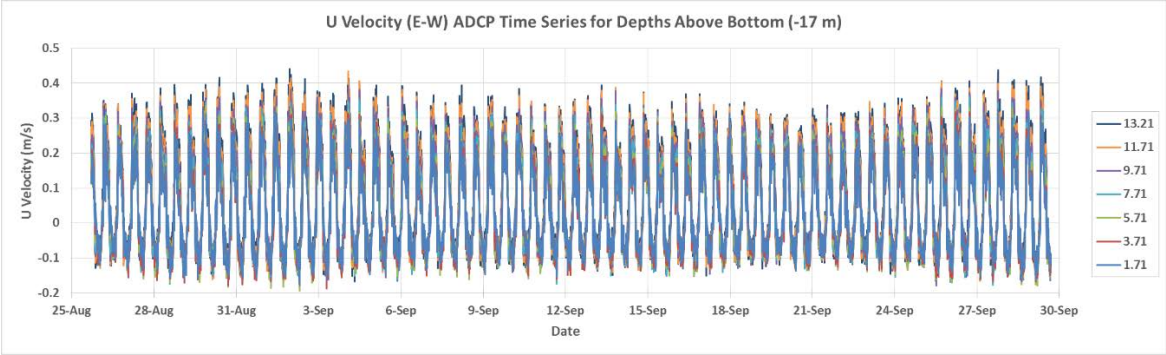

Figure 1-12. Time series of U (east-west) velocities for selected depths from ADCP.

The U and V velocities were rotated by 21° clockwise to match the Along-Channel (21° – 201°) and Across Channel (111°-291°) directions to highlight the flood and ebb directional flows. Figure 1-13 shows the resulting Along-Channel velocities.

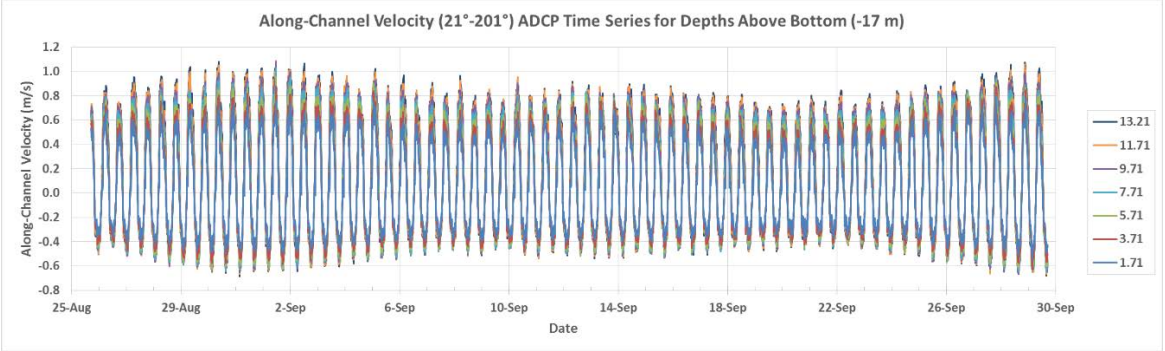

Figure 1-13. Time series of Along-Channel (21° – 201°) velocities for selected depths from ADCP.

A mean tide was chosen from maximum flood (20 September 2015 20:25 UTC) to maximum ebb (21 September 2015 1:35 UTC) to show the vertical structure through that portion of the tide. Figure 1-14 shows how the structure is essentially vertical from maximum flood (negative velocity) to slack high but during the higher velocity ebb (positive north velocity) the bottom friction inhibits the speeds in the deeper layers. The condition of larger ebb velocities than flood (tidal asymmetry) is consistent with other observations (Erturk et al., 2002). This does not invalidate using a vertically averaged modeling approach since the sediment dispersion model reduces the vertical average velocity output from the hydrodynamic model using a log law reduction in the lower layers of its three-dimensional grid. Since the sediment dispersion model uses Lagrangian particles to simulate the sediment movement this approach does not depend on conservation of water mass to accurately transport the sediment particles.

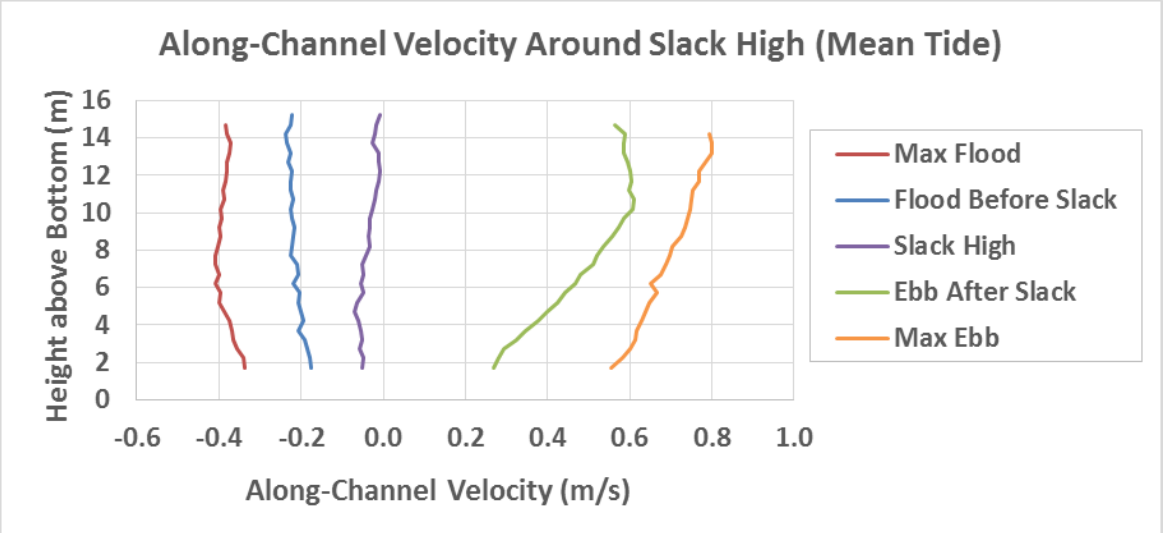

Figure 1-14. Vertical structure of along-channel velocities during a mean tide from maximum flood to maximum ebb.

1.4.2 River Flow

The effect of freshwater flow entering an estuary is based on the volume of flow that may create a vertical structure where low or zero salinity at the surface overrides higher salinity water below. The importance of this effect must be compared to the importance of tidal circulation, which if the tidal prism is significantly higher than the freshwater inflow, then the stronger tidal flow will generate sufficient turbulence to mix the freshwater into the estuary water creating a well-mixed system. The sections below will first examine the amount of freshwater entering the GBES and second, examining whether there is evidence of a vertical salinity gradient in the GBES.

The drainage basins for the rivers that enter the GBES are shown in Table 1-4. Three of the rivers (Lamprey, Squamscott, and Winnicut) flow into Great Bay south of Upper Little Bay and the other four rivers (Salmon Falls, Cocheo, Bellamy and Oyster) flow into Lower Little Bay and the Piscataqua River north and east of Upper Little Bay.

Table 1-5. GBES mean river flow estimates.

River	Short, 1992 m^3/s and (ft^3/s)	Jones, 2000 m^3/s and (ft^3/s)	Ward and Bub, 2000 m^3/s and (ft^3/s)	Bilgili et al., 2005 m^3/s and (ft^3/s)	USGS Present m^3/s and (ft^3/s)
Lamprey	7.9 (279)	7.87 (278)	8.0 (283)	7.9 (279)	8.21 (290)
Squamscott	4.6 (162)	4.62 (163)	3.1 (109)	4.6 (162)	
Oyster	0.5 (18)	0.54 (19)	0.6 (21)	0.5 (18)	0.57 (20)
Bellamy	0.7 (25	0.71 (25)		0.7 (25)	
Cocheco	6.9 (244	6.85 (242	4.7 (166)	6.9 (244)	4.29 (152)
Salmon Falls	5.8 (205	5.78 (204)	5.4 (191)	5.8 (205)	
Winnicut					0.82 (29)
Piscataqua	5.9 (208)	5.95 (210)			
Total	32.3 (1141)	32.31 (1141)	21.8 (770)	26.4 (932)	13.83 (488)

Short (1992) and Jones (2000) presented essentially identical flow estimates. Ward and Bub (2000) presented lower estimates for some rivers and did not include direct runoff. Bilgili et al. (2005) did not account for direct runoff to the GBES so his estimate is somewhat low, 82% of the 32.3 m^3/s (1,140 cfs) average of Short and Jones. The USGS estimate is based solely on the data presently available online. Short (1992) concludes that the Lamprey River accounts for 25% of the total freshwater flow to the GBES (7.9 of 32.3 m^3/s (279 - 1,140 cfs)) and that four times the Lamprey flow is a good proxy for freshwater flow into the GBES.

The total mean freshwater flow into the GBES is less than 2% of the tidal prism and is generally regarded as indicative of a system dominated by tidal flow and not freshwater flow (or salinity variations) and makes the GBES a well-mixed system (Bilgili et al., 2005). The statement that strong tidal currents prevent vertical stratification throughout GBES except for partial stratification during high discharge, particularly in the tidal reaches of the rivers can be traced back at least to Brown and Arellano (1980).

1.4.2.1 USGS River Flow Data

Since the installation of the cables across Upper Little Bay is proposed to occur in the September – October time window, it is instructive to examine the monthly variation of river flow compared to the yearly average. For this analysis, historical discharge measurements were acquired from the USGS website (https://waterdata.usgs.gov/nwis/inventory) for four available sites (Table 1-6.). The record lengths vary from 8 years to 82 years and the mean yearly discharge, calculated from the monthly statistics, ranges from 0.57 m^3/s (Oyster River) to 8.21 m^3/s (Lamprey River).

Table 1-6. USGS discharge station information and mean yearly discharge.

Station Name	USGS Designation	Record Length	Mean Yearly Discharge m^3/s and (ft^3/s)
Lamprey River near Newmarket, NH	01073500	1934-08-01 -> 2016-10-31	8.21 (290)
Cocheco River near Rochester, NH	01072800	1995-03-01 -> 2016-09-30	4.29 (152)
Winnicut River at Greenland, near Portsmouth, NH	01073785	2002-08-01 -> 2016-10-31	0.82 (29)
Oyster River near Durham, NH	01073000	1935-01-01 -> 2016-09-30	0.57 (20)

The mean monthly discharge for each river is summarized in Figure 1-15. The yearly cycle is evident with highest flows in March and April and lowest flows in August and September. The shoulder months of June, July and October are also generally low. The sum of the means of these USGS monitored flows is 43% of the Short (1992) and Jones (2000) total of 32.3 m^3/s (1,140 cfs).

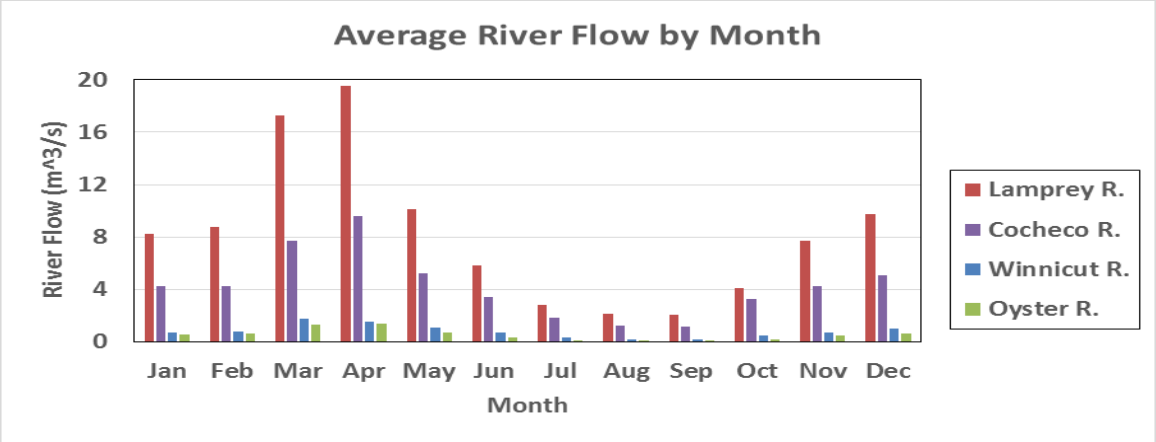

Figure 1-15. Mean monthly river flow from the USGS website.

The monthly mean discharges expressed in percentage of the yearly USGS means are shown in Figure 1-16. Here the annual trend is seen more clearly with highest flows between 15 and 20.2% of the mean flows occurring in March and April, lowest flows between 1.7 and 2.4% of the USGS total mean occurring in August and September and low flows between 3.5 and 6.2% of the USGS total mean in October. Thus the yearly mean flows used by Bilgili (2005) in his hydrodynamic model application described in Section 2 over estimates the flow for September and October but is conservative by a factor of 16.

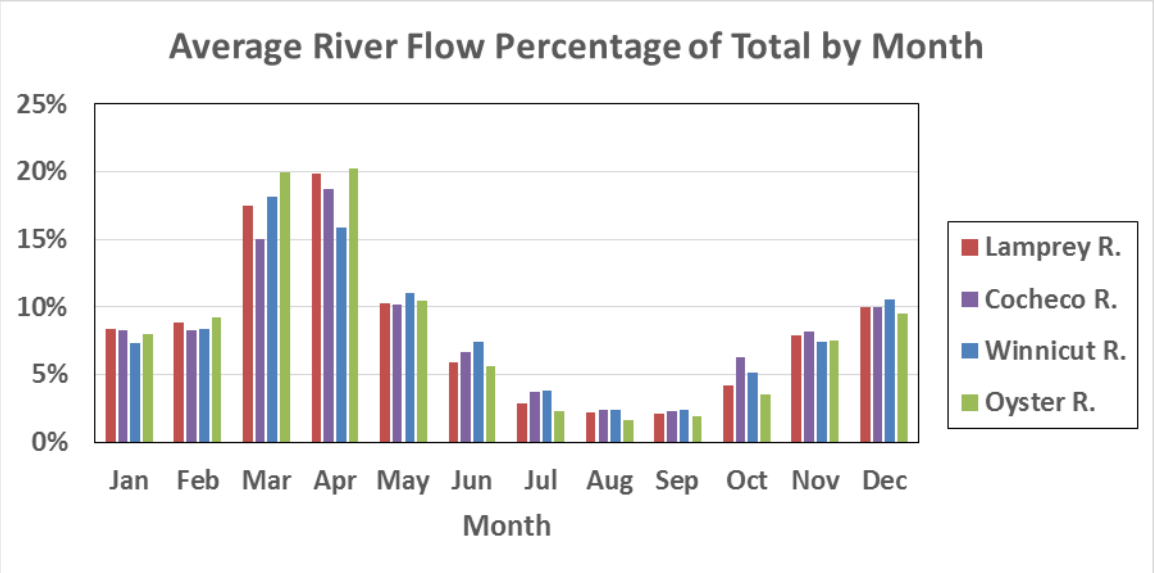

Figure 1-16. Mean monthly river flow as a percentage of mean annual flow.

To further dissect the finer detail of river flow, daily data were downloaded from the USGS website for the September and October months during the 2007 – 2016 decade period. Figure 1-17 shows the results for the Lamprey River, which has the largest flow into GBES (approximately 25% of the total flow), with each year overlain as well as the daily mean flow. The mean daily flow for September and early October is less than 5 m^3/s (176 cfs) and less than

8 m^3/s (282 cfs) by the end of October. The intermittent spikes greater than 10 m^3/s (353 ft^3/s) that occurred (three in 2008, four in 2011, two in 2013) lasted from 3 to 9 days.

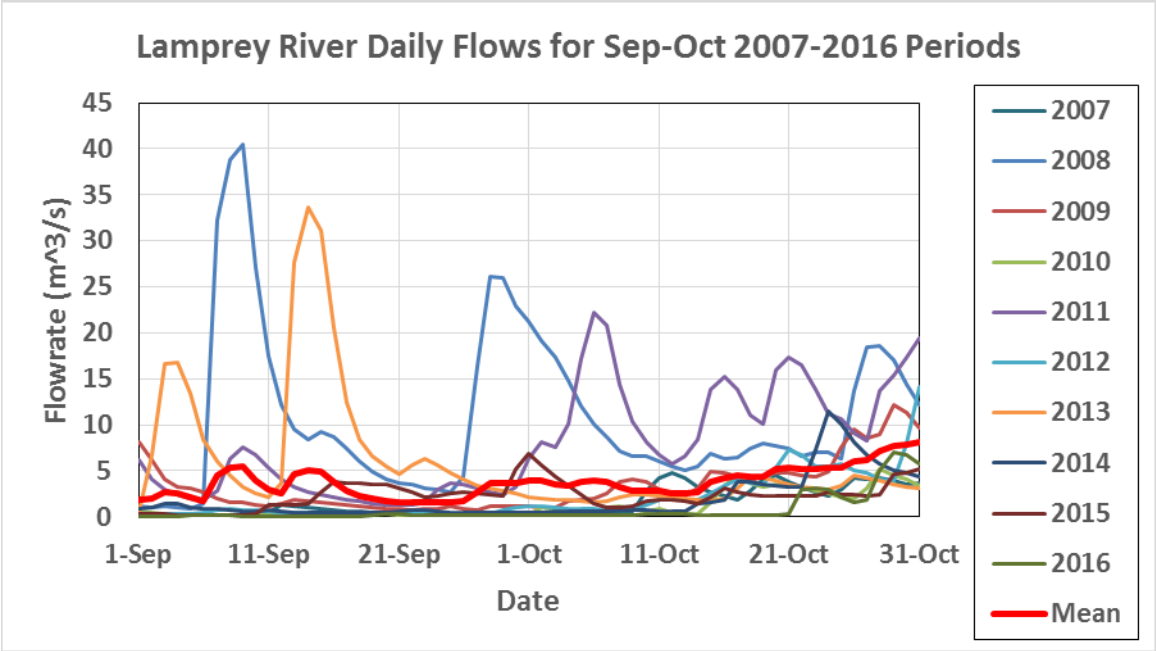

Figure 1-17. Time variations of daily flows of the Lamprey River for the September – October period for the decade 2007-2016.

More detail relative to the distribution of daily flow rates in 1 m^3/s (35.3 cfs) increments is shown in Figure 1-18. A total of 227 days of the 610 total are less than 1 m^3/s (35.3 cfs), 321 days between 1 (35.3 cfs) and less than 9 m^3/s (318 cfs), 43 days between 9 (318) and less than 18 m^3/s (636 cfs) and 18 days between 18 (636 cfs) and the maximum of 40.8 m^3/s (1,440 cfs). This indicates the low likelihood of any significant flow events during the cable installation scheduled for September and October.

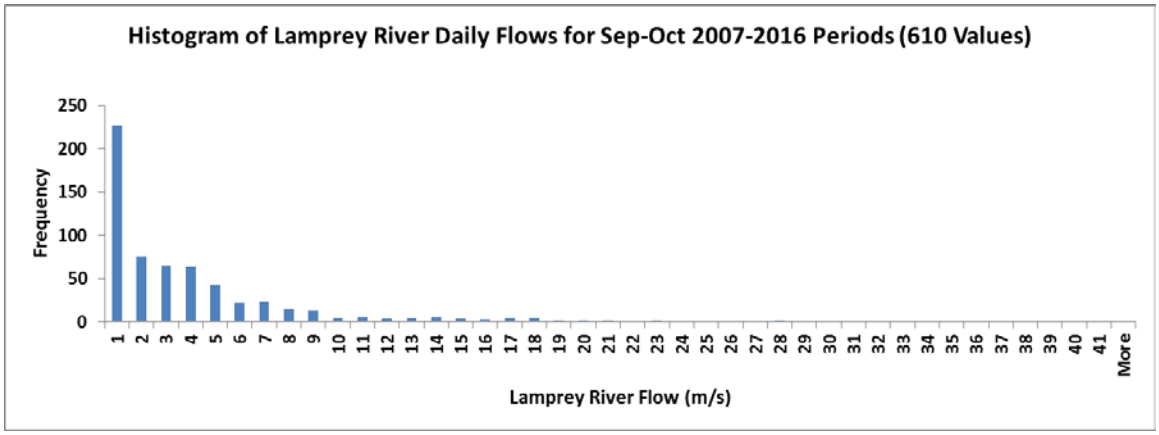

Figure 1-18. Histogram of Lamprey River daily flow for September and October during the 2007-2016 decade.

1.4.2.2 Effect on GBES Salinity

Measurements of the vertical salinity gradient have been collected over many years. The first major effort was that reported by Silver and Brown (1979). A 3-station transect at Adams Point, a 2-station transect between Adams Point and Fox Point, and a 3-station transect at Fox Point were occupied. Based on their measurements they concluded that salinity fronts are typically diffuse and are seen only where the rivers empty into the estuary. They also concluded that "vigorous tidal mixing" and relatively low river flows combine to minimize the salinity structure.

Ward and Bub (2000) reported on a series of 12 cruises, one of which occurred on 13 Oct 1998, where measurements were made at six stations, one of which was in the Furber Strait at the south end of Upper Little Bay. They reported surface (upper 3 m [9.8 ft] average) salinity of 25.7 psu and bottom (lower 3 m [9.8 ft] average) salinity of 25.9 psu [<1 psu vertically mixed] when the average discharge (5 days previous) was 3.4 m^3/s (120 cfs).

Brown and Arellano (1980) analyzed the available data and found, except during high river discharge in spring, most of estuary was considered to be a Hansen and Rattray (1996) classification of 2a, where vertical stratification is small and advection and diffusion processes drive the upstream salt flux. No vertical salinity stratification was observed in Upper Little Bay from the data.

1.4.3 Winds

1.4.3.1 Winds during September – October Period for 2007-2016 Decade

To investigate the potential effects of wind the DS3505 wind records from NOAA for the Pease International Tradeport was downloaded for the decade 2007 – 2016 and the September – October period when the cable installation is proposed to occur. Figure 1-19 shows the wind speed for these periods with each year separated by the intervening 12 months (November – August).

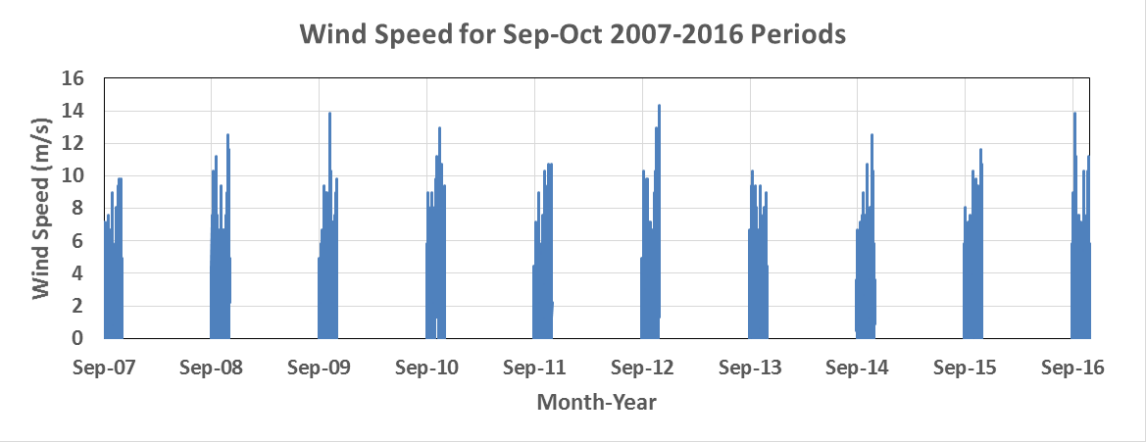

Figure 1-19. Wind speed data from NOAA at Pease International Tradeport for the September – October period over the decade 2007 – 2016.

Due to its time scale the previous figure does not allow a visual examination of the wind variability. Therefore a wind rose was generated (Figure 1-20) that shows the distribution of wind speed, wind direction and frequency of occurrence. The wind is predominantly from the west +or- 22.5° (approximately west northwest to west southwest). The speed was 88% below 5 m/s (11 mph), 11% fell between 5 (11) and less than 9 m/s (20 mph), 0.9% fell between 9 (20) and less than 13 m/s (29 mph) and 0.04% ranged between 13 (29) and 14.3 m/s (32 mph). The peak wind of 14.3 m/s (32 mph), occurring during an event on 29 and 30 October 2013, originated from 50° clockwise from true north while the four associated speeds (three at 13.4 (30) and one at 13.9 m/s [31 mph]) for the same event ranged from 40° to 80°. The directions for the other two events at 13.9 m/s (31 mph) originated from 270° and 310°.

None of the largest wind events originated from the north or northwest or from the south or southeast, the alignment of Upper Little Bay. This indicates that the waves generated by these winds would not be substantial as the wave fetch would be limited to the width (1.1 km [0.7 mi]) of the water body and not its length (3.5 km [2.2 mi]).

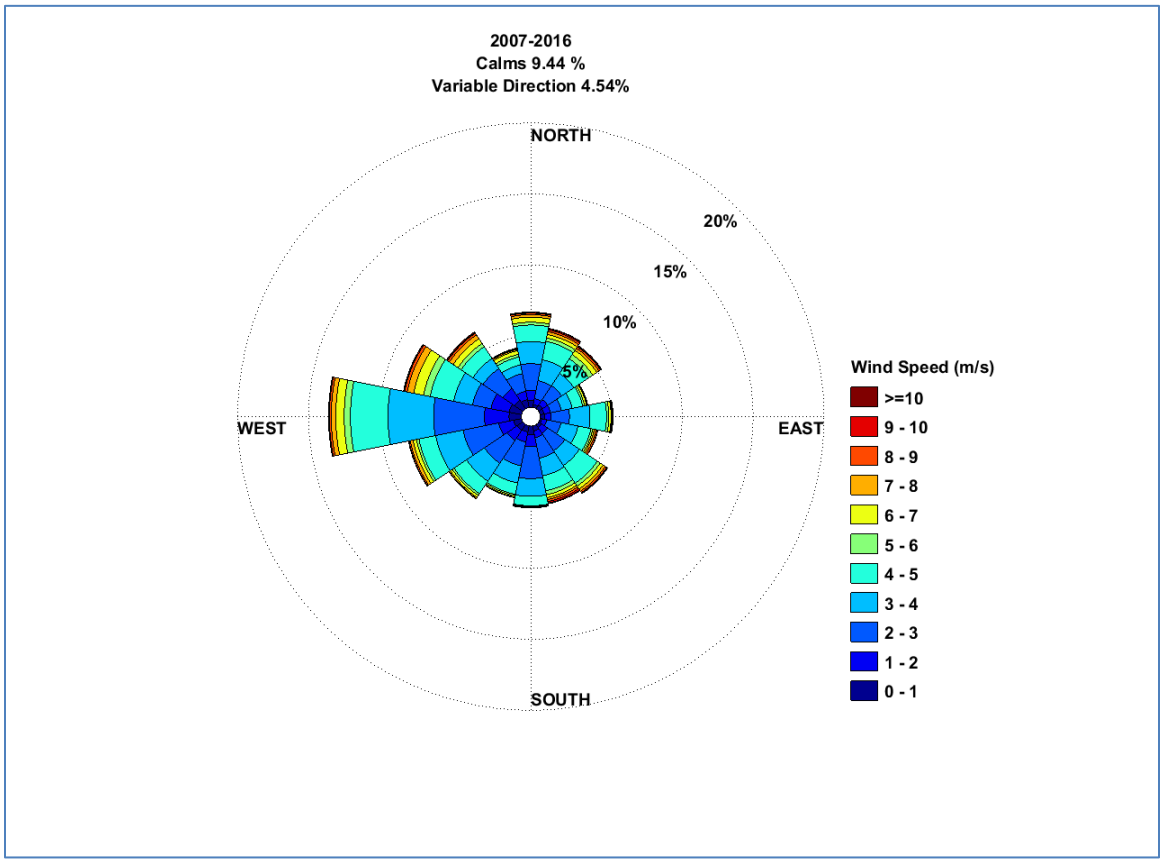

Figure 1-20. Wind rose showing speed (m/s), direction and frequency of occurrence for September – October period during the 2007 – 2016 decade.

1.4.3.2 Winds During ADCP Deployment

To investigate whether winds could cause an appreciable difference in the observed currents from the ADCP deployment the records from 25 August to 30 September 2015 were examined. Figure 1-21 reveals a general diurnal pattern with a pronounced peak at 7:00 on 4 September 2015.

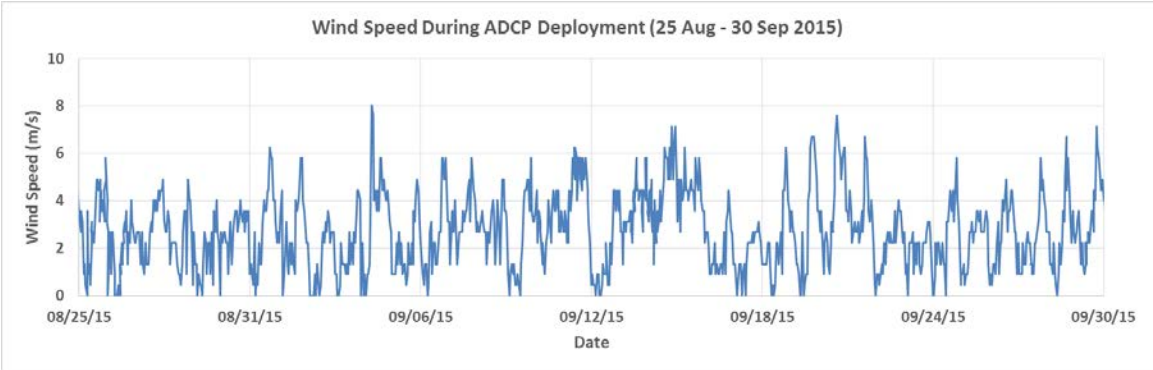

Figure 1-21. Time series of wind speed during ADCP deployment (25 August – 30 September 2015).

A time series of wind speed for the 4 September 2015 event (Figure 1-22) showed that the wind rose quickly from about 1 m/s (2.2 mph) at 4:00 to 8 m/s (18 mph) by 7:00 and then began to drop to about 4 m/s (9 mph) from 9:00 through 13:00. The associated wind direction time series (Figure 1-23) showed that the wind had shifted to 300° by 3:00 and kept moving clockwise to 20° by 6:00 and oscillated between 60° and 10° until 13:00. The largest (8 m/s [18 mph]) winds came from 50° to 60° thus again outside the longitudinal alignment of Upper Little Bay.

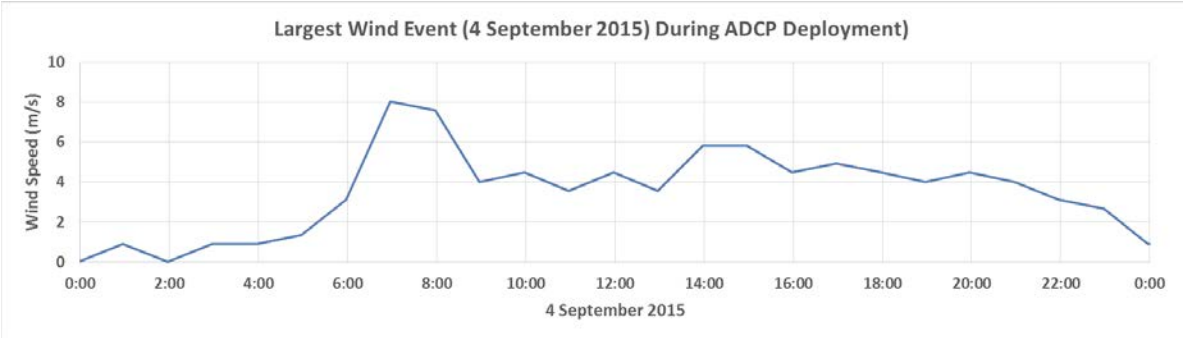

Figure 1-22. Time series of wind speed of largest wind event during ADCP deployment.

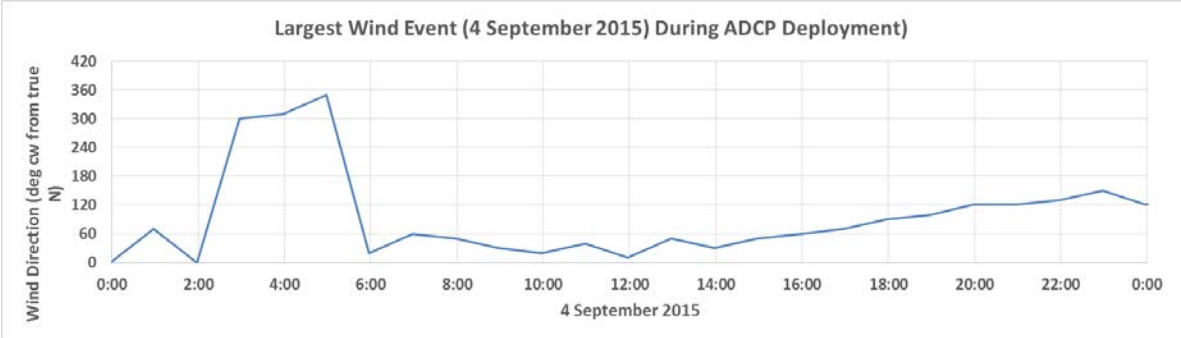

Figure 1-23. Time series of wind direction of largest wind event during ADCP deployment.

To see if the ADCP currents responded to this event Figure 1-24 shows the along-channel currents for the same 4 September 2015 period plus one day on either side for comparison. It does not appear that the velocity structure is different for 4 September from 3 or 5 September.

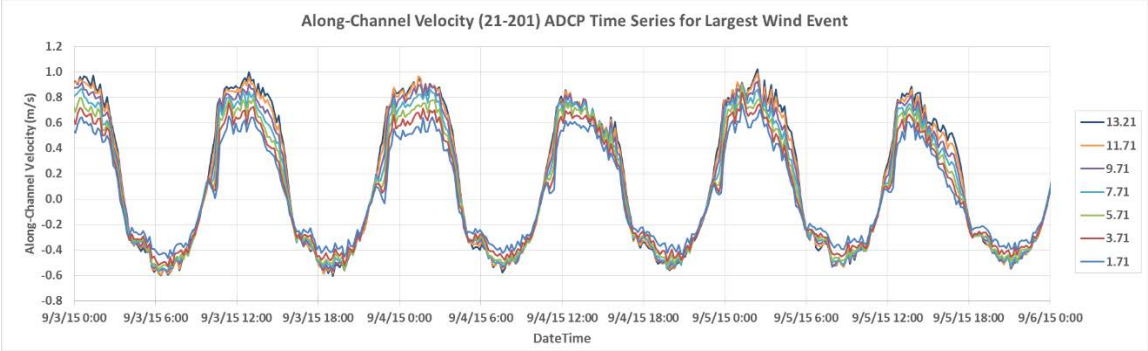

Figure 1-24. Time series of along-channel velocities (m/s) fortide cycles surrounding largest wind event (morning of 4 September 2015) during ADCP deployment. Positive velocity is ebbing and negative velocity is flooding.

2 BELLAMY Hydrodynamic Model

2.1 Model Description

A computer model system developed at Dartmouth College and previously applied by RPS ASA to the Great Bay Estuarine System (GBES) (McLaughlin et al. 2003) was used in this analysis and was based on the recent work of Swanson et al. (2014). The model system includes a finite element, two-dimensional, vertically averaged, time stepping circulation model. The circulation model, known as BELLAMY, can calculate the time varying surface elevation and currents under the influence of tides, winds and river flow on a model domain discretized by a large number of finite element triangles. Due to the fact that Great Bay is tidally dominated (currents up to 2 m/sec) and much of it consists of narrow channels in which the tidal currents mostly flow in flood and ebb directions, the effect of wind is expected to show only in areas with relatively larger wet surface areas such as Great Bay proper and not Little Bay where the cable burial will occur. The model includes simulation of wetting and drying of tidal flats.

All simulation parameters were set to be consistent with previously published work. The reader is referred to Swanson et al. (2014), Bilgili et al. (2005) and McLaughlin et al. (2003) for more detailed information. Sensitivity analyses previously reported are the basis for some of the values chosen. Some key assumptions and resulting parameter values are summarized as follows:

- The model domain consists of the entire GBES plus a stretch of the coastal Atlantic Ocean extending from Portland, ME, in the north to the tip of Cape Ann, MA, in the south to incorporate the effect of the Gulf of Maine coastal current. The Little Bay region is shown in Figure 1-9 between the Lower Piscataqua River-North to the east and Great Bay to the south.
- Tidal forcing used the constituent set of M2, N2, S2, O1, K1 and Z0 as described in previously published work (Bilgili et al. 2005).
- No wind forcing was applied to be consistent with previous studies, which showed the wind effect is short term and minimal, particularly since the modeling focused on steady state conditions.
- The model includes annually averaged freshwater discharges from the major rivers as constant values (Bilgili et al. 2005). The effect of time varying discharges is not investigated due to the fact that the total freshwater volume entering the estuary is less than 2% of the tidal prism (Reichard and Celikkol, 1978). The yearly averaged discharges from the WWTF outfalls are also incorporated as constants since these are considered as additional fresh water sources (Trowbridge, 2009).
- The internal hydrodynamic model time step was 99.36 seconds with model predicted velocities output on a 30-min interval. The model was run to capture the 15-day spring-neap cycle.

BELLAMY has been tested and calibrated extensively in the Great Bay estuary over the past two decades (Ip et al. 1998; Erturk et al. 2002; McLaughlin et al. 2003; Bilgili et al. 2005). One quantitative statistical measure indicating how well the model reproduces observed currents is “skill”, with 0 indicating no match to data and 1 indicating perfect match with data. McLaughlin et al. (2003) report a mean skill of 0.918 while the Bilgili et al. (2005) work improves this to 0.942 for cross-section averaged current velocity comparisons. Point velocity comparisons also

show good fit (McLaughlin et al. 2003; Bilgili et al. 2005), especially considering the inherent variability in this type of measurements.

2.2 Model Results

As noted above the current velocities to be used to disperse the excess suspended sediment were based on previous hydrodynamic modeling of the Great Bay System. Example current vectors for flood and ebb tides in lower Little Bay are shown in Figure 2-1 and Figure 2-2 respectively. The vectors are scaled and contoured by speed in accordance with the legend displayed in the in the upper left portion of the figures. The line shown across the Bay is a representative approximation of the route of the cables. The strength of the currents is similar

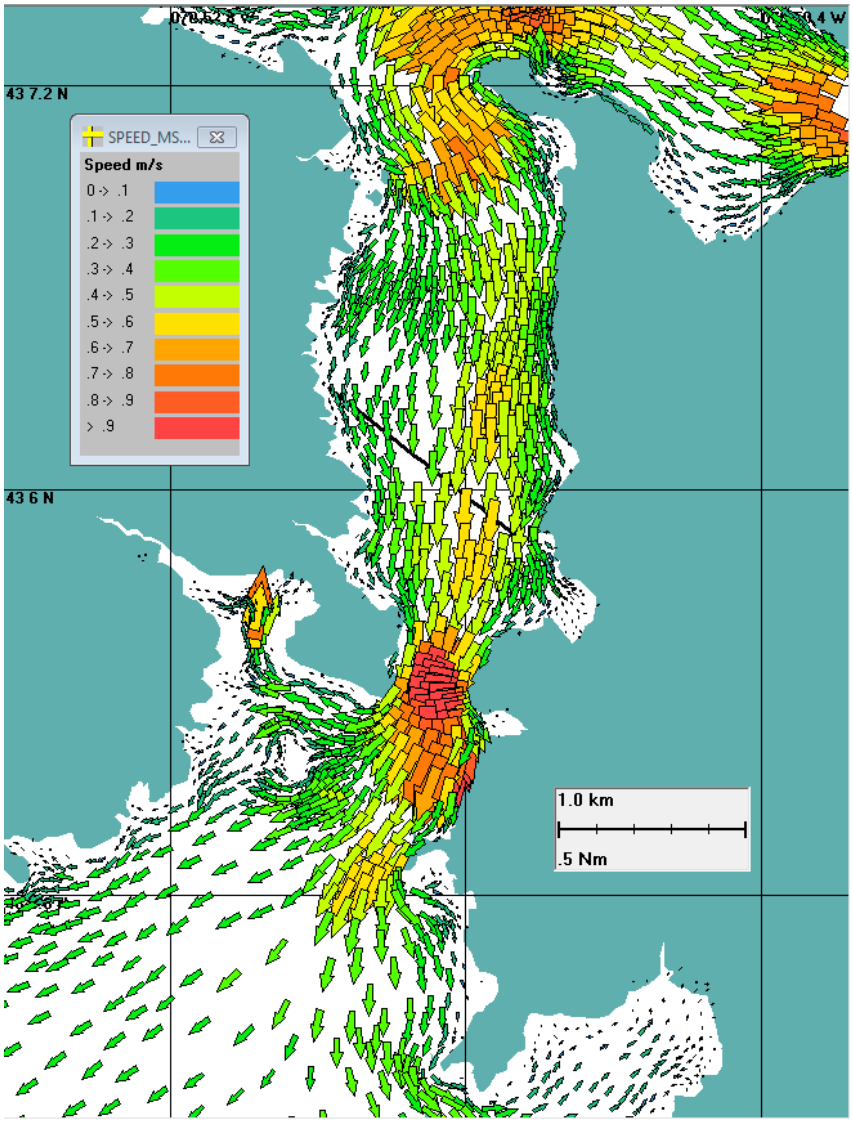

Figure 2-1. Example flood tide currents for lower Little Bay with the solid black line indicating the approximate cable route.

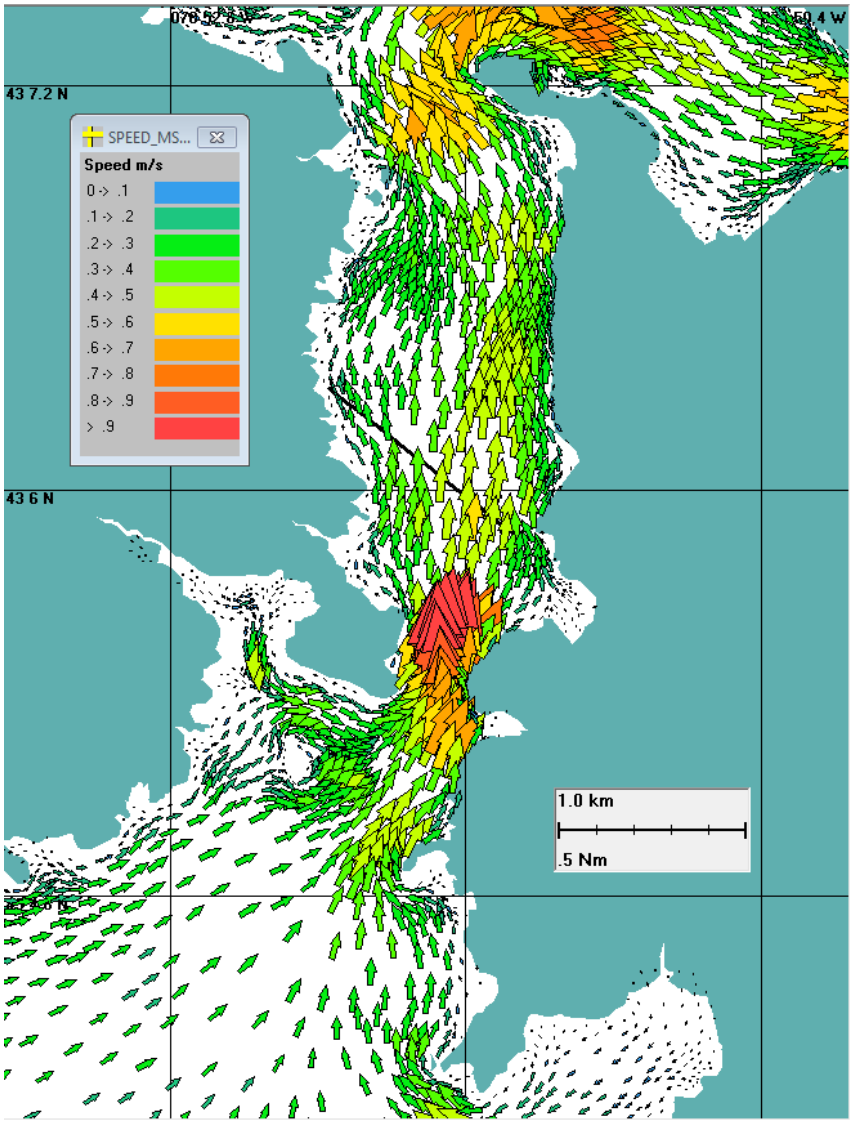

Figure 2-2. Example ebb tide currents for lower Little Bay with the solid black line indicating the approximate cable route.

in both flood and ebb directions. Peak speeds in the shallow areas located on both sides of the Bay peak at speed less than 0.3 m/s (0.58 kt) and the peak speeds in the deeper areas to between 0.4-0.6 m/s (0.78 1.16 kt).

3 SSFATE Sediment Dispersion Model

3.1 Model Description

The SSFATE (Suspended Sediment FATE) model was utilized to predict the excess suspended sediment concentration and the dispersion of suspended sediment resulting from jet plowing and diver hand jetting activities. SSFATE addresses the short-term movement of sediments where sediment is introduced into the water column and predicts the path and fate of the sediment particles using the local currents. Excess water column concentration is defined as the sediment concentration generated by the jet plow or diver activities above ambient suspended sediment concentration. In addition, SSFATE was used to calculate the resulting deposition thickness of resuspended sediments that have resettled back on the bottom.

SSFATE was originally jointly developed by ASA (now RPS ASA) and the U.S. Army Corps of Engineers (USACE) Environmental Research and Development Center (ERDC) to simulate the sediment suspension and deposition from dredging operations. It has been documented in a series of USACE Dredging Operations and Environmental Research (DOER) Program technical notes (Johnson et al. 2000 and Swanson et al. 2000); at a previous World Dredging Conference (Anderson et al. 2001) and a series of Western Dredging Association Conferences (Swanson et al., 2004; Swanson and Isaji, 2006). Since then SSFATE has been extended to include the simulation of dredged material disposal including barge overflows as well as cable and pipeline burial operations using water jet plows (Swanson et al., 2006; Mendelsohn et al., 2012), diver activities and mechanical plows. Many RPS ASA projects have been performed that demonstrate successful application to dredging, cable and pipeline installation. A list of cable or pipeline burial studies is provided in **Error! Reference source not found.**.

Table 3-1. List of similar RPS ASA project experience.

Project Year	Projects Description	Client
2014	Salem Lateral Pipeline Submarine Connection	TRC
2013	Sediment dispersion modeling for pipeline installation, Safaniya, Saudi Arabia	King Fahd University of Petroleum and Minerals
2013	Sediment Dispersion Modeling for Pipeline Installation in Manifa Bay, Saudi Arabia	Saudi Aramco, (Through King Fahd University of Petroleum and Minerals (KFUPM))
2013	Modeling of Sediment Dispersion during Installation of the Proposed West Point Transmission Project Power Cable	West Point Partners, (Through the ESS Group, Waltham, MA)
2011	Sediment Dispersion Analysis of Cable Installation for Deepwater Wind Block Island Wind Farm and Transmission System, RI	Tetra Tech, Boston, MA
2011	Preparation of a Third-Party Environmental Impact Statement for the Aguirre GasPort Project	FERC, (Through Natural Resource Group (NRG), Providence, RI)
2011	Simulations of Sediment Dispersion from Hydraulic Jetting Cable Burial, Lower Chesapeake Bay	Gamesa Offshore Wind Energy, (Through ESS Group, Inc.)
2010	Sediment Dispersion Modeling Of Dredging For Pipeline Installation Across Hudson River	Spectra Energy, (Through TRC Environmental Corp.)
2010	Modeling of Sediment Dispersion during Installation of the Proposed Port Dolphin Gas Pipeline	CSA International
2010	Sediment Dispersion Analysis for the Mid Atlantic Power Pathway: Chesapeake Bay Crossing – Jet Plow Embedment	ESS Group, Inc.

Project Year	Projects Description	Client
2008	Sediment Dispersion Modeling from Electrical Transmission Cable Burial Activities in Eastern Lake Ontario	ESS Group, Inc
2007	Sediment Dispersion Modeling for Proposed Pipeline Construction Activities	CSA International
2007	Simulations of Sediment Transport and Deposition from Jet Plow and Excavation Operations for the Hudson Transmission Project	ESS Group, Inc.
2007	Results from Modeling of Sediment Dispersion during Installation of the Proposed Bayonne Energy Center Submarine Cable	ESS Group, Inc.
2005	Computer Simulation of Sediment Transport Effects from Cable Burial Operations at Amityville Cut in Great South Bay	EEA, Inc
2005	Sediment Transport Study for Northeast Gateway Pipeline Lateral Project in Massachusetts Bay	Project Consulting Services, Inc
2005	Analysis of Potential Impacts from a Proposed Nantucket Sound Wind Farm, Nantucket Sound, MA	Cape Wind Energy, LLC, Boston, MA
2005	Comparison of HDD And Hydraulic Jetting Cable Installation At Northport Landfall	Long Island Power Authority, (Through ESS Group, Inc.)
2003	Model Simulations of Sediment Deposition from Cable Burial Operations in Lewis and Popponesset Bays, MA	ESS Group, Inc
2003	Model Simulations of Sediment Deposition from Cable Burial Operations in New Haven Harbor	ESS Group, Inc
2001	Simulations of Sediment Transport and Deposition from Jet Plow and Excavation Operations for the Cross Hudson Project	ESS Group, Inc
2001	Simulations of Sediment Deposition from Jet Plow Operations in New Haven Harbor	ESS Group, Inc

The SSFATE model has been previously validated with two examples presented. SSFATE was applied to a proposed new dredging project, the Craney Island Expansion, located in the Elizabeth River in Chesapeake Bay in Portsmouth, VA (CHT, 2008). Craney Island had been used for some time as a site for placement of dredged materials and is operated by the U.S. Army Corps of Engineers. Before the Corps proceeded with the project they wanted to know that SSFATE could accurately predict suspended sediment plumes that have previously been observed at the site. An extensive field program was conducted by the Virginia Institute of Marine Sciences to collect suspended sediment data from a maintenance cutterhead dredging operation in September 1978 over three days. The model was calibrated to one day of data and validated to the other two days. Although monitoring suspended sediment plumes is difficult, the comparison of SSFATE predictions to observation agreed well, particularly the vertical structure of the plume.

Another SSFATE validation was conducted in the Lower New York Harbor during installation of an electrical cable from Bayonne, NJ to Brooklyn, NY (Whitney and Herz, 2013). The project was to install a 345 kV cable 4.6 m (15 ft) below the seabed using jet plow technology in 2011. The modeling components included pre-construction predictive modeling, and post construction statistical comparison to installation monitoring field data. Based on initial pre-construction field data the model was run to provide realistic predictions of water column suspended sediment concentrations and seabed deposition. Model results were used to evaluate effects on water quality and marine organisms for use in the permit application and to negotiate permit

conditions. Results were also used to help design the installation monitoring program that included transects of acoustic backscatter data to locate the plume as well as conductivity-temperature-depth-optical backscatter data to draw real time information on the suspended sediment concentrations. Water samples for subsequent TSS analysis were also acquired. RPS ASA (then ASA) performed a statistical analysis comparing the observed plume to the model predictions. This analysis showed the model to successfully capture the main observed features even though some pre-construction assumptions on input data were different from actual installation conditions. The model typically predicted somewhat more conservative TSS concentrations than actual but that the model proved successful predicting cable burial projects using jet plow technology.

The SSFATE modeling system computes suspended sediment distributions and deposition patterns resulting from various seabed activities. The suspended sediment concentrations are computed in three dimensions (the water column) while the depositional patterns are computed in two dimensions (the seabed). The model contains the following features:

- Ambient currents can be imported from a variety of numerical hydrodynamic models;
- The procedure, which is a standard numerical approach, that mimics the mixing of sediment within the water column due to turbulence;
- Simulates suspended sediment source strength and vertical distribution from mechanical (e.g., clamshell, long arm excavator) or hydraulic (e.g., cutterhead, hopper) dredges, and water jet plows, divers and mechanical plows;
- Uses a continuous but time-varying release of sediments with multiple sediment types (different grain sizes and size distributions) specified along route;
- Calculates average excess sediment concentrations within each grid cell at each time step;
- Grid cell dimensions are specified by the user; typical horizontal resolution is ~25m and typical vertical resolution is between 0.2-0.5m.
- Output consists of excess suspended sediment concentration contours in both horizontal and vertical planes, time series plots of concentrations, and the spatial distribution of sediment deposited on the sea floor.

SSFATE is a particle-based (Lagrangian) model and predicts the transport and dispersion of the suspended material generated by seabed activities. In far field calculations, the mean transport and turbulence associated with ambient currents dominate the distribution of the sediment particles. Particle advection (i.e., transport) is based on the simple relationship that a particle moves linearly with a local velocity, obtained from the hydrodynamic model, for a specified model time step. Particle diffusion (i.e., dispersion) is assumed to follow a simple random walk process frequently used in simulating the dispersion of Lagrangian particles.

The particle model allows the user to predict the transport and dispersion of the different size classes of particles e.g., sands, silts, and clays. The particle-based (Lagrangian) approach is extremely robust and independent of the grid spacing. Thus, the method is not subject to artificial diffusion near sharp concentration gradients and is easily interfaced with all types of sediment sources including dredging, jet plowing, and backfilling operations.

In addition to transport and dispersion, sediment particles also settle at some rate through the water column to the bottom. Settling of mixtures of particles, some of which may be cohesive in nature, is a complex but predictable process with the different size classes interacting, i.e., the settling of one particle size is not independent of the other sizes. In addition, the clay-sized particles, typically cohesive, undergo enhanced settling due to flocculation. These processes have been implemented in SSFATE using empirically based formulations based on previous USACE studies (Teeter, 1998).

At the end of each time step, the excess suspended sediment concentration of each particle class, as well as the total concentration, is computed on a numerical concentration grid. The horizontal dimensions of all grid cells stays the same, with the total number of cells increasing as the sediment plumes is transported away from the source. The settling velocity of each particle size class is computed along with a deposition probability based on shear stress. Finally, the deposition of sediment from each size class from each bottom cell during the current time step is computed and the calculation cycle begins anew. Deposition is calculated as the mass of sediment particles that accumulate over a unit area (utilizing the concentration grid). The mass flux is subsequently converted to thickness.

Outputs from the model are total excess sediment concentrations for each grid cell and deposition thicknesses for each grid cell that shares a boundary with the bottom of the water body. Concentrations and thicknesses are available for every time step during the period that the model is run.

3.2 Seabed Sediment Characterization

The sediment grain size information was extracted from vibratory samples that were analyzed by sieve and hydrometer by Alpha Analytical Laboratory (Normandeau Associates Inc., 2016 & Normandeau Associates Inc., 2017). These data were acquired after the previous sediment dispersion modeling report was issued in December 2015 (Swanson et al., 2015b). These new data were more appropriate than the estimates extracted from visual descriptions of sediments because the new data were collected along the route centerline and included more sophisticated analyses. The survey consisted of 12 sampling stations shown in Figure 3-1, some of which had multiple depths. If more than one sediment sample was taken from a vibracore, a composite of the size fractions was calculated based on the relative quantities each sample contributed to the whole. SSFATE represents the grain size distribution through five classes or bins as delineated in Table 3-2. The size thresholds that delineate the classes are accompanied by corresponding settling velocity coefficients associated with the size thresholds as defined by Swanson et al. 2007. The bins define the full range of sediment sizes with bias towards capturing smaller sizes. In this sense, they do not have to be consistent with any standard delineation of descriptive classes (e.g. Wentworth), however they generally align and as such are used to describe the classes.

Table 3-3 summarizes the number of samples at each location, and their respective depth range and percent weighting used to calculate the composited characteristics at any sites with more than one sample in the applicable depth range.

Table 3-2. SSFATE Sediment Class Sizes Delineation.

SSFATE Class Description	Low End (µm) (Greater Than)	High End (µm) (Less Than or Equal To)
Clay	0	7
Fine Silt	7	35
Coarse Silt	35	74
Fine Sand	74	130
Coarse Sand	130	No Limit

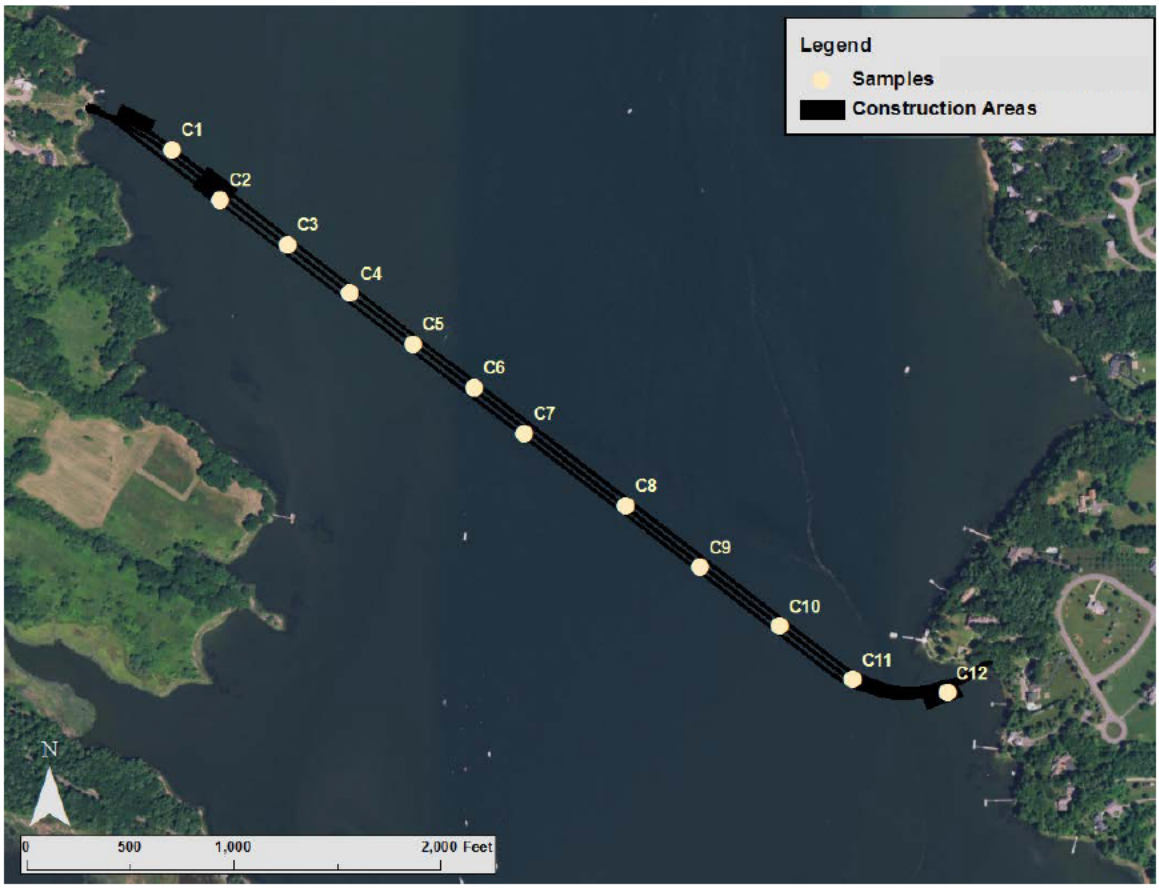

Figure 3-1. Location of vibracore borings across Upper Little Bay along route of center cable crossing (indicated by center of three solid lines in construction area).

Table 3-3. Depths and percent weight (when more than one) from each sample location.

ID	Sample #	Percent Weighted	Depth Range
C1	1	100	0 to 48 in
C2	1	100	0 to 48 in
C3	1	100	0 to 48 in
C4	1	100	0 to 48 in
C5	1	100	0 to 48 in
C6	1	80	0 to 48 in
C6	2	20	48 to 61 in
C7	1	100	48 to 54 in
C8	1	100	0 to 48 in
C9	1	100	0 to 48 in
C10	1	100	0 to 48 in
C11	1	80	0 to 48 in
C11	2	20	48 to 89 in
C12	1	100	0 to 48 in

As presented in Section 1 of this report the new laboratory analysis included a measure of the moisture within the sample. Based on the sample moisture, the percent solids was calculated for each sample (Table 3-5). The water content is used to determine the percent solids in a sample. The greater the water content, the lower the percent solids. The formulas for water content (w) and the associated conversion to percent solids (PS) used in this study are shown below.

$$w = \frac{M_w}{M_s}$$

Where w is water content, M_w is the mass of water and M_s is the dry mass of sediment.

$$PS = \frac{100}{\left(SG_W + SG_S * \frac{w}{100}\right)}$$

Where PS is percent solids, SG_w is the specific gravity of water, SG_s is the specific gravity of sediment and *w* is water content.

It was realized through further investigation into the lab data sheets that the moisture value presented was defined by a different laboratory method and had a different meaning than presented above. The lab general chemistry data presented both a moisture value along with a total solids value; these values reflected the mass of the water and dry sediment relative to the

total mass respectively. This led to a slight over estimate of the percent solids by volume. A comparison of what was assumed and what the actual value should be is provided in Table 3-4; it can be seen from this table that the values used had approximately 10% more assumed mass. This overestimate provides a degree of conservatism in the modeling with more mass introduced to the water column than expected.

Table 3-4. Summary of east diver burial route distance modeled in previous and present study.

Percent Solids		
ID	**Value Used**	**Actual Value**
C1	47.7	34.9
C2	49.2	37.2
C3	50.6	39.2
C4	51.8	41.1
C5	54.3	44.5
C6	53.4	42.6
C7	56.5	47.9
C8	56.0	47.2
C9	67.3	62.8
C10	64.1	58.5
C11	54.3	44.8
C12	60.5	53.6

Table 3-5 and Figure 3-2 show the grain size as defined by five SSFATE classes. The percentage in each bin was determined from the sieve and hydrometer analysis performed by Alpha Analytical. Sediment grain size was generally similar over much of the route, but predominantly consisted of coarse silt (samples C1 through C7), predominately coarse sand (samples C8, C9, and C10, and samples C11 and C12 have roughly equal components of coarse sand and coarse silt. All samples have less than ~20% mass within the two smaller diameter classes (clay and fine silt). In general, the sediments with higher fines fractions will tend to generate larger suspended sediment plumes while those with higher sand fractions smaller plumes. The percent solids assumed in the modeling ranged from 48-67% with the higher percent solids near the deeper portion of the channel that has predominantly coarse sand.

Table 3-5. Sediment characteristics for vibracore stations (composited over vertical).

Specific gravity for all samples was 2.65.

ID	Percent Coarse Sand	Percent Fine Sand	Percent Coarse Silt	Percent Fine Silt	Percent Clay	Moisture (%)	Percent Solids
C1	27.99	1.91	49.52	13.33	7.25	41.30	47.7
C2	45.91	2.29	44.66	6.42	0.72	38.90	49.2
C3	35.02	3.88	47.53	8.58	4.99	36.90	50.6
C4	26.47	5.63	50.62	11.58	5.70	35.10	51.8

ID	Percent Coarse Sand	Percent Fine Sand	Percent Coarse Silt	Percent Fine Silt	Percent Clay	Moisture (%)	Percent Solids
C5	35.69	10.31	43.20	7.85	2.95	31.70	54.3
C6	35.99	4.89	48.05	6.53	4.55	32.98	53.4
C7	32.93	13.17	40.28	7.02	6.60	29.10	56.5
C8	72.81	9.29	16.09	0.99	0.81	29.70	56,0
C9	67.18	1.62	21.01	5.36	4.82	18.30	67.3
C10	68.20	25.10	5.78	0.59	0.33	21.10	64.1
C11	41.31	10.05	36.51	8.09	4.04	31.76	54.3
C12	43.39	12.31	35.90	5.10	3.30	24.60	60.5

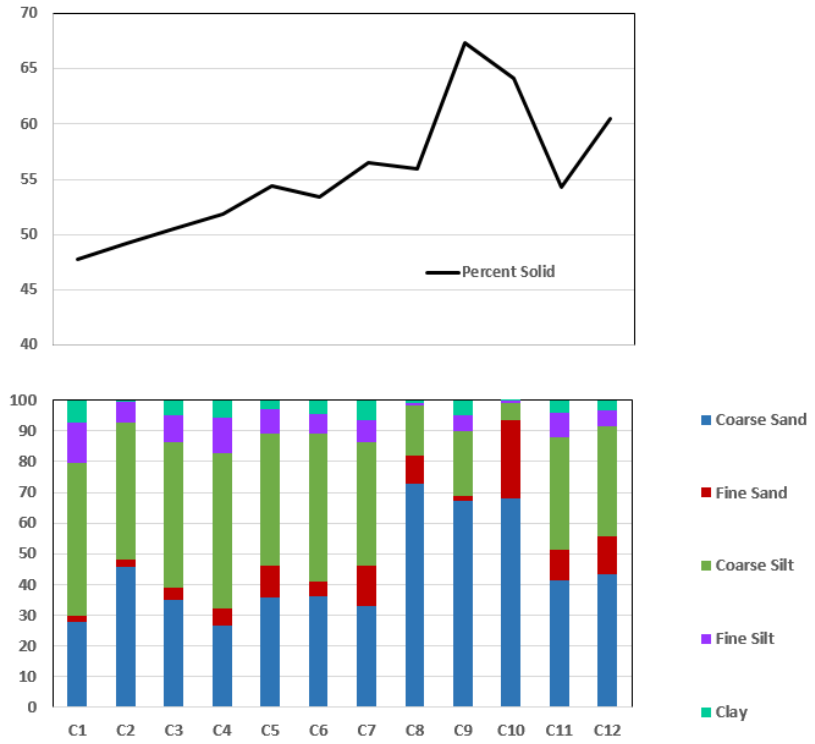

Figure 3-2. Percent solids (top) and histogram (bottom) of grain size distributions (in percent) for vibracore stations along route.

3.3 Model Input Parameters

Details of the model input parameters for the base case and sensitivity runs are provided in the following sections.

3.3.1 Jet Plow Burial – Route

The planned route across Upper Little Bay is shown in Figure 3-3; the extent of the jet plow installation is outlined by the red box. The lengths of all the three cable routes were defined to be 559 m (1,835 ft) for the shallow burial and 741 m (2,431 ft) for the deeper burial for a total of 1,300 m (4,265 ft). The associated depth of burial is shown in Figure 3-4 (shown only for the center route). Along the jet plow (parallel lines) portion of the crossing the three bundled cables are separated by 9.4 m (30 ft).

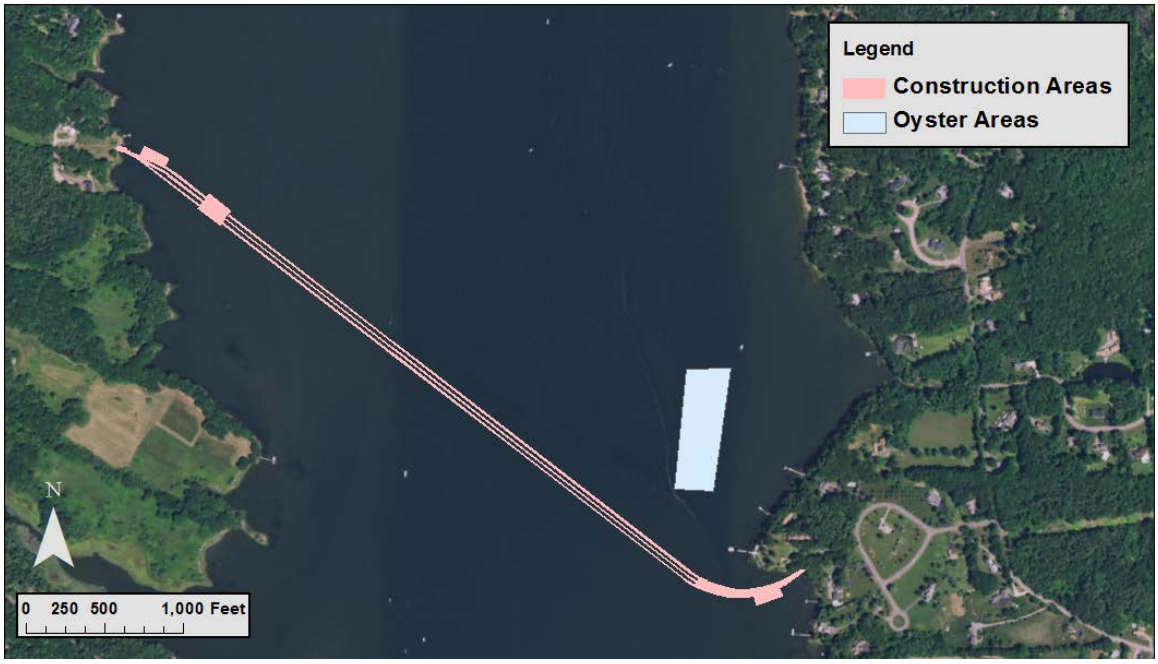

Figure 3-3. Proposed cable route (LS Cable & System, 2017).

Figure 3-4. Proposed minimum burial depths.

3.3.2 Jet Plow Burial – Advance Rate

The jet plow rate of advance was recommended by the cable installer, Durocher. They noted that during operations the rate of advance can be variable (from 36.6 – 402.3 m/hr [120 - 1320 ft/hr]) for short periods but recommended an average rate of 183 m/hr (600 ft/hr), particularly in the shallows where the plow would be advanced using a skeeter barge. It was decided collectively that for the sensitivity runs an average advance rate of 91.4 m/hr (300 ft/hr) and 274.3 m/hr (900 ft/hr) would capture the range of advance rates. Like the previous modeling the central cable route among the three cable bundles crossing Upper Little Bay was chosen for modeling since the cables were to be separated by only 9.4 m (30 ft). Table 3-6 provides a summary of the advance rates and associated activity duration and Figure 3-5 illustrates how the exposure to tides and currents (speed and direction) changes depending on advance rate. For the present start time (high tide) both the base and fast rate runs will be exposed to primarily ebbing (northward) currents (North/South velocity component is greater than zero) while using the slow advance rate the activity will take place in both ebbing and flooding (southward) currents (velocities move from positive to negative back to positive).

Table 3-6. Summary of previous (for reference) and present advance rates for the base case (average) and sensitivity runs (slower and faster advance).

Activity	Activity Advance Rate			Length of Route	Duration to Complete per Cable	Duration to Complete per Cable
	ft/min	ft/hr	m/hr	m	hr	Days
Previous (for Reference)– Jet Advance Rate	5.47	328	100	1300	13.0	0.54
Present – Typical/Average Jet Advance Rate (Base)	10	600	182.9	1300	7.1	0.30
Present – Low Jet Advance Rate (Sensitivity)	5	300	91.4	1300	14.2	0.59
Present – High Jet Advance Rate (Sensitivity)	15	900	274.3	1300	4.7	0.20

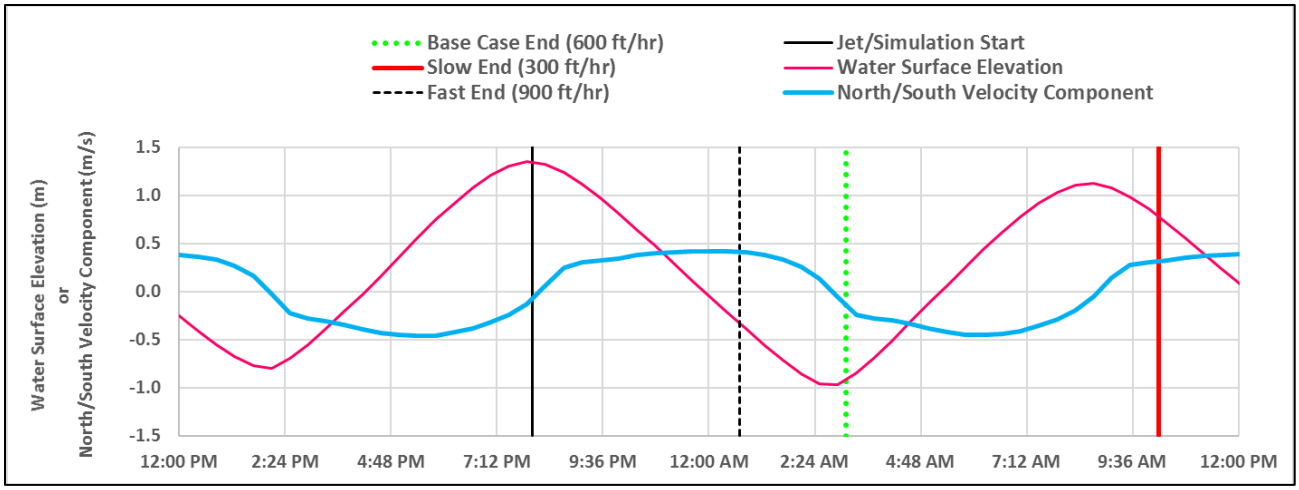

Figure 3-5. Illustration of timing of different advance rates with the tides and current velocity.

3.3.3 Jet Plow Burial – Cross Sectional Area

One of the inputs required to define the mass of sediment introduced in the water column is the cross-sectional area that is to be fluidized. The cables are to be buried by jet plowing to minimum depths of 1.07 m (3.5 ft) deep in the shallows adjacent to the western coast and 1.52 m (5 ft) in the center and east sections. For ease of discussion, this report refers to the jet plow disturbance as a trench although, while the jet plow will be occupying a three-dimensional space, the "trench" is not open but contains sediment that has been injected with jets of water. The total depth of the trench included the minimum burial depth plus the cable diameter of 0.15 m (6 in) and an overage of 0.20 m (8 in) totaling 1.42 m (56 in) for the western section and 1.88 m (74 in) for the central and eastern sections. The vertical walled trench width was defined as 0.32 m (12.75 in) resulting in a trench cross sectional area of 0.46 m^2 (5.0 ft^2) in the shallow western portion and an area of 0.66 m^2 (7.1 ft^2) in the deeper central and eastern portions. Table 3-7 summarizes the trench dimensions including the cross-sectional area that is input to the model.

Table 3-7. Summary of trench dimensions and SSFATE input parameters for the jet plow portion of the cable burial simulation.

Parameter	Shallow Jet Plow Burial	Deep Jet Plow Burial
Cable burial depth	1.07 m (3.50 ft)	1.52 m (5.00 ft)
Cable diameter	0.15 m (0.5 ft)	0.15 m (0.5 ft)
Overage amount	0.2 m (0.67 ft)	0.2 m (0.67 ft)
Total trench depth Burial + cable diameter + overage	**1.42 m (4.67 ft)**	**1.88 m (6.16 ft)**
Trench width	0.32 m (12.75 in)	0.32 m (12.75 in)
Trench cross sectional area	0.46 m^2 (4.96 ft^2)	0.66 m^2 (7.05 ft^2)

3.3.4 Jet Plow Burial – Loss Rate

The base case simulations assumed 25% of the material in the trench would be resuspended into the water column by the jetting activity; this is consistent with the previous modeling study. This is a conservative estimate consistent with previous studies that found a range of 10 to 35% (Foreman, 2002). Two sensitivity runs were simulated to assess the sensitivity or the results to the loss rate assumption. A summary of the loss rates used in the base case and sensitivity runs are presented in Table 3-9; this table also includes the previous value for reference.

Table 3-8. Summary of loss rates used in previous and present modeling including sensitivity runs.

SSFATE Class Description	Loss Rate (%)
Previous (Reference)	25
Present - Base	25
Present – Low (Sensitivity)	10
Present – High (Sensitivity)	35

3.3.5 Jet Plow Burial – Mass Initialization in the Vertical Dimension

The model input also requires a specification of the initialization of sediment in the water column through specifying the percent mass released at various depths in the water column. This initialization represents the location and mass of sediment introduced in to the water column from the proposed construction methods. The vertical distribution is defined using five bins which vary in depth and percent of the total mass. Table 3-9 summarizes the profile of mass initialization to the water column for both the shallow (< 3 m [10 ft] water depth) and deep (> 3 m [10 ft]) portions of the route.

Table 3-9. Initial vertical distribution of sediment for jet plow.

Cumulative % of mass released	Individual % of mass released	Height above bottom m (ft)	Height above bottom m (ft)
29	29	0.17 (0.56)	0.33 (1.08)
57	28	0.33 (1.08)	0.66 (2.17)
85	28	0.50 (1.64)	1.00 (3.28)
95	10	1.00 (3.28)	2.00 (6.56)
100	5	1.50 (4.92)	3.00 (9.84)

3.3.6 Jet Plow Burial – Tide

The model run was started on the west side of Upper Little Bay during a spring tide at slack high water which is the beginning of the ebb tide. It was determined that this was the most favorable stage of the tide for operations in the shallow water areas. A sensitivity to tidal amplitude was also performed by starting the simulation at the slack high water of a neap tide. Table 3-10 summarizes the simulation start and Figure 3-6 illustrates the spring and neap start

times overlaid on an example month-long time series of water surface elevation and current speed from the Bellamy model. It should be noted that the sensitivity runs for advance rate (slower and faster) also inherently include variation of the tidal currents to which the sediments are subject.

Table 3-10. Summary of simulation start times.

Simulation	Timing Shallow Jet Plow Burial	Timing Deep Jet Plow Burial
Base Case	Start at high slack during a *spring* tide	Continue after shallow portion
Sensitivity	Start at high slack during a *neap* tide	Continue after shallow portion

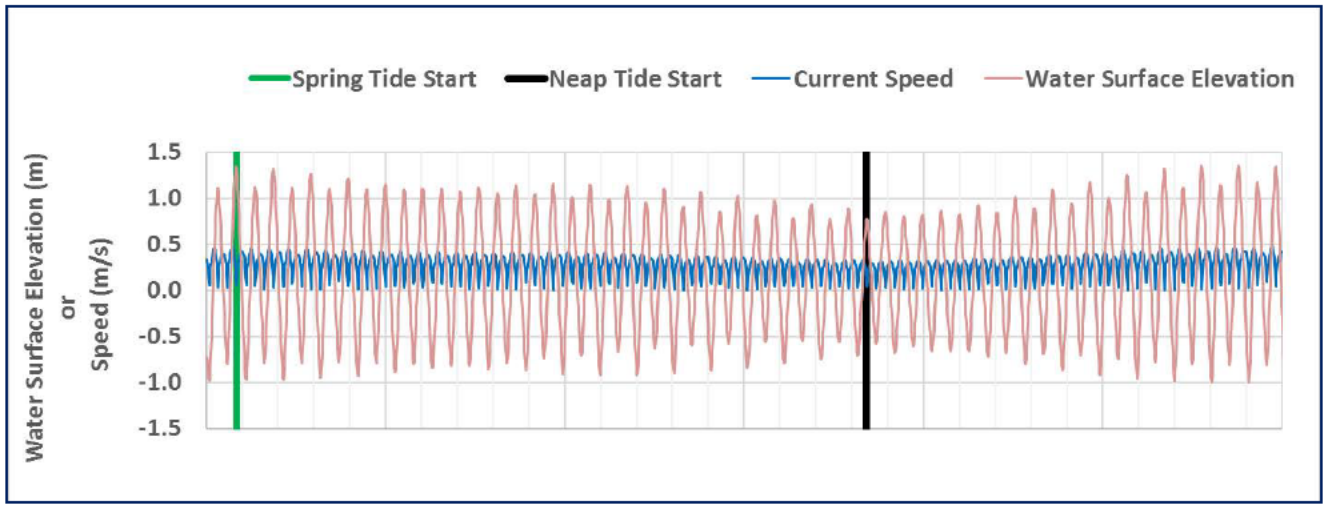

Figure 3-6. Illustration of jet simulation start timing relative to spring and neap tide amplitude and current speed based on Bellamy model output.

3.3.7 Jet Plow Burial – Continued Resuspension

Prior to the construction activity the sediments in the seabed are primarily consolidated, which serves to reduce the likelihood of resuspension, particularly for cohesive sediments (clays and silts). When artificial processes like construction disturb sediments, they are released to the water column, transported and eventually settle out to the bottom. These sediments can continue to resuspend when the bottom stress exceeds the critical shear stress (e.g. high current velocities) during subsequent tidal cycles. Further, freshly deposited sediments may be more easily resuspended due to the lack of consolidation. The SSFATE model has an option to simulate continued resuspension based on the method detailed in Swanson et al. 2007. This option is useful for identifying whether the potential for resuspension exists and further identifying the areas that will likely have some level of resuspension.

The SSFATE model predictions for resuspended concentrations are highly conservative, however, as the model does not include details about whether the particles were in a floc when they settled/deposited, does not include a cohesive sediment model (electromagnetic attraction of clays), does not consider the order in which the particles were deposited (i.e. if clays get covered by coarse sands), and does not include any interaction with the ambient suspended sediments or bottom sediments. Since the height of resuspension above the bottom is a

function of the sediment type and the bottom stress, for the depths and speeds associated with this application, the it was typically within tens of centimeters above the bottom; therefore, the concentrations of resuspended sediments were located only at the bottom of the water column and most of the water column remained clear. To demonstrate the potential for resuspension a sensitivity simulation was run with this option activated.

3.3.8 Jet Plow Burial – Summary of Base and Sensitivity & Additional Simulations

A series of sensitivity runs were simulated where all parameters except one were kept the same as the Base Case (most expected values). A summary of the sensitivity runs and the values of the varied parameters is provided in Table 3-11.

Table 3-11. Summary of sensitivity and additional simulations.

ID	Parameter	Advance Rate m/hr (ft/hr)	Loss Rate (%)	Tidal Range	Continued Resuspension
1	Base Case	183 (600)	25	Spring	Off
2	Sensitivity to Advance Rate - Slow	91 (300)	25	Spring	Off
3	Sensitivity to Advance Rate -Fast	274 (900)	25	Spring	Off
4	Sensitivity to Loss Rate -Low	183 (600)	10	Spring	Off
5	Sensitivity to Loss Rate - High	183 (600)	35	Spring	Off
6	Sensitivity to Tide	183 (600)	25	Neap	Off
7	Additional Run to Investigate Continued Resuspension	183 (600)	25	Spring	On

3.3.9 Diver Hand Jet Burial

The western and eastern ends connecting the jet plowing portions to the land are represented by non-parallel routes ending at the shore which use divers to hand jet bury the cables; the separation of these lines was initially 9.1 m (30 ft) however this distance decreases as the cable routes approach the shore (Figures 3.3 and 3.4). The diver installation portion of the route was significantly smaller than the jet plow (~ 16% of jet plow route). The model required description of the advance rate, cross section, loss rate, initial vertical distribution, and start times for the diver hand jet burial; these parameters are described below.

The diver rate of advance was much slower than the jet plow at 2.3 m/hr (7.5 ft/hr). The central cable route among the three cable bundles crossing Upper Little Bay was chosen for modeling since the cables are to be initially separated by a maximum of 9.1 m (30 ft).

The cables are to be buried by divers using hand jets to create trenches with a minimum depth of 1.07 m (42 in) deep in the shallows on both the western and eastern portions of Upper Little Bay. The model simulation installation route lengths are to be 91.4 m (300 ft) in the western portion and 165 m (541 ft) in the eastern portion. The diver burial will utilize silt curtains for the entire western route and for 94.7m (311 ft) of the eastern route, leaving 70 m (230 ft) of the

diver burial adjacent to the jet plowed route without silt curtains. See Figure 1-2 for delineation of silt curtain areas on the western diver route.

The total depth of the trench included the minimum burial depth plus the cable diameter of 0.15 m (6 in) which equals 1.22 m (48 in). Based on installation specification the trench width was defined as 1.22 m (48 in) resulting in a trench cross sectional area of 1.49 m^2 (16.0 ft^2).

It was also assumed, based on past experience, that 50% of the material in the trench would be resuspended into the water column for diver hand jetting activities outside the silt curtain. This rate is twice the rate for jet plowing because the technology used, diver controlled high pressure water hoses, focuses the pressure at the surface of the substrate rather than from within. The vertical profile defining the initial vertical distribution of the sediment mass for diver hand jet burial is summarized in Table 3-12.

Table 3-12. Initial vertical distribution of sediment for diver hand jet burial.

Cumulative % of release	Individual % of release	Height above bottom m (ft)
29	29	0.11 (0.36)
57	28	0.22 (0.72)
85	28	0.33 (1.08)
95	10	0.67 (2.20)
100	5	1.00 (3.28)

The model run was started two hours before high slack water and continued for four hours due to diver requirements of working in as deep water as possible. Each model run was simulated using the same spring tide, as that would provide the greatest potential for advection, but only one four-hour activity was assumed per day. The individual daily runs were then combined to develop the footprint for the diver activity in total.

Silt curtains can greatly reduce the magnitude and extent of the water column areas affected. The US Army Corps of Engineers refers to reductions in loss rates of 80 to 90% when silt curtains are correctly employed (Francingues and Palermo, 2005). A recent model application by the USACE (Lackey, et. al., 2012) assumed reductions of 90 to 100% in loss rates due to the use of silt curtains to protect of coral reefs in Guam. Based on these studies the loss rate used in the modeling of regions protected by silt curtains was assumed to be 10% of the activity loss rate of 50% which is therefore 5% of the total volume. The area inside the silt curtains adjacent to the cable routes will, of course, see a local increase in concentrations. Silt curtains will be used along the entire western diver burial route and on the eastern end of the eastern diver burial route.

Table 3-13 summarizes the trench dimensions and SSFATE input parameters used in the diver hand jetting portion of the simulation. The east area is divided into two portions: with and without the use of silt curtains

Table 3-13. Summary of trench dimensions and SSFATE input parameters for the diver jetting portion of the single cable burial simulation.

Parameter	West Diver Burial (with silt curtains)	East Diver Burial (with silt curtains)	East Diver Burial (w/o silt curtains)
Cable burial depth	1.07 m 3.50 ft	1.07 m 3.50 ft	1.07 m 3.50 ft
Cable diameter	0.15 m 0.5 ft	0.15 m 0.5 ft	0.15 m 0.5 ft
Total trench depth **Burial plus cable diameter**	**1.22 m** **4.00 ft**	**1.22 m** **4.00 ft**	**1.22 m** **4.00 ft**
Trench width	1.22 m 4.00 ft	1.22 m 4.00 ft	1.22 m 4.00 ft
Trench cross sectional area	1.49 m^2 16.0 ft^2	1.49 m^2 16.0 ft^2	1.49 m^2 16.0 ft^2
Route distance	91.4 m 300 ft	94.8 m 311 ft	70.1 m 230 ft
Trench Surface Area	111.5 m^2 1200 ft^2	115.6 m^2 1244 ft^2	85.47 m^2 920 ft^2
Advance rate (mean)	2.29 m/hr 7.5 ft/hr	2.29 m/hr 7.5 ft/hr	2.29 m/hr 7.5 ft/hr
Duration (mean)	4 hr/day for 10 days	4 hr/day for 10.3 days	4 hr/day for 7.7 days
Timing	Start 2 hrs before high slack	Start 2 hrs before high slack	Start 2 hrs before high slack
Final resuspension fraction outside silt curtain if used	5% of trench volume	5% of trench volume	50% of trench volume

3.4 Model Results

3.4.1 Jet Plow Results – Base Case

3.4.1.1 Water Column Concentrations

Under the base case conditions the total duration of the cable burial by jet plowing was 7.1 hours based on an average advance rate of 183 m/hr (600 ft/hr) and a route distance of 1,300 m (4,266 ft). The simulation was continued after jet plowing was completed (7 hours and 6 minutes after start) to ensure that all residual concentrations had dissipated; concentrations at or above 10 mg/L ceased to persist after 7 hours and 45 minutes.

To best display the resulting water column concentration a series of figures was generated for each hour of the crossing resulting in seven "snapshots" of the submerged plume at that time. Figure 3-7 and Figure 3-8 show the plan and vertical section views of the predicted instantaneous maximum excess SS concentration in 1-hr increments after the start of jet plowing at high slack tide. Figure 3-9 shows the last time step to have water column concentrations present; this occurs at 7 hours and 55 minutes after the start. These figures show the maximum concentration present from within all the vertical layers, which is invariably the

lowest layer adjacent to the bottom. The submerged SS concentration plume remained close to the route and extended slightly north of the cable route for hours 1 through 7 indicating an ebb tide condition and began to extend south of the route as operations were ending and after they ceased as shown at 7 hours and 55 minutes (flood tide condition). The water column concentration contours shown, which are defined by a single concentration level, surround an enclosed area where concentrations are at or above the specified concentration, i.e., the area is cumulative. Thus, the areas with higher concentrations must be smaller than areas with lower concentrations since those areas are enclosed within the lower concentration contour.

The contours showed a decreasing concentration away from the immediate location of the jet plow on the cable route as material diluted and settled out. The colored contours can be identified from the legend in the central left side of each panel showing concentrations from 10 mg/L and higher. A larger SS concentration legend is shown in the upper left panel of Figure 3-7. A vertical section view defined along the cable route looking north is inserted at the bottom of each hourly panel. The insert showed that the highest concentrations occurred just above the jet plow near the bottom with reduced concentrations extending somewhat up into the water column above the plow. In the shallows, suspended sediments from the jet plow activity were likely to reach nearly to the water surface. In the channel, excess suspended sediments were restricted to the lower half of the water column.

The plume orientation aligns with the current direction. At the onset when the currents are low (high slack water) at the western shore where activity starts, the plume is relatively wider however the shape of the plume becomes narrower and elongated with the faster currents.

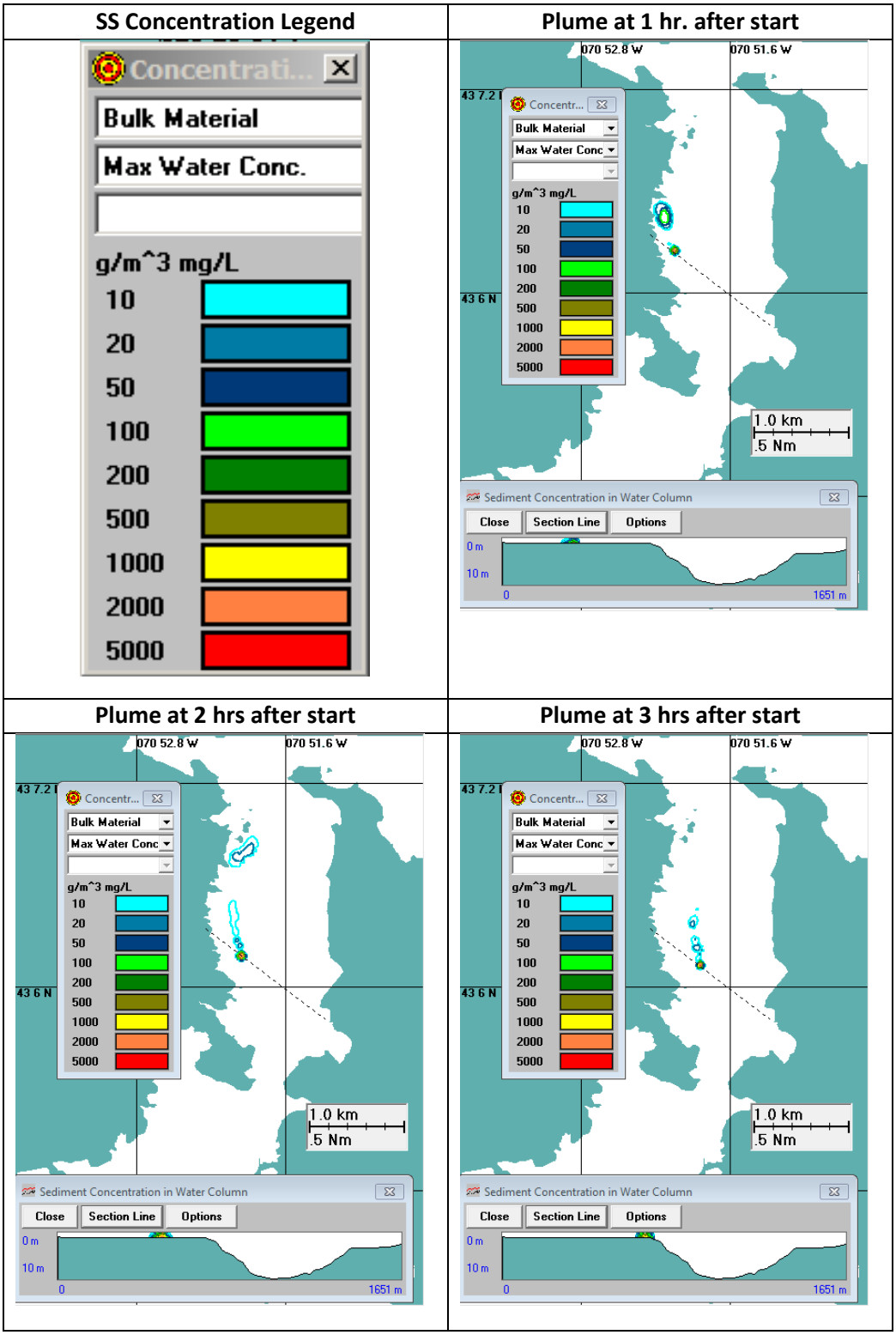

Figure 3-7. Plan view of instantaneous excess SS concentrations at 1 through 3 hrs after start of jet plowing for base case with spring tide. Vertical section view at bottom of each panel.

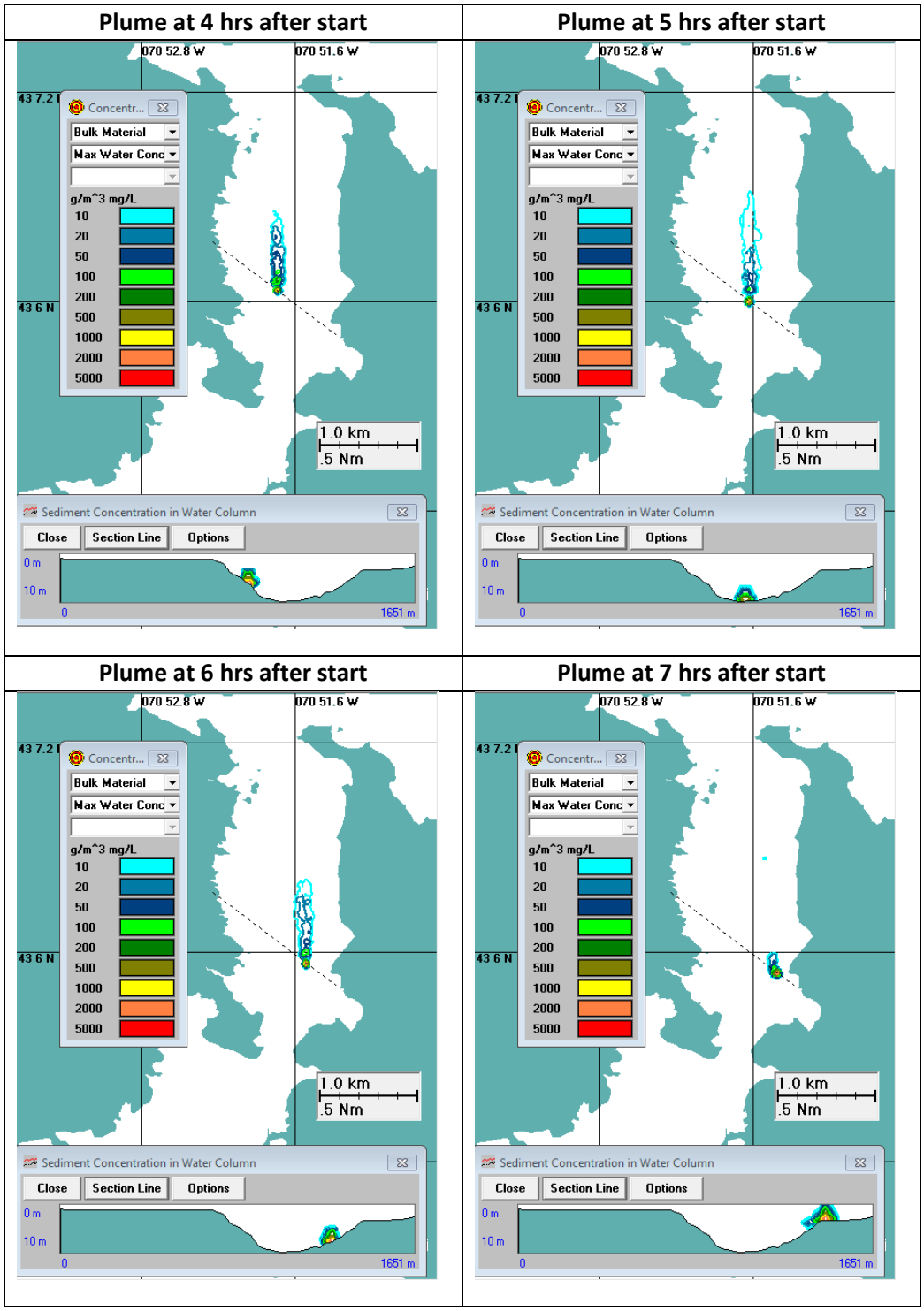

Figure 3-8. Plan view of instantaneous excess SS concentrations at 4 through 7 hrs after start of jet plowing for base case with spring tide. Vertical section view at lower portion of each panel.

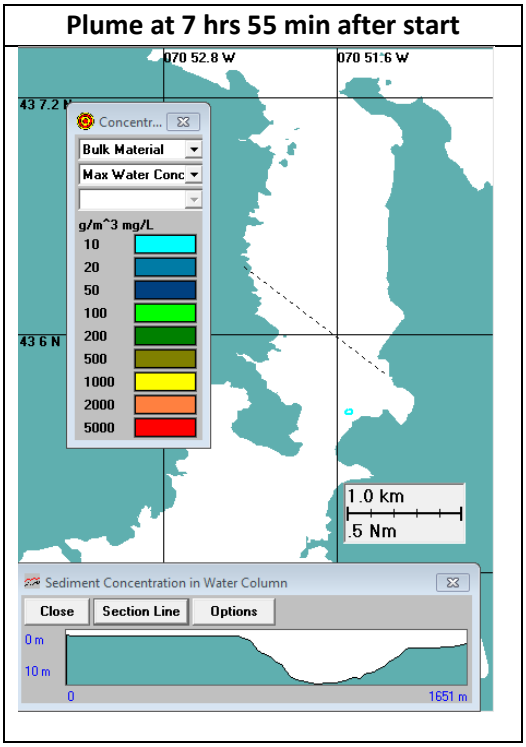

Figure 3-9. Plan view of instantaneous excess SS concentrations at 7 hrs and 55 minutes after start of jet plowing for base case with spring tide. Vertical section view at bottom of each panel. Last time step with concentrations.

The instantaneous total enclosed area of the excess SS concentration plumes seen in Figure 3-7 and Figure 3-8 is quantitatively summarized in Table 3-14 (in area units of hectares) and Table 3-15 (in units of acres) for each 1-hr increment identified at the top of each figure panel. On average the entire area enclosed by the plume (as defined by the 10 mg/L excess SS concentration contour) was 8.10 ha (20.02 ac), ranging from a low of 2.52 ha (6.22 ac) at 7 hrs to a high of 14.30 ha (35.34 ac) at 5 hrs. These total enclosed areas dropped dramatically for the higher concentrations, averaging 0.64 ha (1.58 ac) at 100 mg/L, 0.08 ha (0.20 ac) at 1,000 mg/L and 0.006 ha (0.014 ac) at 5,000 mg/L. indicating that the extent of the plume was small for higher concentrations. For reference the trench surface area is 0.042 ha (0.104 ac).

Figure 3-10 shows the plan view of the maximum time-integrated excess SS concentration contours. The time-integrated maximum concentration is generated from the model results by determining the highest concentration in each SSFATE grid cell which overlays Upper Little Bay during the entire simulation. These maximum concentrations did not occur throughout the water column and were generally restricted to one vertical layer (20 cm thickness) at the bottom. Further, these concentrations do not occur simultaneously. The timing of the start and the advance rate are such that the activity took place primarily during ebb currents, and as such the plume was transported primarily to the north of the cable route until it reached the eastern end of the route and the currents began to flood and the plume headed towards the south. The contours showed decreasing concentration from either side of the cable route with higher concentrations adjacent to the jet plow route. A vertical section view defined by the jet plow route is shown at the bottom of the figure. The highest concentrations occurred just above the

bottom at the jet plow with reduced concentrations extending up into the water column along the route.

Table 3-14. Summary of the total area (hectares) enclosed by the excess SS threshold concentration contours shown in due to jet plowing. Hours start at high slack tide.

TSS (mg/L)	Area (ha) 1 hr	Area (ha) 2 hr	Area (ha) 3 hr	Area (ha) 4 hr	Area (ha) 5 hr	Area (ha) 6 hr	Area (ha) 7 hr	Area (ha) Average
	Ebb	Ebb	Ebb	Ebb	Ebb	Ebb	Ebb	
10	5.43	9.07	3.32	9.15	14.30	12.94	2.52	8.10
20	3.99	3.08	1.28	6.43	4.31	6.43	1.84	3.91
50	2.24	0.52	0.52	2.56	1.36	1.64	1.00	1.40
100	1.32	0.36	0.36	0.80	0.36	0.68	0.60	0.64
200	0.20	0.20	0.20	0.32	0.20	0.20	0.32	0.23
500	0.20	0.20	0.20	0.20	0.20	0.20	0.20	0.20
1000	0.04	0.20	0.04	0.04	0.04	0.12	0.08	0.08
2000	0.04	0.04	0.04	0.04	0.04	0.04	0.04	0.04
5000	0.00	0.00	0.04	0.00	0.00	0.00	0.00	0.01

Table 3-15. Summary of the total area (acres) enclosed by the excess SS threshold concentration contours shown is due to jet plowing. Hours start at high slack tide.

	Area (ac)	Area (ac)	Area (ac)	Area (ac)	Area (ac)	Area (ac)	Area (ac)	Area (ac)
TSS (mg/L)	1 hr	2 hr	3 hr	4 hr	5 hr	6 hr	7 hr	Average
	Ebb	Ebb	Ebb	Ebb	Ebb	Ebb	Ebb	Ebb
10	13.42	22.40	8.19	22.60	35.34	31.97	6.22	20.02
20	9.87	7.60	3.16	15.89	10.66	15.89	4.54	9.66
50	5.53	1.28	1.28	6.32	3.36	4.05	2.47	3.47
100	3.26	0.89	0.89	1.97	0.89	1.68	1.48	1.58
200	0.49	0.49	0.49	0.79	0.49	0.49	0.79	0.58
500	0.49	0.49	0.49	0.49	0.49	0.49	0.49	0.49
1000	0.10	0.49	0.10	0.10	0.10	0.30	0.20	0.20
2000	0.10	0.10	0.10	0.10	0.10	0.10	0.10	0.10
5000	0.00	0.00	0.10	0.00	0.00	0.00	0.00	0.01

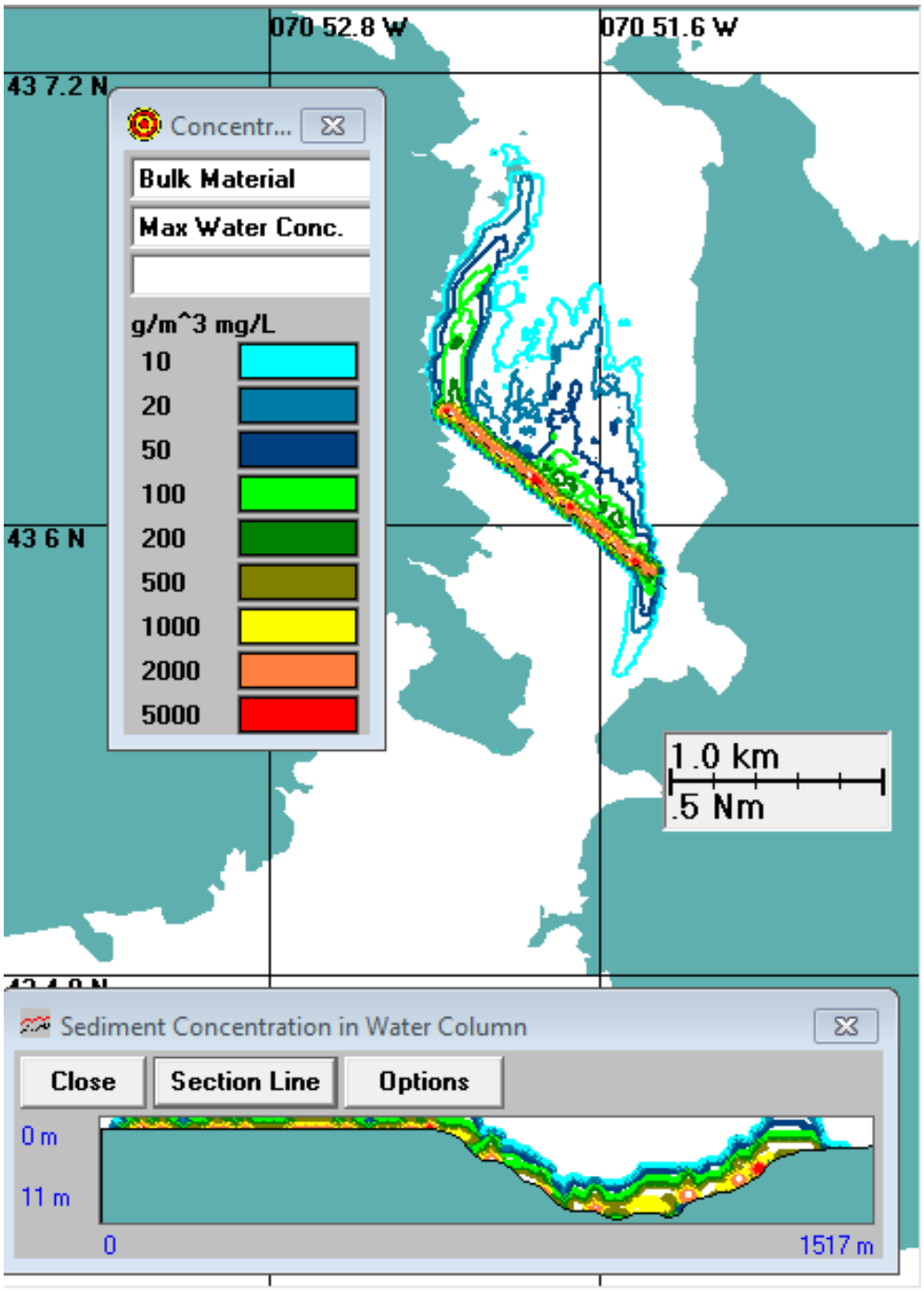

Figure 3-10. Plan view of maximum time integrated excess SS concentration contours over the entire jet plowing operation and the post operational period (while concentrations dissipate) for base case with spring tide. Vertical section view at bottom of figure.

Table 3-16 summarizes the total area enclosed by the maximum time-integrated excess SS concentration contours over the entire jet plowing operation and the brief post operational period (while concentrations dissipate) as shown graphically in Figure 3-10. This table showed that an area of 105.5 ha (260.69 ac) was experienced a maximum of 10 mg/L concentration but at different times during the simulation; i.e., the area experiencing excess SS of 10 mg/L is not

continuous in space or time. The 5,000 mg/L time integrated enclosed area was 0.4 ha (1.09 ac) and was restricted to small discontinuous features along the cable route.

Table 3-16. Summary of the total area (hectares and acres) enclosed by the maximum time-integrated excess SS concentration contours over the entire jet plowing operation and the post operational period (while concentrations dissipate) in Figure 3-10.

TSS (mg/L)	Area (ha)	Area (ac)
10	105.5	260.69
20	72.9	180.11
50	37.8	93.35
100	20.2	49.84
200	9.2	22.80
500	6.9	16.98
1000	5.1	12.53
2000	2.6	6.41
5000	0.4	1.09

An important metric defining the plume is its duration for different concentrations, which could have biological significance if exposure (duration multiplied by concentration) is sufficiently elevated. Figure 3-11 and Table 3-17 summarize the area that experiences a specific exposure (duration at or above the concentration) due to jet plow operations; note that these areas are summations and not necessarily contiguous in space or time. Areas totaling 36.9 ha (91.2 ac and 0.1 ha (0.2 ac) were exposed to a concentration of 10 mg/L or greater for 1 hr, and 2 hrs, respectively, while no areas were exposed to such a concentration for a duration of three hours. Approximately 14.5 ha (35.8 ac) were exposed to a concentration of 20 mg/L for approximately 1 hour. The area coverages dropped dramatically for the exposures to concentrations greater than 20 mg/L near the jet plow indicating that the duration and extent of the plume was relatively limited. Furthermore, once the jet plow stopped operating, no additional sediments were dispersed into the water column and concentrations above 10 mg/L dissipated within one hour.

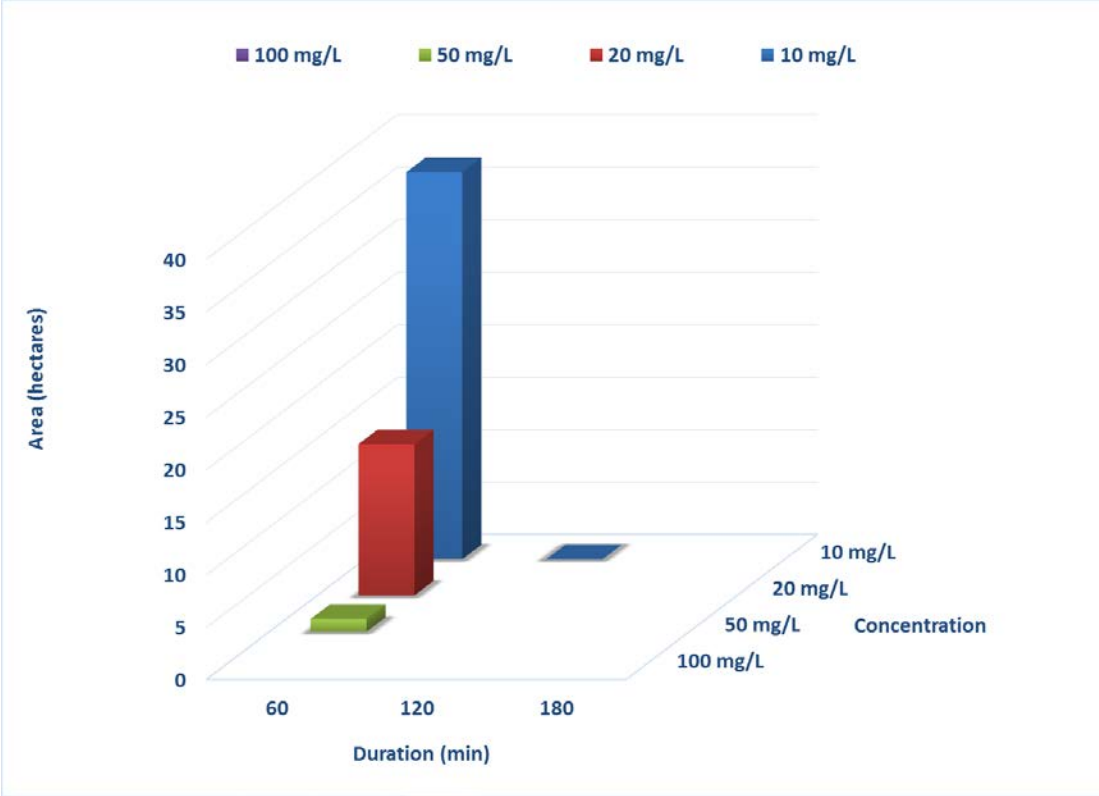

Figure 3-11. Area (hectares) exposed to excess SS concentrations for various durations over the entire jet plowing operation and the post operational period (while concentrations dissipate).

Table 3-17. Duration (minutes) and total enclosed area (hectares and acres) of maximum time integrated excess SS concentration contours over the entire jet plowing operation and the post operational period (while concentrations dissipate).

SS Concentration	Hectares			Acres		
	60	120	180	60	120	120
(mg/L)	(min)	(min)	(min)	(min)	(min)	(min)
10	36.9	0.1		91.2	0.2	
20	14.5			35.8		
50	1.3			3.3		
100						

3.4.1.2 Bottom Deposition

Figure 3-12 shows the plan view of the bottom deposition thickness distribution from 0.1 to 10 mm (0.004 to 0.4 in) due to jet plowing all three cable routes combined and assuming any sediment deposited on the bottom remains in place. The color filled areas are defined by the legend for different deposition thickness ranges, e.g., 1 mm to 5 mm (0.04 to 0.2 in) denoted by yellow. In contrast to the water column concentration contours, which are defined by a single

concentration value surrounding an enclosed area where concentrations are at or above the specified concentration (i.e., the area is cumulative), the bottom deposition thickness is defined for the area exclusively between the range of thicknesses described (i.e., the area is not cumulative). Thus, the areas with larger thicknesses are not necessarily smaller than areas with smaller thicknesses. The shape of the distribution pattern was generally similar to the water column plume but reduced in extent. The higher deposition areas were at and adjacent to the cable route.

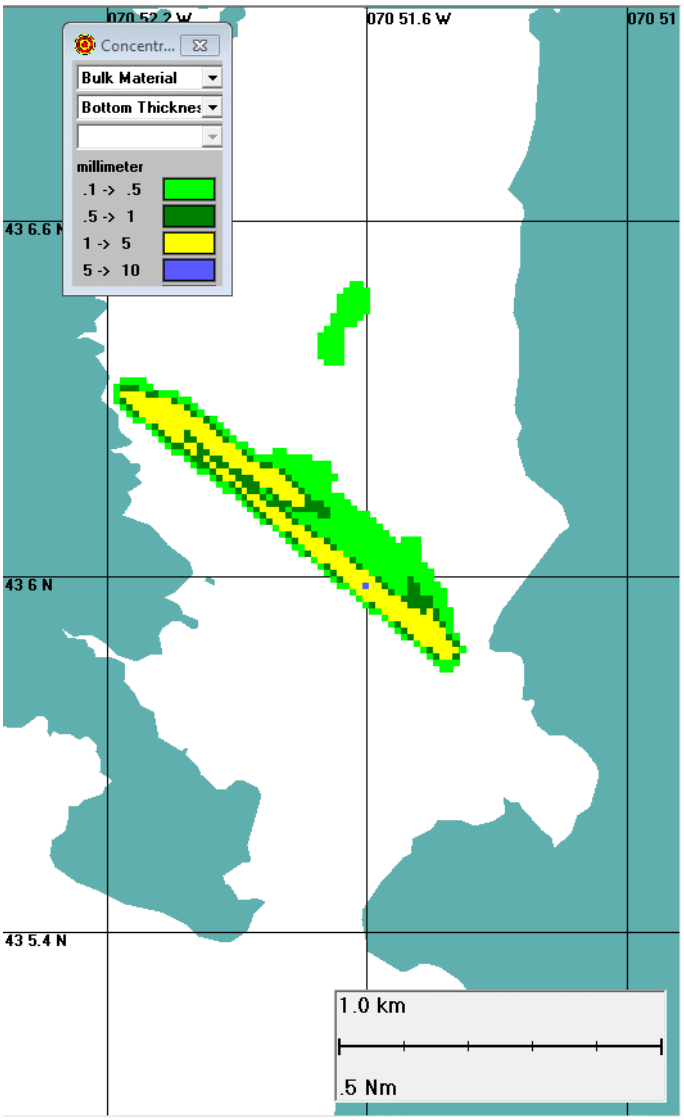

Figure 3-12. Plan view of integrated bottom thickness (mm) distribution due to jet plowing for the three cable trenches combined for base case with spring tide.

The areal sizes of the deposition thickness patterns seen in Figure 3-12 are summarized in Table 3-18 for each thickness increment range. At the range of 0.1 to 0.5 mm (0.004 to 0.02 in) thickness range the area was 13.26 ha (32.76 ac) due to jet plowing the three cable routes. These areas generally dropped in size, but not always, for the higher deposition thicknesses. For

example, the area of 9.09 ha [22.47 ac] for the 1 to 5 mm [0.04 to 0.2 in) thickness range was larger than the 0.5 to 1 mm (0.02 to 0.04 in) area of 5.05 ha (12.47ac).

Table 3-18. Bottom thickness (millimeter and inch) areal distribution (hectare and acre) due to jet plowing for the three cable routes combined.

Thickness (mm)	Area (ha)	Thickness (in)	Area (ac)
0.1 to 0.5	13.26	0.004 to 0.02	32.76
0.5 to 1	5.05	0.020 to 0.04	12.47
1 to 5	9.09	0.04 to 0.2	22.47
5 to 10	0.04	0.2 to 0.4	0.10
Totals 0.1 to 10	27.44	0.004 to 0.4	67.81

3.4.2 Jet Plow Results – Sensitivity and Additional Runs

A few sensitivity runs were simulated holding all parameters the same as the base case except for the single parameter of interest. The sensitivity to advance rate, loss rate, tide range (spring/neap) were investigated. In addition, a run with continued resuspension simulated was performed to investigate the areas where sediment from installation activities may be transported after they initially settle. To provide a relative comparison, the maximum time integrated concentrations for each sensitivity run are shown along with the base case.

Advance Rate

Figure 3-13 illustrates the sensitivity to advance rate as defined by maximum time integrated excess SS concentration. The upper right panel shows the base case of 183 m/hr [600 ft/hr], and the lower left and lower right panels show a slower (91 m/hr [300 ft/hr]) and faster (274 m/hr [900 ft/hr] rate) advance rate, respectively. While the total mass introduced to the water column remains the same in each case, the changes in the advance rate modify the source strength (flux [mass/time] of sediment to the water column), the timing with the tidal currents and the overall duration of the activity. The slower advance rate, with lower mass loading flux to the water column showed lower peak concentrations along the route compared to the base case. Further the slower advance rate showed more variability in the footprint, with exposure to both flood and ebbtides. The base and faster advance rates had short enough durations that they were exposed primarily to ebb currents. The faster advance rate had more prevalent high concentrations (5,000 mg/L) along the route, due to the increased mass loading rate.

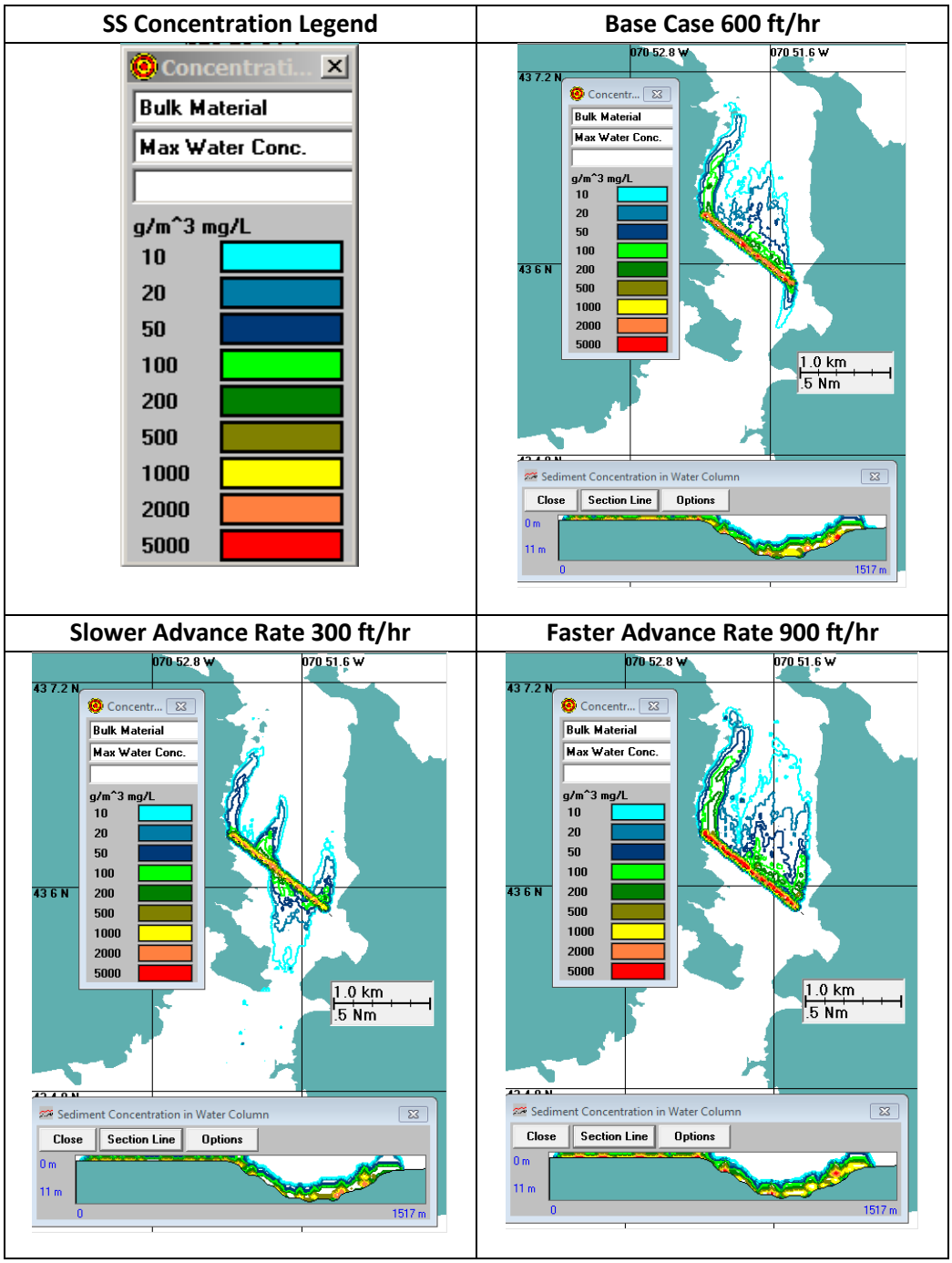

Figure 3-13. Plan view of maximum time integrated excess SS concentrations base and sensitivity to advance rate simulations. Base case (top right), slower advance rate (bottom left) and faster advance rate (bottom right). Vertical section view at bottom of each panel.

Sediment Loss Rate

Figure 3-14 illustrates the sensitivity to loss rate as defined by maximum time integrated excess SS concentration. The upper right figure shows the base case of 25%, and the lower left and

lower right panels show lower (10%) and higher (35%) rates. Changes in the loss rate modified the source strength (flux of sediment to the water column) and total mass disturbed. The lower loss rate, with lower mass loading flux to the water column showed lower peak concentrations along the route as well as a smaller footprint than the base case. Alternatively, the higher loss rate, with greater mass flux, showed a greater extent of water column concentrations and greater extent within the footprint of individual contour levels. Such trends were evident by comparison of maximum integrated excess concentrations in Figure 3-14.

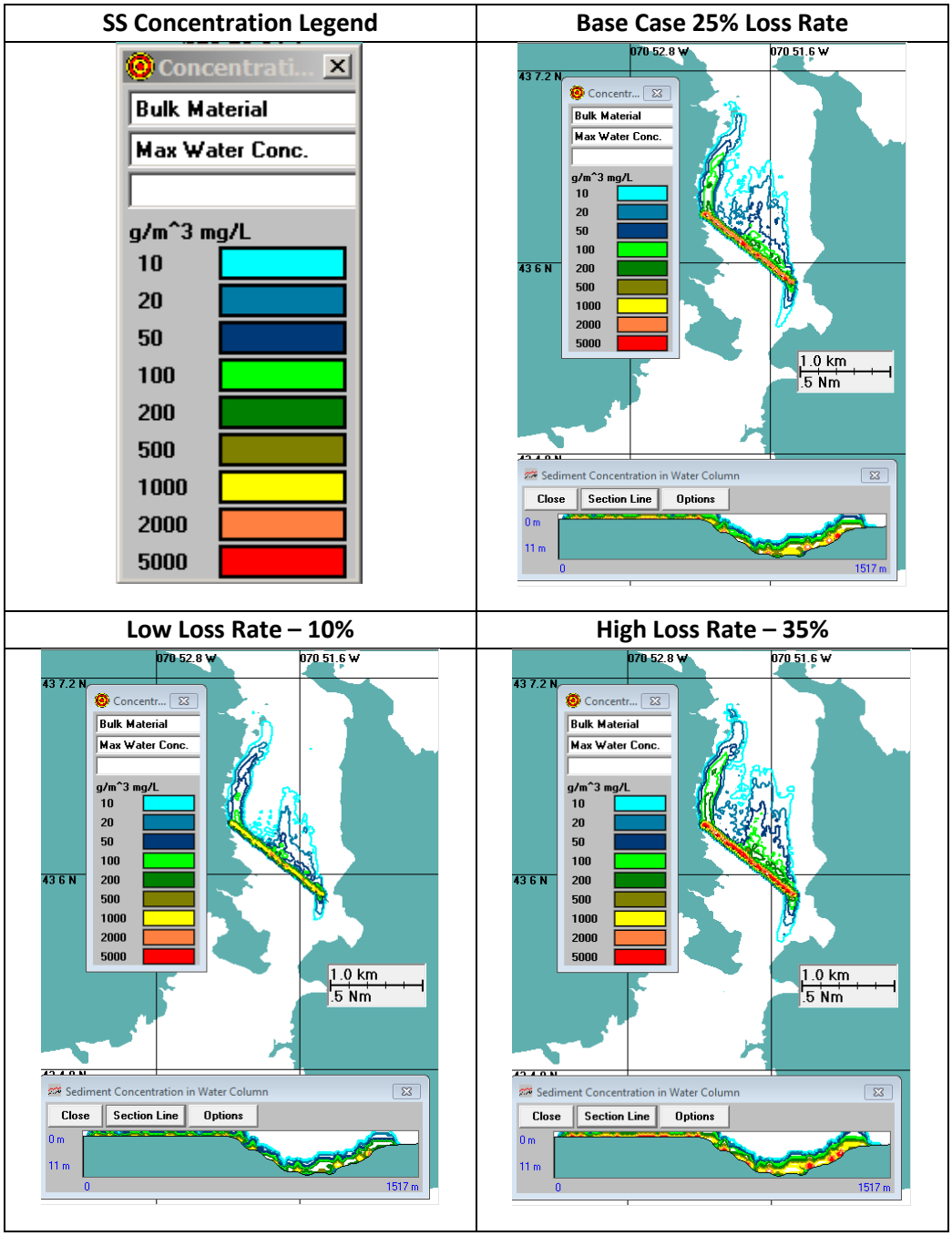

Figure 3-14. Plan view of maximum time integrated excess SS concentrations base and sensitivity to loss rate. Base case (top right), low loss rate (bottom left) and high loss rate (bottom right). Vertical section view at bottom of each panel.

Influence of Tidal Amplitude

Figure 3-15 illustrates the sensitivity to tide. The base case was simulated during a spring tide (to identify maximum extent of the plume) and the sensitivity run was simulated for a neap tide. A spring tide has a larger tidal amplitude/range and faster currents and a neap tide has a smaller tidal amplitude/range and reduced currents. Both runs were started at high water slack current and both runs simulated activities that took place for just over 7 hours. The comparison of the maximum time integrated concentration was similar for both the spring tide and neap tide, though the overall footprint for the spring tide is greater and there are some differences in the extent of the individual contour levels. Concentrations 20 mg/L and less generally extend further in the spring tide and concentrations above 20 mg/L do not extend as far in spring as compared to neap; this is due to less advection of the sediments in the neap tide.

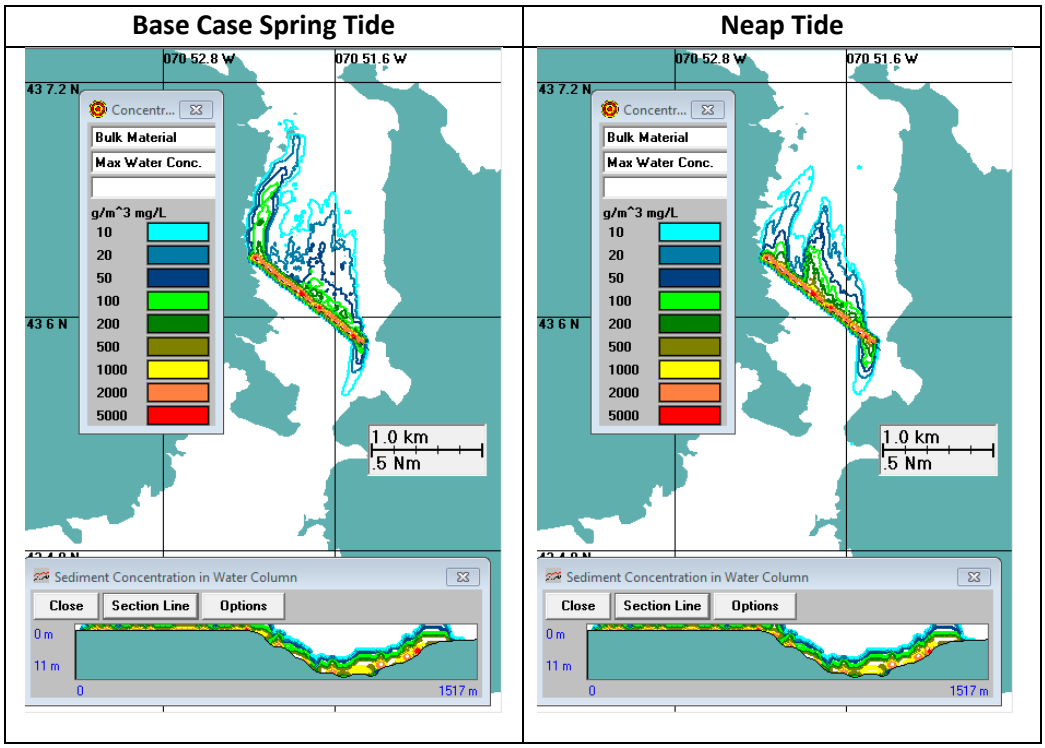

Figure 3-15. Plan view of maximum time integrated excess SS concentrations base and sensitivity to tidal amplitude. Base case run for a spring tide (left), sensitivity run during a neap tide (right); both start at high slack. Vertical section view at bottom of each panel.

Resuspension

A measure of the stability of deposited sediments to the seabed is a function of the erosion velocity for each grain size in the sediment. This relationship is shown via a Hjulstrom diagram as shown in Figure 3-16. Here the y-axis is the current velocity and the x-axis is sediment grain size. Since the freshly deposited sediment is unconsolidated, the fine grains (clay and silt) and sand would be eroded at a velocity of about 20 cm/s (0.4 kt). Examining the example figures of flood and ebb tide velocities in Figure 2-1 and Figure 2-2, respectively, this minimum speed is exceeded at peak tides across most of Upper Little Bay except in the shallow tidal flats very near

the shore where there could be some accumulation. Thus, most of the fine sediment is likely to be resuspended on subsequent tides and dispersed from the areas initially affected by deposition unless flocculation of the clay particles occurs and they remain in place. The larger grain sizes will quickly drop back into the channel when first resuspended by the jetting process.

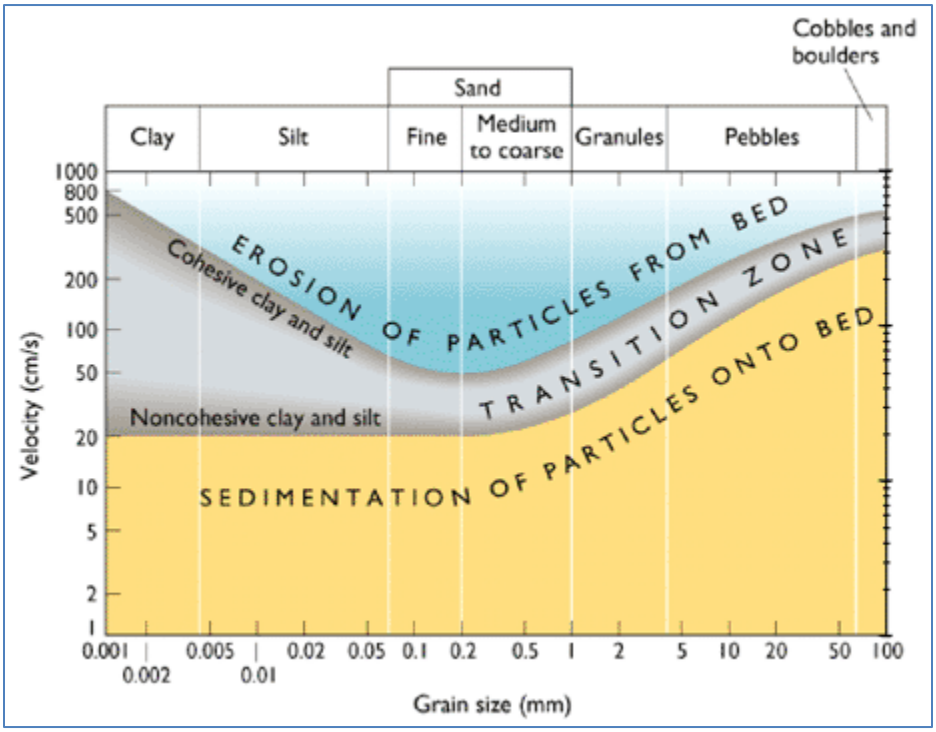

Figure 3-16. Hjulstrom diagram showing relationship between velocity and grain size (from http://eesc.columbia.edu/courses/ees/lithosphere/homework/hmwk1_s08.html).

An additional model run was simulated that include the effects of continued resuspension. This run showed a much larger footprint of SS excess concentrations, though the concentrations were present intermittently and confined to the very bottom of the water column. Figure 3-17 illustrates the maximum time integrated excess SS concentration footprint of this run which was simulated for a week-long period after the onset of construction. As expected, this footprint is a significantly larger extent because it simulates potential movement after the initial settling of the sediments, and the footprint covers new areas that only see concentrations for a brief amount of time local to the bottom due to the continued resuspension. Much of the area has the potential for continued resuspension due to the relatively strong currents. Since the model did not include a cohesive sediment model, a sediment consolidation model, adjustments for settled flocs (larger diameters), or interactions with the background suspended sediments and bedload, these predictions are an extremely conservative estimate of the potential impacts. To provide a sense of the temporal characteristics of the continued resuspension several time series were extracted at the points shown in Figure 3-17; the corresponding instantaneous concentration time series plots (truncated to 3 days since concentrations were zero from that point forward) are embedded in Figure 3-17. The footprint of maximum time integrated concentration is based on the model instantaneous concentration output at a 5-minute interval; the instantaneous concentrations have higher peak values that are not sustained and therefore

have less potential for physical or biological effects. A summary of the duration over various concentration thresholds at each of the time series locations is presented in Table 3-19; this shows how the concentrations do not persist, particularly at the higher levels. Appendix A illustrates hourly snapshots of the concentrations to provide a temporal and spatial summary of this simulation.

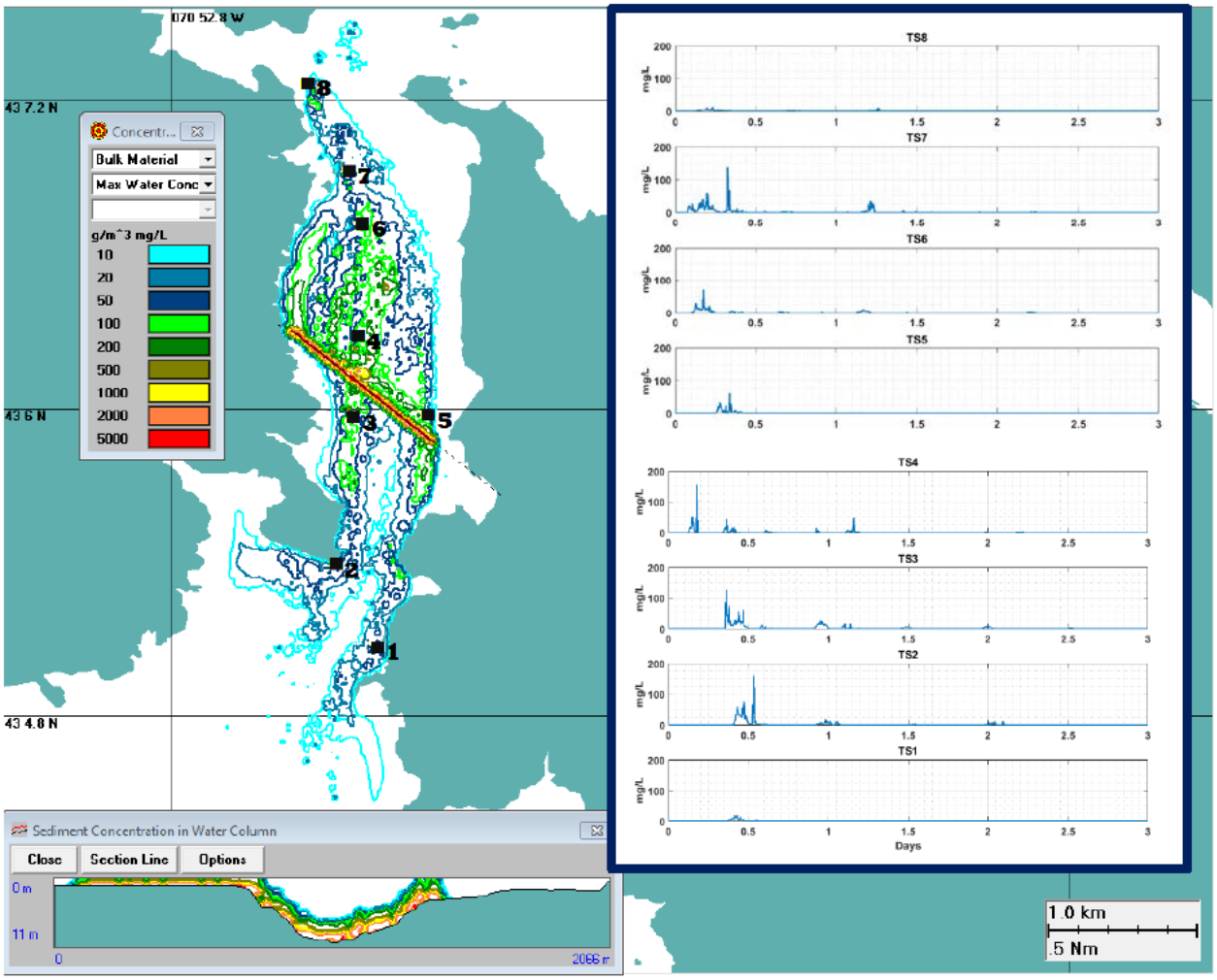

Figure 3-17. Plan view of maximum time integrated excess SS concentrations for continued resuspension simulation. Vertical section view at bottom of each panel. Embedded time series with short duration spikes at select locations TS1 –8.

Table 3-19. Summary of duration over concentration thresholds for the eight time series locations identified in Figure 3-17

Concentration Threshold mg/L	Time Over Concentration Threshold (minutes)							
	TS1	TS2	TS3	TS4	TS5	TS6	TS7	TS8
20	10	115	120	50	25	25	95	0
40	0	45	35	30	5	5	30	0
60	0	20	15	5	5	5	10	0
80	0	5	5	5	0	0	5	0
100	0	5	5	5	0	0	5	0
120	0	5	5	5	0	0	5	0
140	0	5	0	5	0	0	0	0
160	0	5	0	0	0	0	0	0
180	0	0	0	0	0	0	0	0
200	0	0	0	0	0	0	0	0

3.4.3 Diver Hand Jet Burial Results

3.4.3.1 Water Column Concentrations

The diver hand jet burial activity is assumed to take place intermittently (4 hrs/day) over approximately 10 days for the west and 18 days for the east if a single dive team is used. This is based on the route lengths, an average advance rate of 2.3 m/hr (7.5 ft/hr) and 4 hrs a day of operations. The total duration of activity is based only on the advance rate and route length; the calendar span over which it takes place depends on the tides (minimum water depth required is 1 ft) and operations (e. g., multiple dive teams). A summary of the route length, activity duration and the span of time over which it was modeled is presented in Table 3-20, this

Table 3-20. Summary of diver hand jetting route length, activity duration and modeled calendar span (based on 4 hrs/day). Also included are lengths of routes within silt curtain.

	West	East
Length (m)	91.4	164.9
Length (ft)	300	541
Length within Silt Curtain (m)	91.4	94.8
Length within Silt Curtain (ft)	300	311
Length outside Silt Curtain (m)	0.0	70.1
Length outside Silt Curtain (ft)	0	230
Percent within Silt Curtain	100.0	57.5
Activity Duration (hr)	39.7	71.7
Activity Duration (day)	1.7	3.0
Modeled Calendar Span (days)	10	18

table also includes the length of the routes that will be within silt curtains. Note that silt curtains were simulated as a reduced loss rate to the water column outside the areas enclosed by the curtains themselves, however the portion within the curtains is not modeled and would be expected to have higher concentrations.Since the diver burial takes place over many discrete intervals, the results are presented two ways; one a snapshot of a representative day with simultaneous east and west diver burial activity and the other as the cumulative footprint of all days.

Figure 3-18 shows the plan view of the predicted instantaneous maximum (vertically) excess SS concentration contours for both the west and east area; note the east area day shown had activity outside the silt curtains. The water column concentration contours shown, which are defined by a single concentration level, totally surround an enclosed area where concentrations are at or above the specified concentration, i.e., the area is cumulative. Thus, the areas with higher concentrations must be smaller than areas with lower concentrations since those areas are enclosed within the lower concentration contour.

Figure 3-18 illustrates that the plume associated with activities without silt curtains (western side of east portion) will be larger than the plume associated with the activities that take place while using silt curtains. The figure also illustrates that the plume is aligned with the current direction with a trend of decreasing concentration away from the location of the diver activities on the cable route as material dilutes and settles out.

A vertical section view defined along the cable route looking north is inserted at the bottom of the figure. The insert shows that the highest concentrations occur near the bottom with reduced concentrations extending up into the water column. In the western shallows, suspended sediments from the diver burial activity are likely to reach nearly to the water surface. In the somewhat deeper eastern area, excess suspended sediments will be restricted to the lower half of the water column.

The instantaneous total enclosed area of the excess SS concentration plumes for the west and east diver burial sections seen in Figure 3-18 is summarized in Table 3-21 for concentration levels that occurred during activity. At 10 mg/L excess SS concentration the total area enclosed by the contour is 0.44 ha (1.09 ac) for the west section and 3.47 ha (8.58 ac) for the east section. However, these total enclosed areas drop dramatically for the higher concentrations near the diver burial activities, i.e., the area at 100 mg/L is only about 0.24 ha (0.59 ac) for the west section and do not reach that threshold for the east section, indicating that the extent of the plume is relatively limited for higher concentrations. Figure 3-19 illustrates time history of excess SS concentrations during activity at a location close to the source during diver activity. This figure also has an inset with the location of the queried point overlaid on the maximum excess SS concentration for that day. This figure illustrates that the concentrations diminish to zero within approximately 20 minutes after activity stops.

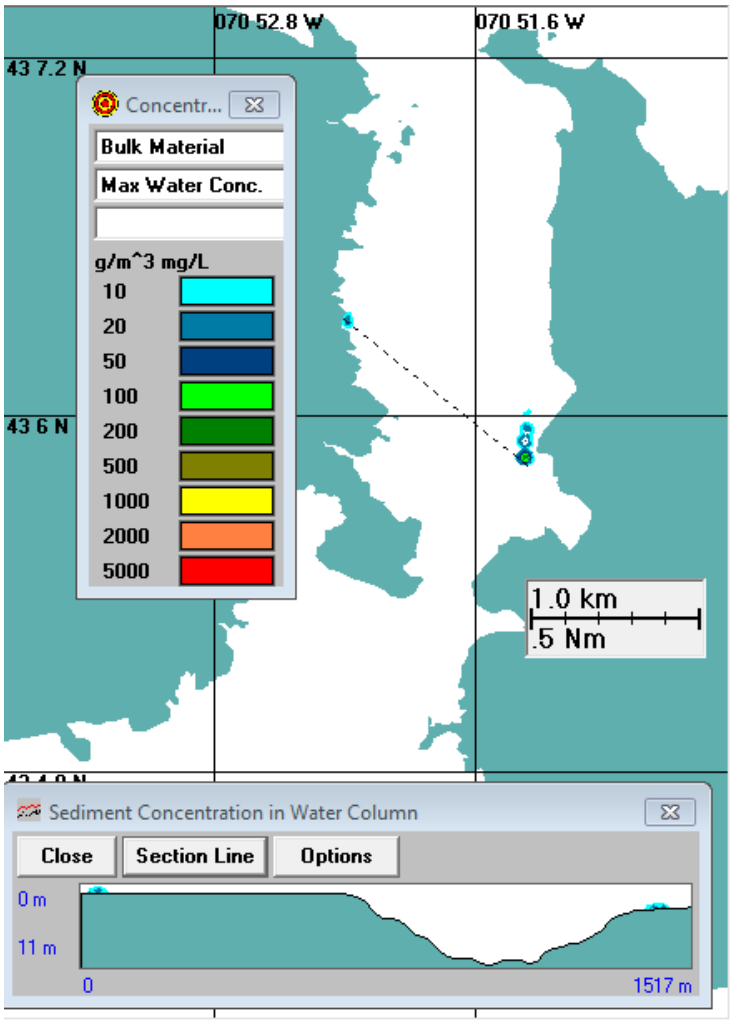

Figure 3-18. Plan view of instantaneous maximum (vertically) excess SS concentration contours for 1 day approximately midway across the west and east diver hand jet burial sections. Vertical section view at lower left. Assumes silt curtains were used on the entire west route and eastern portion of east route.

Table 3-21. Summary of the total area (hectares and acres) enclosed by the excess SS threshold concentration contours shown in Figure 3-18 due to diver hand jet burial. Assumes silt curtains were used on the entire west route and eastern portion of east route.

TSS (mg/L)	West Section		East Section	
	(ha)	(ac)	(ha)	(ac)
10	2.44	6.02	9.58	23.68
20	1.24	3.06	4.83	11.94
50	0.36	0.89	2.16	5.33
100	0.08	0.20	0.80	1.97
200			0.60	1.48
500			0.20	0.49
1000				

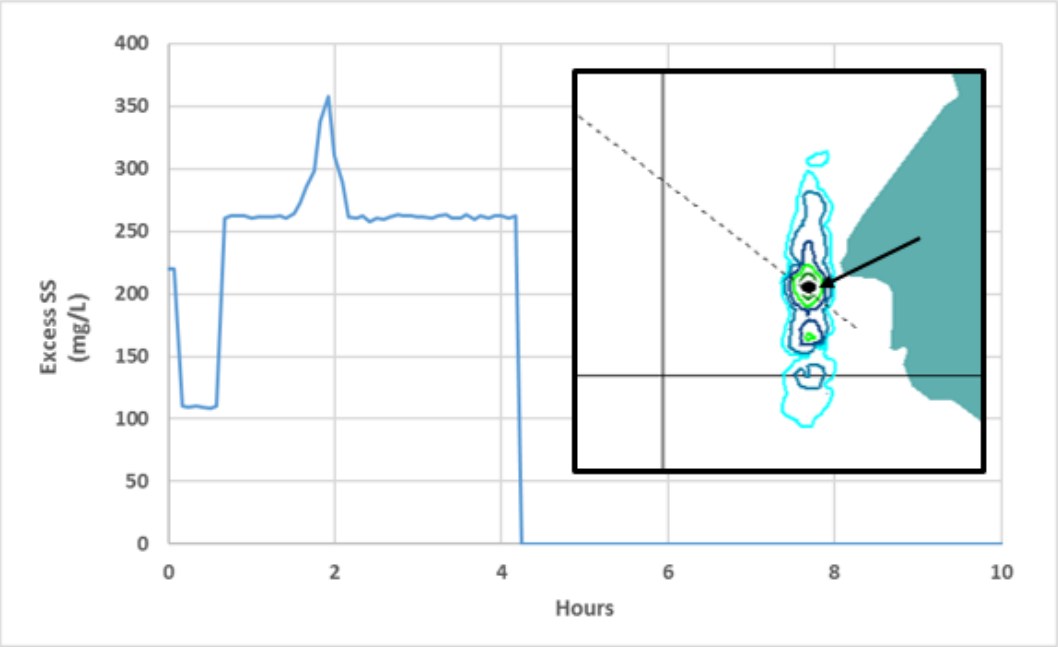

Figure 3-19. Time history of concentrations taken from a point close to the route centerline. Black arrow points to black dot of location where time history was queried.

Figure 3-20 shows the plan view of the maximum time-integrated excess SS concentration contours for all diver hand jet burial sections. These concentrations are generated from the model results by determining the highest concentration in each SSFATE grid cell during the entire simulation of all diver simulations. This plot shows only the maximum excess SS concentration integrated over time as well as space (vertically within the water column) and would not occur simultaneously in the Bay. The contours show decreasing concentration from either side of the cable route with higher concentrations adjacent to the jet plow route. This model run assumed silt curtains were used in the western shore entire route and the eastern end of the eastern route.

A vertical section view defined by the jet plow route is shown at the bottom of the figure. The highest concentrations on the west are 100 mg/L and the highest on the east are 500 mg/L. These peak concentrations occur just above the bottom with reduced concentrations extending up into the water column along the route.

Table 3-22 summarizes the total eastern area enclosed by the maximum time-integrated excess SS concentrations over the diver burial operations shown in Figure 3-20. This table shows that during the diver burial activities a total enclosed area of 2.44 ha (6.02 ac) sees a minimum 10 mg/L concentration at different times during the simulation. For the east side the 10 mg/L concentration contour encloses a total area of 9.58 ha (23.68) ac.

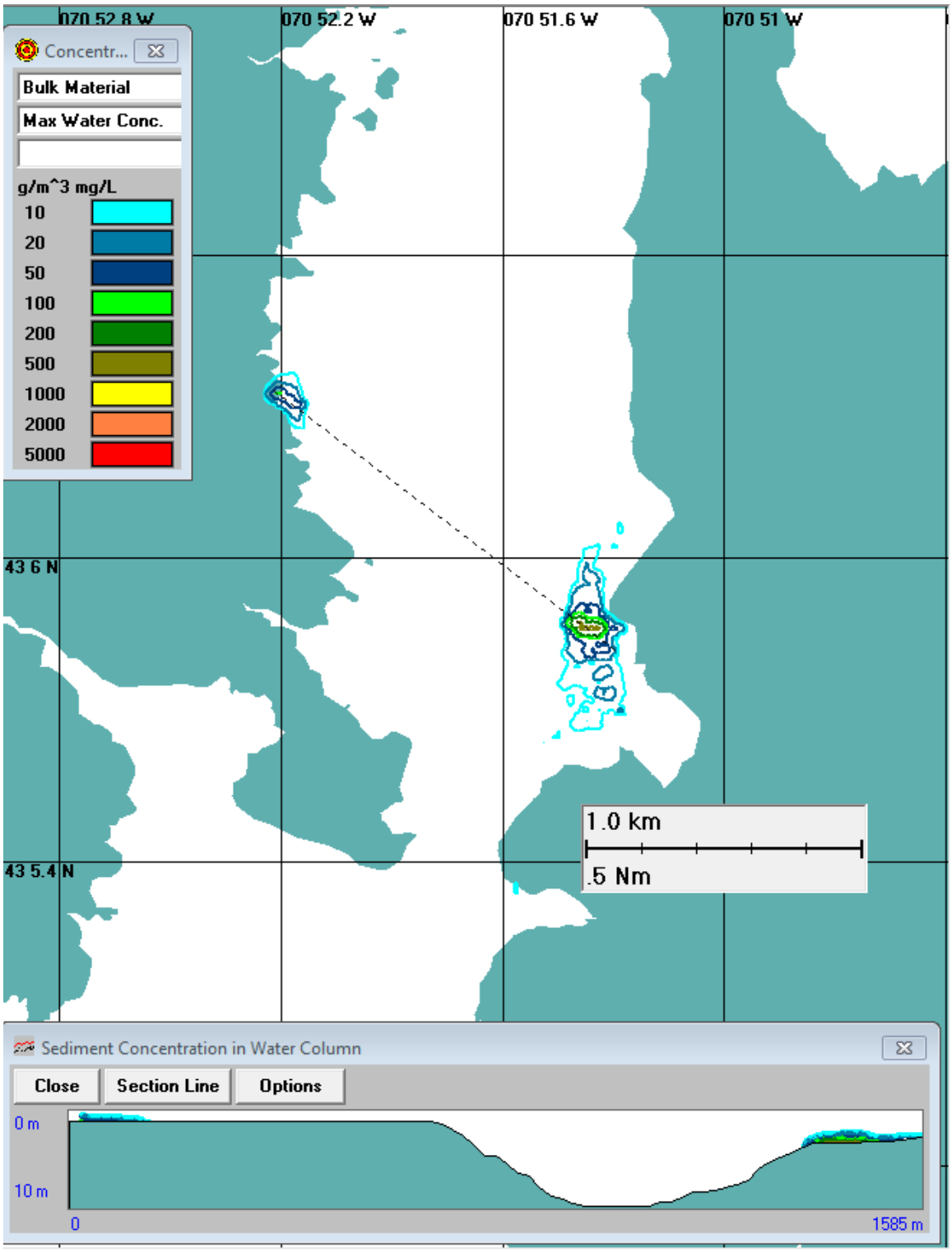

Figure 3-20. Plan view of maximum time integrated excess SS concentration contours over diver hand jet burial operations. Vertical section view at lower left. Assumes silt curtains were used on the entire west route and eastern portion of east route.

Table 3-22. Summary of the total area (hectares and acres) enclosed by the maximum time-integrated excess SS threshold concentration contours shown in Figure 3-20 due to diver hand jet burial for the west and east sections combined. Assumes silt curtains were used on the entire west route and eastern portion of east route.

	Total Diver Burial	Total Diver Burial
TSS	Area	Area
(mg/L)	(ha)	(ac)
10	11.34	28.02
20	5.75	14.21
50	2.36	5.82
100	0.84	2.07
200	0.68	1.68
500	0.24	0.59
1000	0.00	0.00

An important metric defining the plume is its duration for different concentrations, which could have biological significance if exposure (duration multiplied by concentration) is sufficiently elevated. The area exposed to various concentration thresholds for different durations is presented in Figure 3-21 and is summarized in Table 3-23 and Table 3-24 for the combined east and west diver burial activities. In total concentrations, up to 100 mg/L will be present for up to a day (1440 minutes) for a small area (0.1 ha [0.2 ac]); the exposure however will be intermittent over the course of approximately 30 days. A maximum concentration of 500 mg/L persists for an hour at an area of 0.2 ha (0.6 ac). The area decreases for extended durations and similarly the area is smaller at higher thresholds. The duration of excess concentrations is due mainly to the duration of the activity.

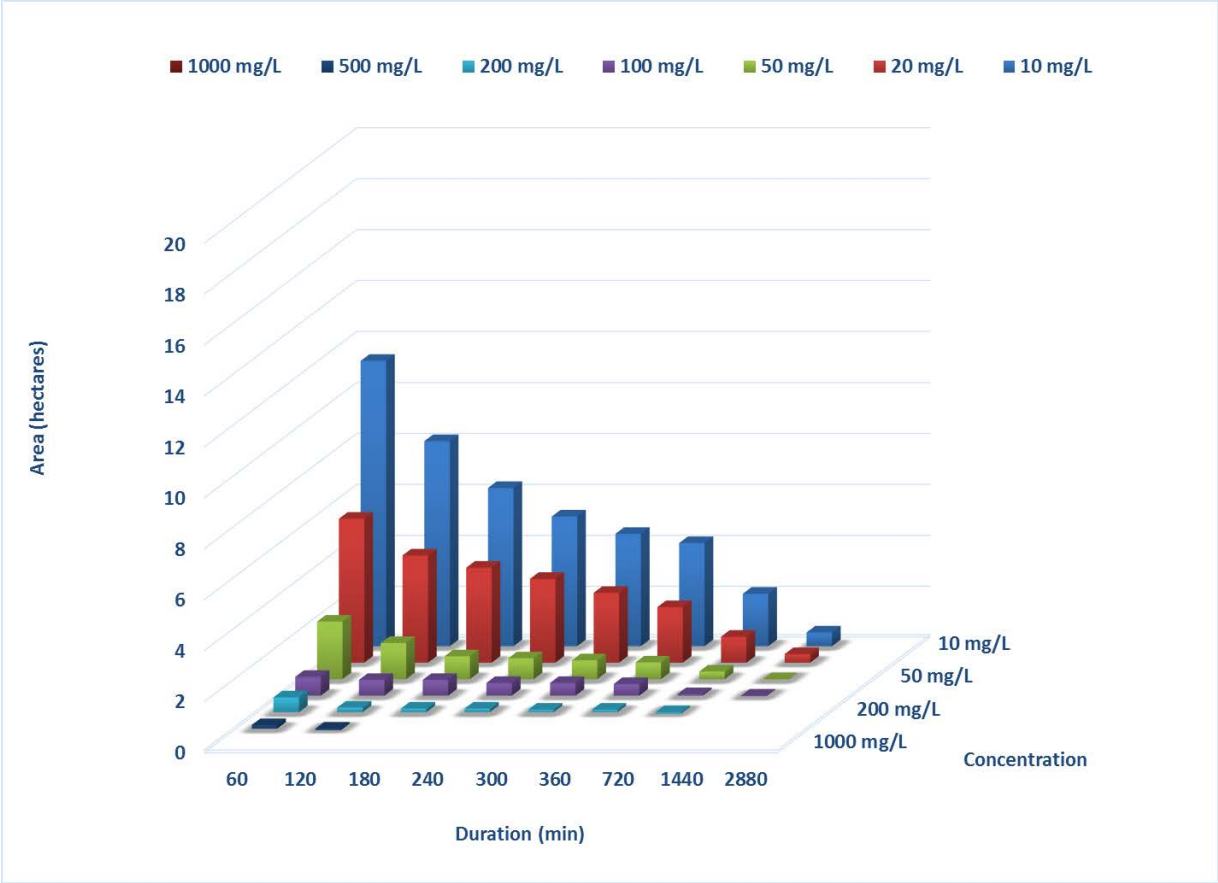

Figure 3-21. Area (hectares) exposed to excess SS concentrations for various durations from diver burial (east and west combined). Assumes silt curtains were used on the entire west route.

Table 3-23. Area (hectares) exposed to excess SS concentrations for various durations from diver burial (east and west combined). Assumes silt curtains were used on the entire west route.

SS Concentration	Hectares								
	60	120	180	240	300	360	720	1440	2880
(mg/L)	(min)	(min)	(min)	(min)	(min)	(min)	(min)	(min)	(min)
10	11.3	8.2	6.3	5.2	4.5	4.2	2.2	0.6	
20	5.8	4.3	3.8	3.4	2.8	2.3	1.1	0.4	
50	2.4	1.5	1.0	0.9	0.8	0.8	0.4	0.1	
100	0.8	0.7	0.7	0.6	0.6	0.6	0.2	0.1	
200	0.7	0.3	0.2	0.2	0.2	0.2			
500	0.24	0.04							
1000									

Table 3-24. Area (acres) exposed to excess SS concentrations for various durations from diver burial (east and west combined). Assumes silt curtains were used on the entire west route.

SS Concentration	Area (ac)								
	60	120	180	240	300	360	720	1440	2880
(mg/L)	(min)	(min)	(min)	(min)	(min)	(min)	(min)	(min)	(min)
10	27.9	20.1	15.6	12.8	11.1	10.3	5.3	1.6	0.0
20	14.2	10.6	9.5	8.4	7.0	5.6	2.8	1.1	0.0
50	5.8	3.8	2.5	2.3	2.1	1.9	1.0	0.2	0.0
100	2.1	1.8	1.8	1.5	1.5	1.4	0.4	0.2	0.0
200	1.7	0.7	0.6	0.6	0.5	0.5			
500	0.59	0.1							
1000									

3.4.3.2 Bottom Deposition

Figure 3-22 shows the plan view of the bottom deposition thickness distribution from 0.1 mm to 10 mm (0.004 to 0.4 in) due to diver hand jetting activity for both the west and eastern sections of all three cable routes. This footprint assumed that any sediment deposited on the bottom remained in place. The color filled areas are defined by the legend for different deposition thickness ranges, e.g., 1 mm to 5 mm (0.04 to 0.2 in) denoted by yellow. The bottom deposition thickness is defined for the area exclusively between the range of thicknesses described, i.e., the area is not cumulative. Thus the areas with larger thicknesses are not necessarily smaller than areas with smaller thicknesses. The distribution pattern is generally similar to the maximum water column plume footprint but reduced in extent. The higher deposition areas are adjacent to the cable route.

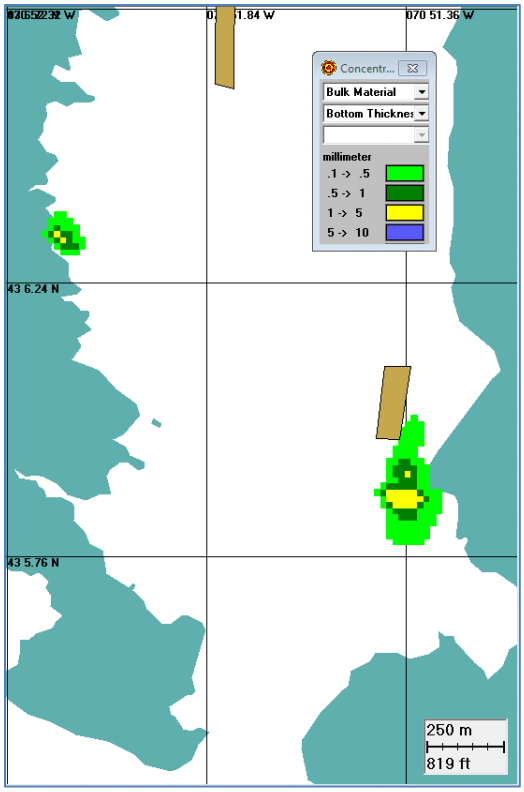

Figure 3-22. Plan view of time integrated bottom thickness (mm) distribution due to diver burial for west and east sections for three cable routes combined. Assumes silt curtains were used on the entire west route and eastern portion of east route. Brown polygons represent oyster lease areas.

The areal sizes of the deposition thickness patterns seen in Figure 3-22 for the combined west and east sections are summarized in Table 3-25 for each thickness increment range. At the 0.1 to 0.5 mm (0.004 to 0.02 in) thickness range the area is 4.37 ha (10.79 ac) accounting for all the three cable routes combined. At higher thickness intervals/thresholds the footprint is smaller.

Table 3-25. Bottom thickness (millimeter and inch) areal distribution (hectare and acre) due to diver burial for west and east sections for the three cable routes combined. Assumes silt curtains were used on the entire west route and eastern portion of east route.

Diver Burial			
Thickness	**Area**	**Thickness**	**Area**
(mm)	**(ha)**	**(in)**	**(ac)**
0.1 to 0.5	4.37	0.004 to 0.02	10.79
0.5 to 1	1.52	0.02 to 0.04	3.76
1 to 5	0.72	0.04 to 0.2	1.78
5 to 10	0.00	0.2 to 0.4	0.00
Totals 0.1 to 50	6.61	Totals 0.004 to 2	16.33

The area inside the silt curtains adjacent to the cable routes will, of course, see a significant local increase in bottom deposition thickness. The project proposes that silt curtains will be used to enclose the entire three western diver hand jet burial routes 91.4 m (300 ft) long with an area of 2,323 m^2 (25,000 ft^2) and also used along a portion (94.8 m [311 ft]) of the three-eastern diver hand jet burial routes enclosing an area of 2,480 m^2 (26,700 ft^2). Approximately 70.1 m (230 ft) of each of the three cables on the eastern end of the route closest to the jet plow activity will not be enclosed by silt curtain during diver hand jet burial. Based on the trench geometry for diver burial summarized in Table 3-4 90% of the entire west resuspension volume or 61.2 m^3 (2,160 ft^3) spread over the enclosed area results in an average deposition thickness of 26 mm (1.0 in) while 90% of the enclosed east resuspension volume or 63.4 m^3 (2,239 ft^3) spread over the enclosed area results in an average deposition thickness of 26 mm (1.1 in). Larger thicknesses would be found closest to the burial routes and smaller thicknesses are expected at increased distance from the routes.

3.5 Effects of Multiple Cable Laying Operations

Since there are three cable to be installed in separate but parallel routes the question arises as to what happens to the water column concentration and bottom deposition created by one single pass and whether it might affect the subsequent passes. The current schedule to embed each cable by jet plowing plans for a 5 to 7 day interval between installations. The water column concentration duration analysis shows that the excess concentration will drop to zero within approximately 1 hour following cessation of jet plowing. With continued resuspension enabled the simulation shows excess concentration will drop to zero within 3 days. Thus there will be no cumulative increases in suspended sediment concentrations as a result of these installations.

There will be a cumulative threefold increase in deposition inside the silt curtains, however, for the three cables. This results in three times increase in deposition thickness; the maximum deposition thickness is 44 and 43 mm (3.1 and 3.0 in) for the west and east curtains,

respectively. Greater deposition thicknesses would be found closest to the burial routes and smaller thicknesses found closer to the silt curtains distant from the routes.

4 Conclusions

Two computer models were used in the analysis: BELLAMY, a hydrodynamic model used for predicting the currents in Upper Little Bay, and SSFATE, a sediment dispersion model used for predicting the fate and transport of sediment resuspended by the jet plowing and diver burial operations. BELLAMY is a finite element, two-dimensional, vertically averaged, time stepping circulation model developed at Dartmouth College and previously applied to the Great Bay Estuarine System. The SSFATE (Suspended Sediment FATE) model was utilized to predict the excess suspended sediment concentration and the dispersion of suspended sediment resulting from jetting activities. The model predicts excess concentration, which is defined as the concentration above ambient suspended sediment concentration generated by the seabed activities. Summaries and conclusions for the BELLAMY and SSFATE model results and associated analyses are presented below

4.1 BELLAMY Hydrodynamic Model

The BELLAMY model used had previously been successfully applied to the Great Bay Estuary System over the last 15 years. Its use was found entirely appropriate as follows:

- The tides in the GBES are known at mesoscale with a range between 2 and 4 m. This tidal amplitude generates a tidal prism of 64 x 10^6 m^3 and induces high tidal-induced turbulence conducive to energetic mixing in the system.
- A recent measurement program conducted in Upper Little Bay using a bottom mounted Acoustic Doppler Current Profiler (ADCP) showed that the the structure is mostly vertical from maximum flood to slack high but during the higher velocity ebb the bottom friction inhibits the speeds in the deeper layers. This does not invalidate using a vertically averaged modeling approach since the currents in a vertically averaged model somewhat overestimates near bottom currents and overestimates near surface currents, which provides a conservative (higher) current that transports the sediment released by jetting activities.
- The freshwater flow into an estuary can cause stratified salinity conditions and resultant complex currents if sufficiently large. The annual average freshwater flow to the GBES is 32.3 m^3. This means that the flow is less than 2% of the tidal prism and that the GBES is dominated by tidal flow and the GBES is thus considered a well-mixed system as has been consistently pointed out in the scientific literature for at least the last 35 years.
- An examination of previous salinity measurements in the Little Upper Bay area show very little salinity stratification due to vigorous tidal mixing and relatively low river flow.
- A review of the U.S. Geology Survey gauge data shows that the average flow in the September-October period when the cables will be installed is less than 6.2% of the annual flow thus significantly reducing the effects of river flow even further. The use of average flows in the BELLAMY model overestimates the flow for September-October by a factor thus is highly conservative.
- The USGS daily flow was examined for the 2007-2016 decade showed that high flows (due to precipitation events are rare in the September-October period.The winds for Pease International Tradeport from the NOAA DS3505 database were examined for the September-October period for the decade 2007-2016. It was found the 88% of the winds were below 5 m/s and that only 0.4% exceed 10 m/s with none of the with none of the largest wind events originating from the north or northwest or from the south or

southeast, the alignment of Upper Little Bay, thus making it very unlikely that wind-induced effects would be significant.

The use of the BELLAMY model was thus fully justified for this project (and a number of others) to simulate currents in the GBES

4.2 SSFATE Sediment Dispersion Model

The SSFATE sediment dispersion model was successfully applied to simulate the cable installation activities across Upper Little Bay. The analysis was updated to reflect new or refined inputs and the modeling study was expanded in order to address the sensitivity of the results to some of the modeling assumptions.

A number of input parameters have been updated since the previous modeling.

- The burial route was updated to reflect the latest plans. The route is primarily the same except for minor revisions to the diver burial route on the eastern shore.
- The use of silt curtains was accounted for in the regions where they will be implemented; this includes the entire western diver burial and approximately 57.5 % of the eastern diver burial route.
- The minimum burial depth for the jet plow installation in waters greater than 10 ft has changed from 8 ft to 5 ft.
- The sediment grain size characteristics have been updated based on refined laboratory analysis. The new information shows that the sediment has more mass in larger sizes than had been assumed in the previous analysis.
- The percent solids have been updated based on laboratory analysis of moisture. This provides a better estimate of the sediment loading to the water column.

Multiple simulations were completed as part of this revised study. These included

- Updated base case of the jet plow
- Sensitivity to Advance Rate (slower and faster) of the jet plow
- Sensitivity to loss rate (lower and higher) for the jet plow
- Sensitivity to tide range (spring vs neap) for the jet plow
- Additional run to evaluate the effects of continued resuspension for the jet plow
- Updated base diver burial simulations

Based on the set of model simulations the following conclusions can be made

- The jet plow installation is anticipated to need approximately 7.1 hours of active sediment disturbing activity to install each cable.
- Each cable is anticipated to be installed with continuous operations without long stoppages; the advance rate modeled and the duration of 7.1 hours is an average rate provided by the installers.
- The sediment plume is temporary, present when construction takes place and dissipates within an hour after construction stops
- The sediment plume follows the currents. Times of weaker currents (neap tide) have a smaller overall footprint but have some contours within the footprint that extend further due to the diminished advection.

- The base case found areas totaling 91.2 ac and 0.2 ac were exposed to a concentration of 10 mg/L or greater for 1 hr, and 2 hrs, respectively, while no areas were exposed to such a concentration for a duration of three hours.
- The base case deposition thickness patterns found the footprint over 0.1 mm extended 67.81 ac due to jet plowing the three cable routes. Areas with thickness over 5 mm are 0.1 acres.
- The sensitivity runs to advance rate showed that the footprint changed primarily due to the change in exposure to currents due to the different timing relative to the tides. Further the region immediately adjacent to the route showed increasing peak concentration with increasing advance rate.
- The sensitivity to loss rate showed that the lower loss rate (15% less than the base) had a more drastic change than the higher loss rate (10% greater than the base). This is expected due to the trend of mass released based on the loss rate.
- An additional model run was simulated that include the effects of continued resuspension. This run showed a footprint of SS excess concentrations that was larger than the base case, though the concentrations were present intermittently and confined to the very bottom of the water column. Much of the area has the potential for continued resuspension due to the relatively strong currents. Resuspension was most pronounced on the first tide following jet plowing and fully dissipated by the third day. The model does not include all processes that would interact with the continued resuspension and serves as a conservative prediction.
- The diver hand jetting takes place intermittently over a longer span of time (4 hours a day between 9-18 days for west and east routes respectively) as compared to the jet plow operations. The intermittent installation is due to operational constraints limited by water depth and currents. The duration of active sediment disturbing activities is 1.7 days for the west route and 3.0 days for the eastern route.
- The diver hand jetting assumes use of silt curtains for the entire west route and 57.5% of the east route.
- The diver concentrations are intermittent and dissipate quickly due to the relatively low mass flux, particularly in regions within the silt curtain.
- The diver hand jetting results in concentration plumes local to the areas of hand jetting and do not extend as far as the jet plow plume.
- The maximum excess SS concentration due to diver burial is 500 mg/L, which will occur over an area of 0.59 ac. Lower concentrations will extend over a greater area, with excess SS of 20 mg/L covering 14.21 acres at some point in time. Concentrations diminish shortly after diver activity ceases, for example a time history of concentration local to diver activity showed that the signal of excess concentration mimicked the duration of activity with concentrations diminished to zero after 20 minutes.
- The deposition due to diver burial is generally similar to the maximum water column plume footprint but reduced in extent. The higher deposition areas are adjacent to the cable route. A total of 10.79 ac will accrue deposition greater than 0.004 in.
- The current schedule to embed each cable by jet plowing plans for a 5 to 7-day interval between installations. The water column concentration duration analysis shows that the excess concentration will drop to zero within approximately 1 hour following cessation of jet plowing. With continued resuspension enabled the simulation shows excess concentration will drop to zero within 3 days. Thus, there will be no cumulative increases in suspended sediment concentrations because of these installations.

- There will be a cumulative threefold increase in deposition inside the silt curtains, for the three cables averaging 3 in.

5 References

Anderson, E.L., Johnson, B., Isaji, T., and E. Howlett. 2001. SSFATE (Suspended Sediment FATE), a model of sediment movement from dredging operations. WODCON XVI World Dredging Congress, 2-5 April 2001, Kuala Lumpur, Malaysia.

Bilgili A., Proehl J. P., Lynch D. R., Smith K., Swif, M. R., 2005. Estuary-Ocean Exchange and Tidal Mixing in a Gulf of Maine Estuary: A Lagrangian Modeling Study, Estuarine, Coastal and Shelf Science Volume 65, No. 4, 607-624 pp. doi:10.1016/j.ecss.2005.06.027

Brown, W. S. and Arellano, E., 1980. The application of a segmented tidal mixing model to the Great Bay Estuary, N. H., Estuaries, Vol. 3, No. 4, p 248-257.

CHT, 2008. Modeling suspended sediment plumes created by dredging operations for the Craney Island Expansion Project. Contract Report CHT 08-02, Computational Hydraulics and Transport, Edwards, MS.

Ertürk S. N., Bilgili A., Swift M. R., Brown W. S., Çelikkol B., Ip J. T. C , Lynch D. R., 2002. Simulation of the Great Bay Estuarine System Tides with Tidal Flats Wetting and Drying, Journal of Geophysical Research - Oceans, 107(C5), doi:10.1029/2001JC000883, pp. 29.

Eversource Energy, 2017. Response to Comments on Little Bay Crossing from Counsel for the Public and Town of Durham/University of New Hampshire. July 1, 2017. Seacoast Reliability Project, Eversource Energy.

Flemming, B.W., 2000. A Revised Textural Classification of Gravel-Free Muddy Sediments on the Basis of Ternary Diagrams. Continental Shelf Research, Volume 20, pages 1125-1137.

Foreman, J., 2002. Resuspension of sediment by the jet plow during submarine cable installation. Submitted to GenPower, LLC, Needham, MA. Submitted by Engineering Technology Applications, Ltd, Romsey, Great Britain, May, 2002.

Francingues, N. R., and Palermo, M. R. (2005). “Silt curtains as a dredging project management practice,” DOER Technical Notes Collection (ERDC TN-DOER-E21). U.S. Army Engineer Research and Development Center, Vicksburg, MS. http://el.erdc.usace.army.mil/dots/doer/doer.html.

Hansen, V. D., and Rattray Jr., M., 1996. New dimensions in estuary classification. Limnol. Oceanogr. 11(3):319-326.

Ip J. T., Lynch D. R., Friedrichs C. T., 1998. Simulation of Estuarine Flooding and Dewatering with Application to Great Bay, New Hampshire. Estuarine Coastal & Shelf Science 47, 119-141.

Isaji, T., E. Howlett, C. Dalton and E. Anderson, 2001. Stepwise- continuous-variable rectangular grid, in Proceedings of the 7th International Conference on Estuarine and Coastal Modeling, St. Pete Beach, FL, November 5-7, 2001.

Johnson, B.H., E. Anderson, T. Isaji, and D.G. Clarke. 2000. Description of the SSFATE numerical modeling system. DOER Technical Notes Collection (TN DOER-E10). U.S. Army Engineer Research and Development Center, Vicksburg, MS. http: //www.wes.army.mil/el/dots/doer/pdf/doere10.pdf.

Jones, S. H., 2000. A technical characterization of estuarine and coastal New Hampshire. New Hampshire Estuaries Project, Portsmouth, NH, 274 pp.

Lackey, T., J. Gailani, S-C. Kim, D. King, and D. Shafer, 2012. Transport of resuspended dredged sediment near coral reefs at Apra Harbor, Guam. Proceedings of 33rd Conference on Coastal Engineering, Santander, Spain, 2012. Edited by P. Lynett and J. M. Smith.

Normandeau Associates, Inc. 2016. Public Service of New Hampshire Seacoast Reliability Project Characterization of Sediment Quality Along Little Bay Crossing. Prepared for Public Service Company of New Hampshire. 22p. + appendices

Normandeau Associates, Inc. 2017. Supplement to Public Service of New Hampshire Seacoast Reliability Project Characterization of Sediment Quality Along Little Bay Crossing. Prepared for Public Service Company of New Hampshire. 22p. + appendices

McLaughlin JM, Bilgili A, Lynch DR (2003) Dynamical Simulation of the Great Bay Estuarine System Tides with Special Emphasis on N2 and S2 Tidal Components, Estuarine, Coastal and Shelf Science, Volume 57, No. 1-2, pp. 283-296.

Mendelsohn, D., N. Cohn and D. Crowley, 2012. Sediment transport analysis of cable installation for Block Island Wind Farm and Block Island Transmission System, ASA Project 2011-243, RPS ASA, 92 pgs.

Meeker, S., Reid, A., Schloss, J., Hayden, A., 1998. Great Bay watch a citizens water monitoring program. NHU-H-98-001.Mendelsohn, D., N. Cohn and D. Crowley, 2012. Sediment transport analysis of cable installation for Block Island Wind Farm and Block Island Transmission System, ASA Project 2011-243, RPS ASA, 92 pgs.

Reichard R. P., Celikkol B., 1978. Application of a Finite Element Hydrodynamic Model to the Great Bay Estuary System, New Hampshire, USA, J.C.J. Nihoul (Ed.), Hydrodynamics of Estuaries and Fjords, Elsevier Scientific Publishing Co., Amsterdam, Netherlands, pp. 349‑372

Short, F.T., 1992. The estuarine hydrosystem. In: Short, F.T. (Ed.), The Ecology of the Great Bay Estuary, New Hampshire and Maine: An Estuarine Profile and Bibliography. NOAA-Coastal Ocean Publications, pp. 31-38.

Silver and Brown (1979. Great Bay estuarine field program, 1975 data report, Part 2: temperature, salinity and density. UNH Sea Grant Technical Report UNH-SG-163, 65 pp.

Swanson, C., A. Bilgili and D. Lynch, 2014. Long Term Simulations of Wastewater Treatment Facility Discharges into the Great Bay Estuarine System (New Hampshire). Water Quality, Exposure and Health, accepted for publication.

Swanson, C. and T. Isaji, 2006. Simulation of sediment transport and deposition from cable burial operations in Nantucket Sound for the Cape Wind Energy Project. Prepared for Cape Wind Associates, Inc., Boston, MA, ASA Project 05-128, 47 p.

Swanson, J. C., Isaji, T., & Galagan, C., 2007. Modeling the ultimate transport and fate of dredge-induced suspended sediment transport and deposition. Proceedings of the WODCON XVIII, 27.

Swanson, J.C, and T. Isaji. 2006. Modeling dredge-induced suspended sediment transport and deposition in the Taunton River and Mt. Hope Bay, Massachusetts. Presented at WEDA XXVI / 38th TAMU Dredging Seminar, June 25-28, San Diego, CA.

Swanson, J. C, Isaji, T., Clarke, D., and Dickerson, C. 2004. Simulations of dredging and dredged material disposal operations in Chesapeake Bay, Maryland and Saint Andrew Bay,

Florida. Presented at WEDA XXIV / 36th TAMU Dredging Seminar, 7-9 July 2004, Orlando, Florida.

Swanson, J.C., T. Isaji, M. Ward, B.H. Johnson, A. Teeter, and D.G. Clarke. 2000. Demonstration of the SSFATE numerical modeling system. DOER Technical Notes Collection (TN DOER-E12). U.S. Army Engineer Research and Development Center, Vicksburg, MS. http://www.wes.army.mil/el/dots/doer/pdf/doere12.pdf.

Swenson, E., Brown, W.S., Trask, R., 1977. Great Bay Estuarine Field Program 1975 Data Report Part 1: currents and sea levels. UNH Sea Grant Technical Report # UNH-SG-157, University of New Hampshire, New Hampshire, USA, 109 pp

Teeter, A.M. 1998. Cohesive sediment modeling using multiple grain classes, Part I: settling and deposition. Proceedings of INTERCOH 98 - Coastal and Estuaries Fine Sediment Transport: Processes and Applications, South Korea.

Trowbridge P, 2009. Environmental Indicators Report, Piscataqua Region Estuaries Partnership, 174 pp.

Ward, L. G. and Bub, F. L., 2000. Suspended particulate material and physical properties (salinity, temperature, turbidity) of the Great Bay Estuary: distribution of major controlling processes. NOAA/UNH Cooperative Institute for Coastal and Estuarine Environmental Technology (CICEET), Technical Report, Durham, NH, 62 pp.

Whitney, P., and S. Herz, 2013. Submarine cable embedment: integrating suspended sediment modeling and monitoring into the regulatory permit process. ESS Group Coastal Whitepaper, downloaded from http://www.essgroup.com/images/stories/pdfs/Submarine-Cable-Embedment-and-Suspended-Sediment-Modeling.pdf.

RPS

Revised Modeling Sediment Dispersion from Cable Burial for Seacoast Reliability Project, Upper Little Bay, New Hampshire

APPENDIX A: CONTINUED RESUSPENSION SIMULATION HOURLY SNAPSHOTS

The following pages contain hourly snapshots of excess SS concentrations from the continued resuspension simulation. Each figure shows a plan view and a cross sectional view at the bottom. The plan view shows the maximum water column concentration within the vertical column. An enlarged contour legend is shown below.

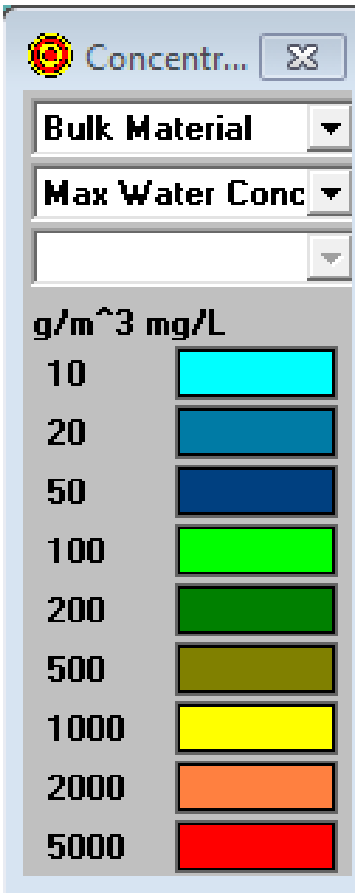

Water column concentration legend

The snapshots start at the first hour after the beginning of a cable installation pass and continue for 64 hours; cable installation activity ceases at approximately 7.1 hours. The concentrations shown during the first 7 hours include the initial plume from construction activities and resuspension of any settled sediments. Starting at hour 8 and beyond the concentrations are due to resuspended sediments. Resuspension is triggered when the currents produce a high enough shear stress to suspend settled sediments depending on the sediment size. Triggering resuspension depends on what sediments have settled, and the current patterns where they have settled. The resuspension occurs during larger velocities in the ebb and flood portions of the tide with diminishing concentration and duration as time passes.

Hour 01	Hour 02	Hour 03	Hour 04
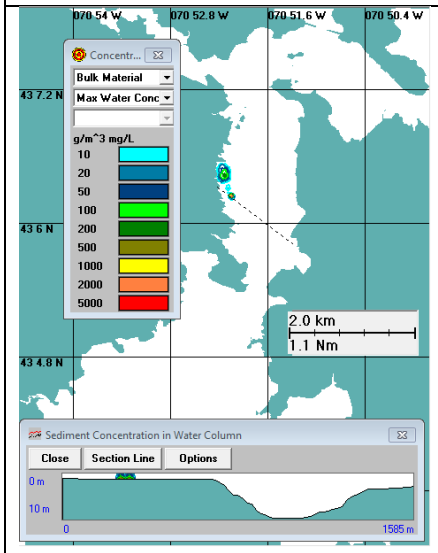	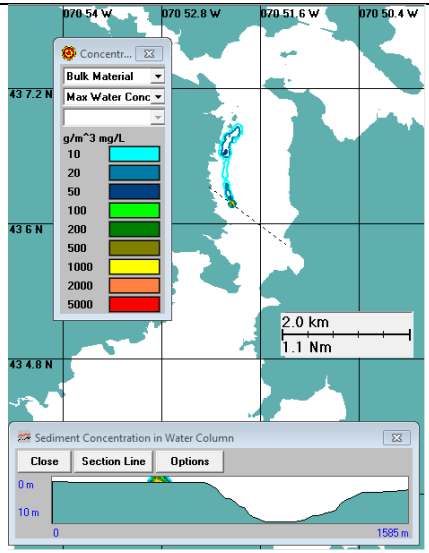	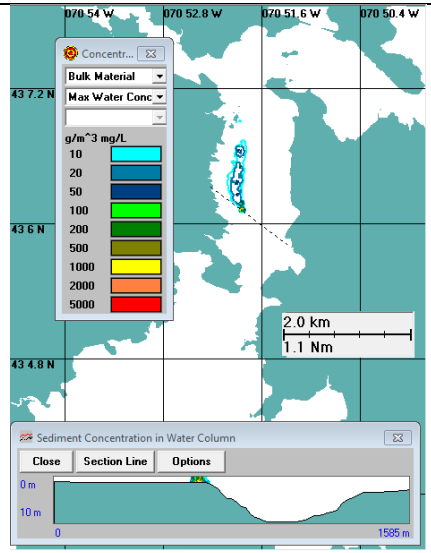	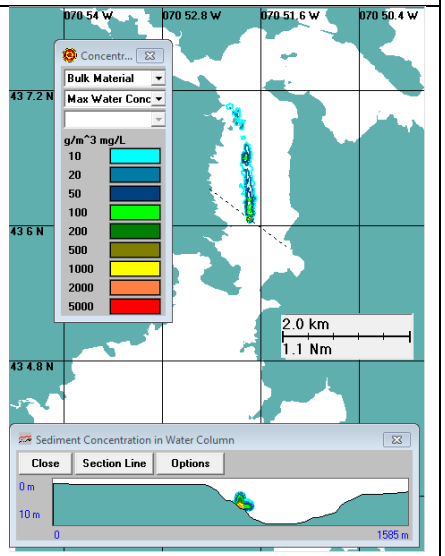
Hour 05	**Hour 06**	**Hour 07**	**Hour 08**
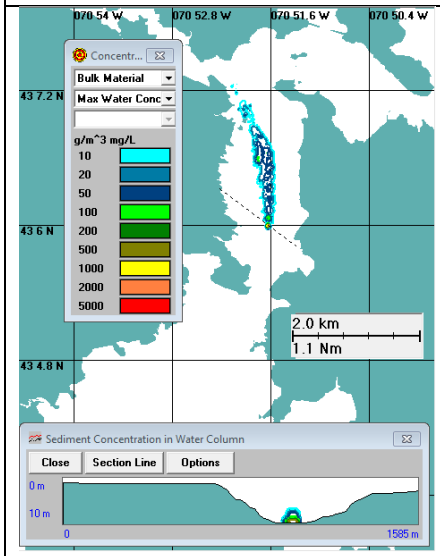	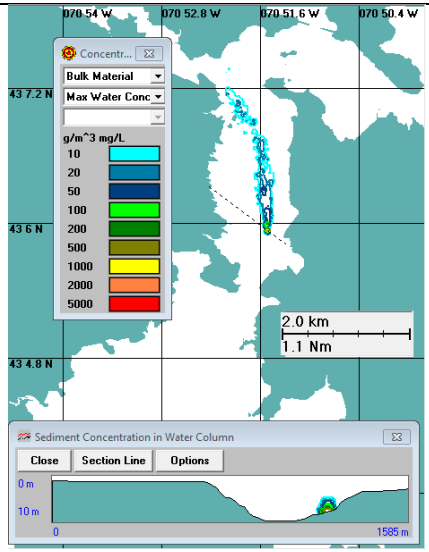	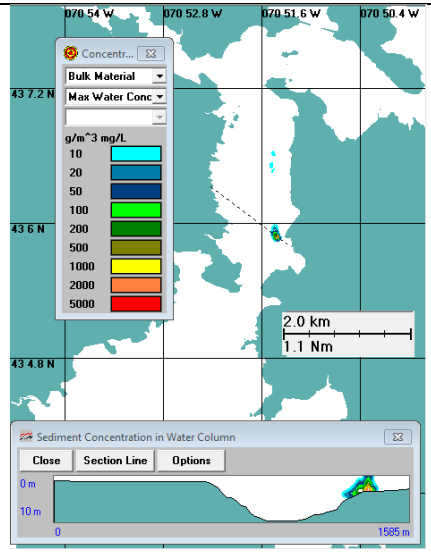	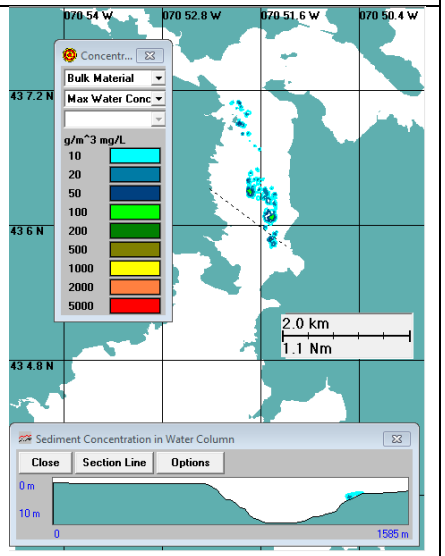

Hour 09	Hour 10	Hour 11	Hour 12
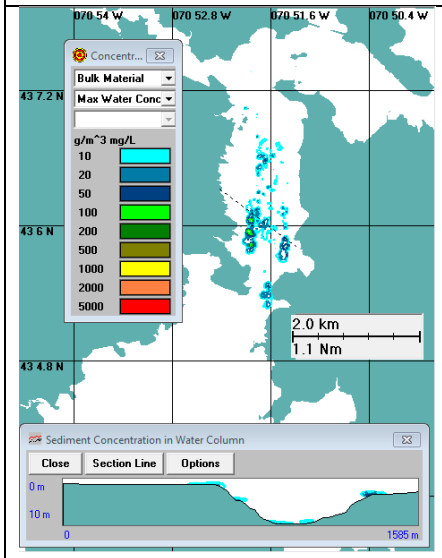	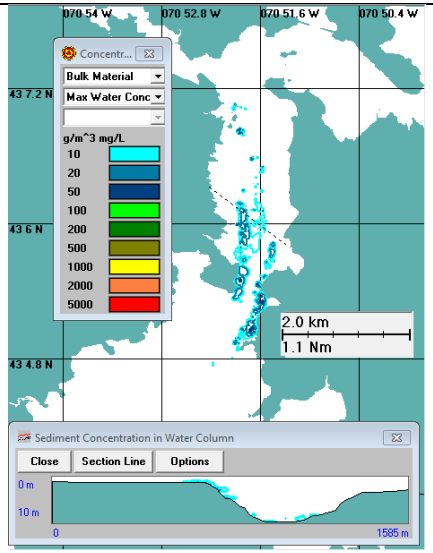	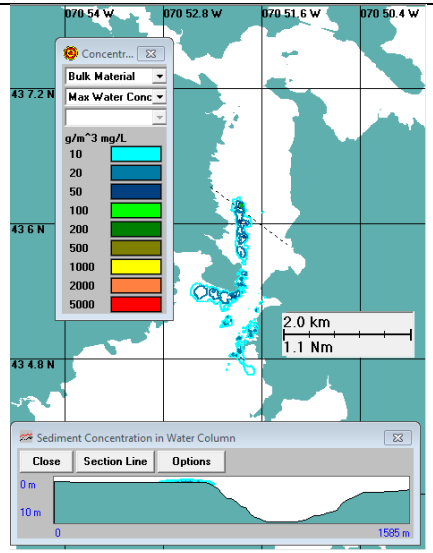	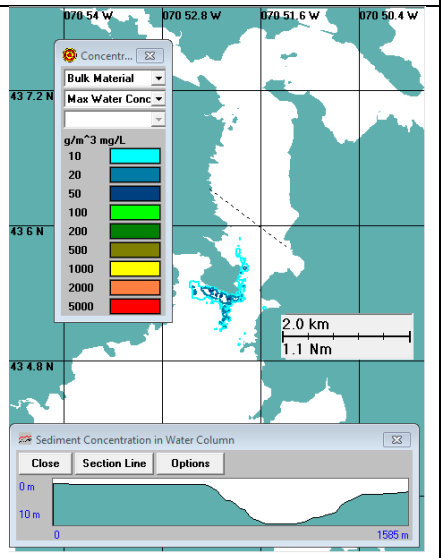
Hour 13	**Hour 14**	**Hour 15**	**Hour 16**
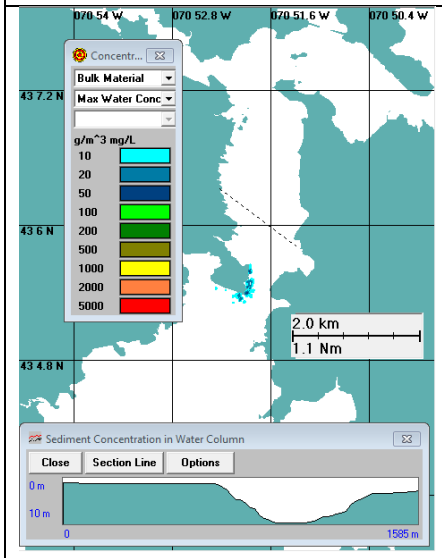	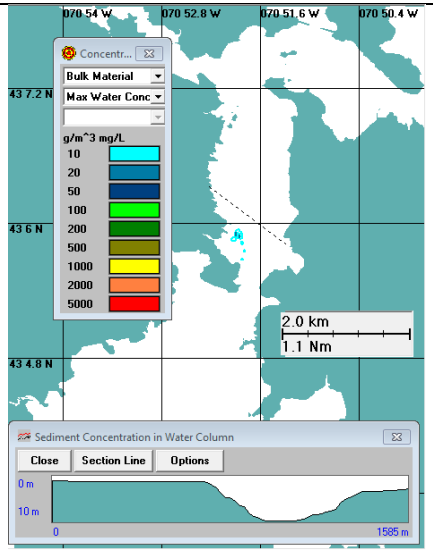	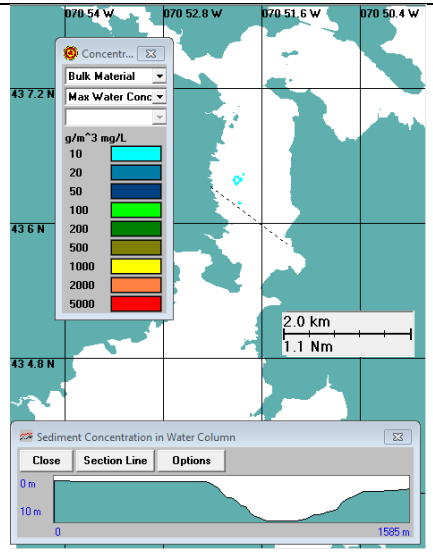	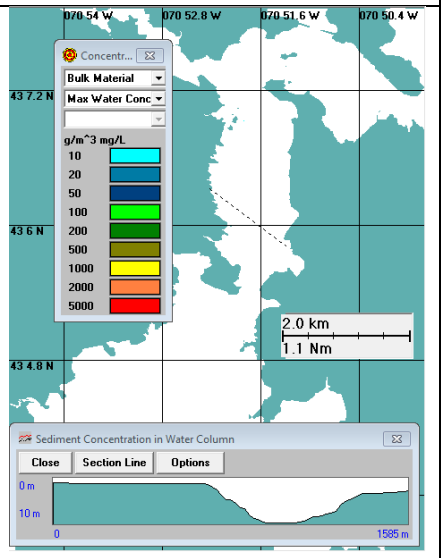

Hour 17	Hour 18	Hour 19	Hour 20
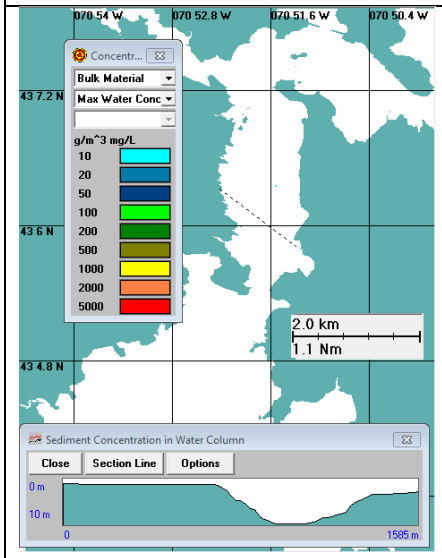	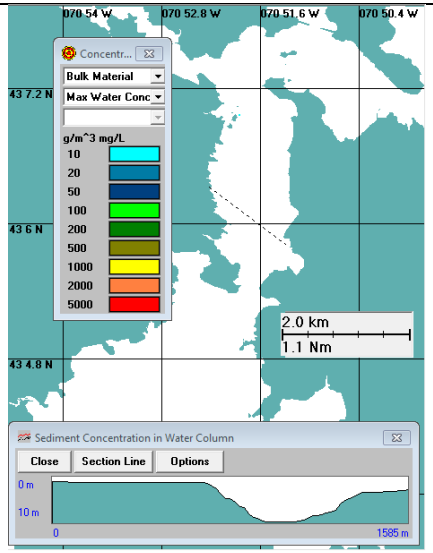	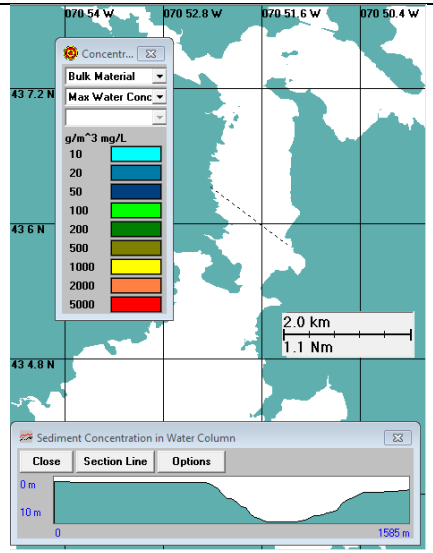	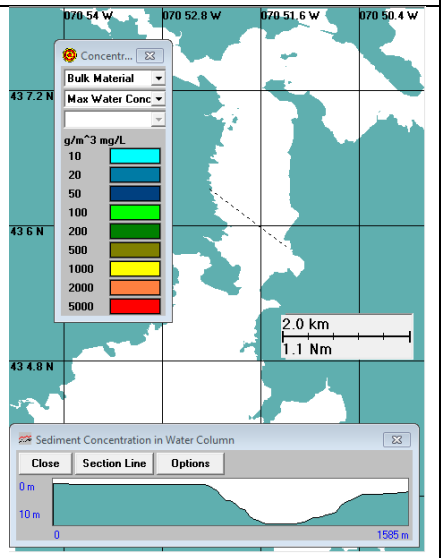
Hour 21	**Hour 22**	**Hour 23**	**Hour 24**
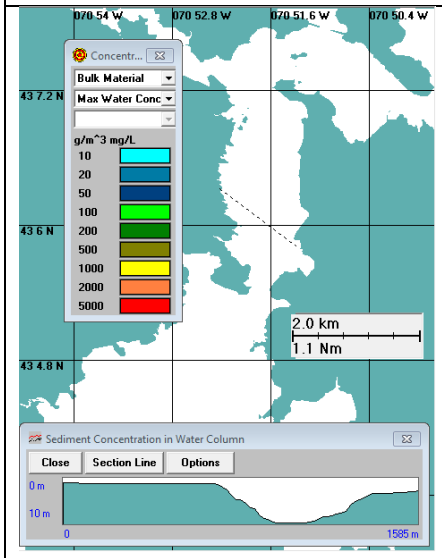	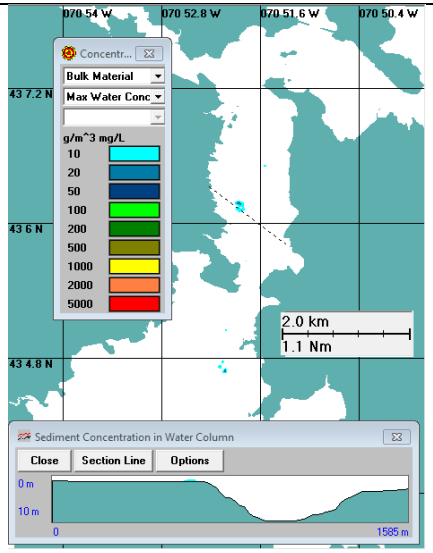	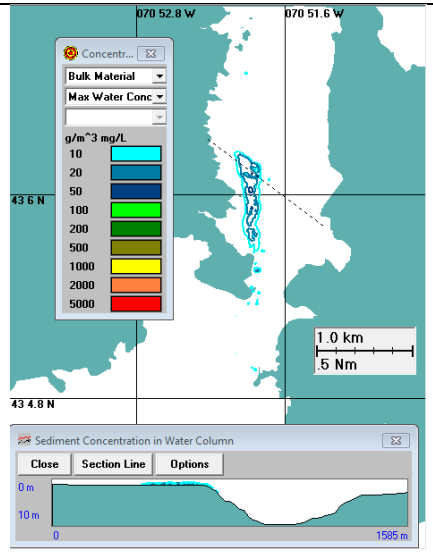	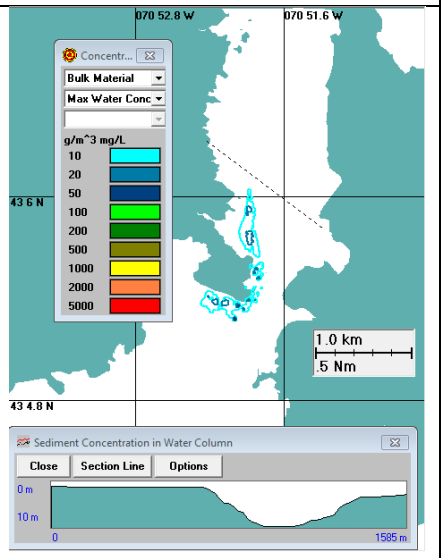

Hour 25	Hour 26	Hour 27	Hour 28
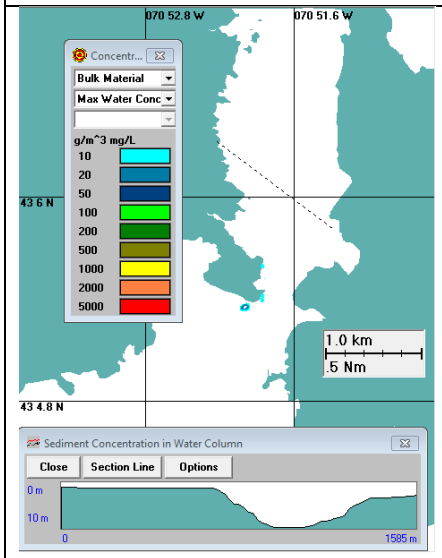	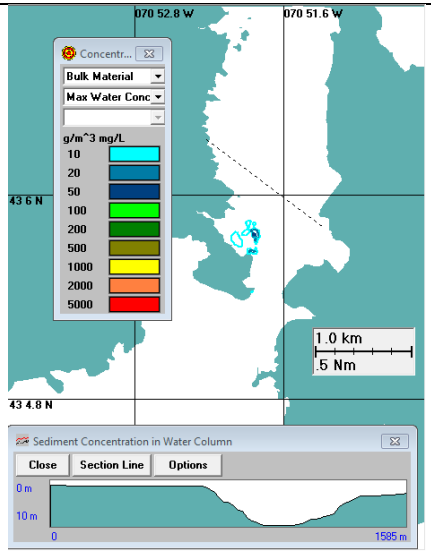	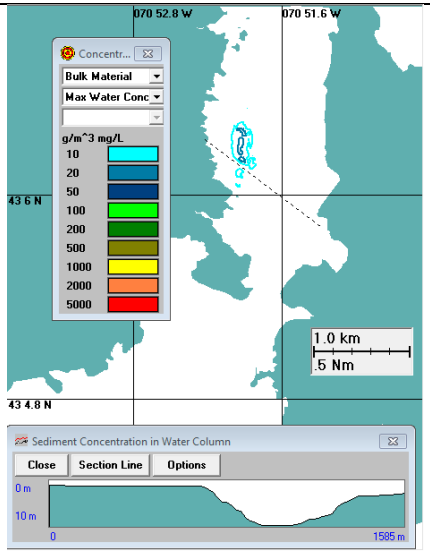	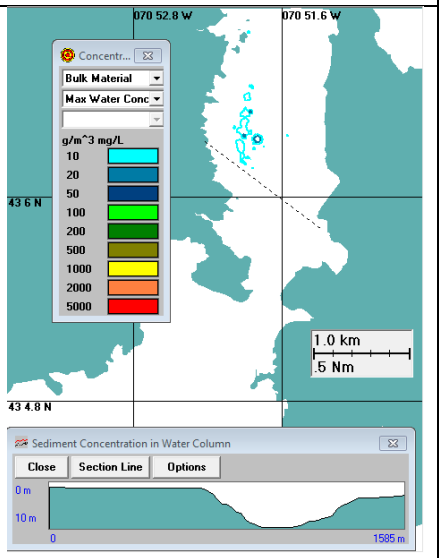
Hour 29	**Hour 30**	**Hour 31**	**Hour 32**
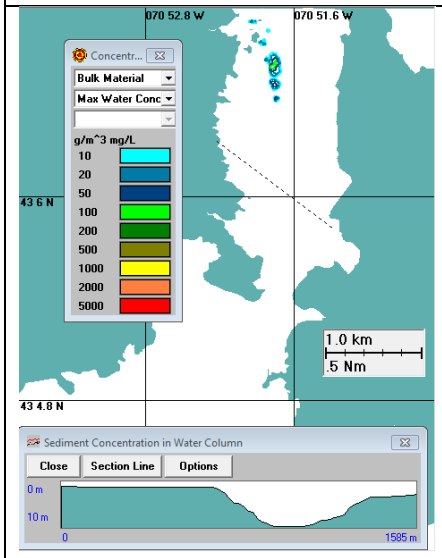	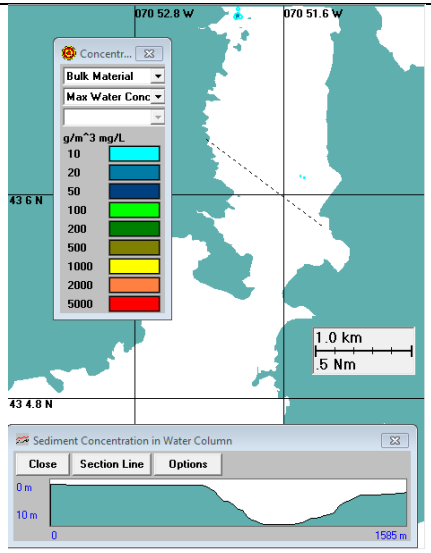	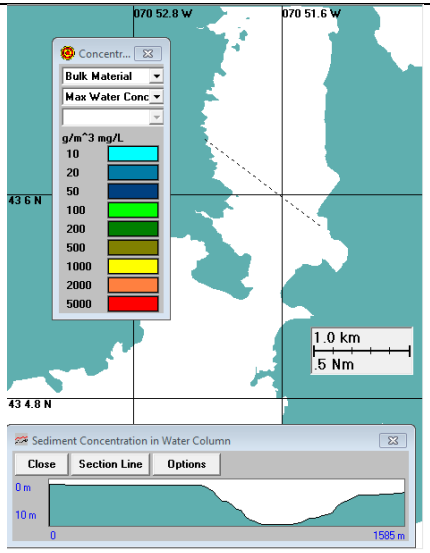	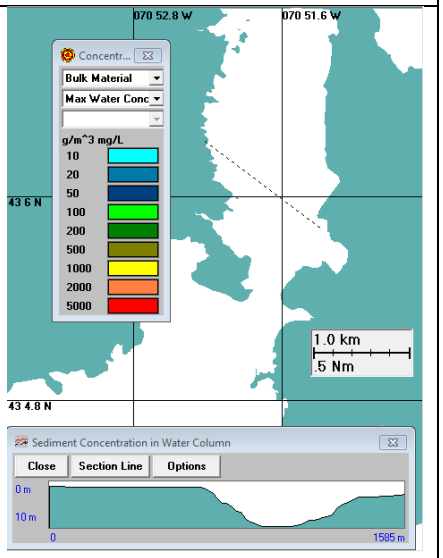

Hour 33	Hour 34	Hour 35	Hour 36
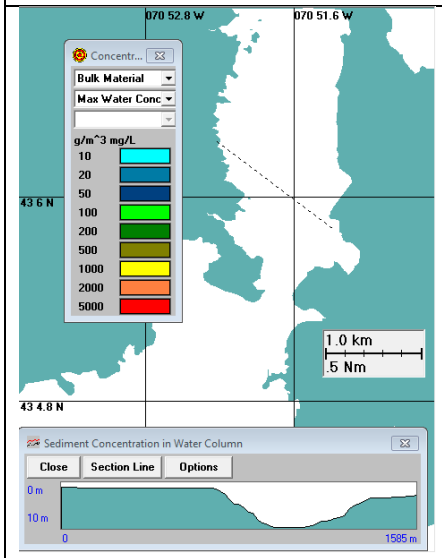	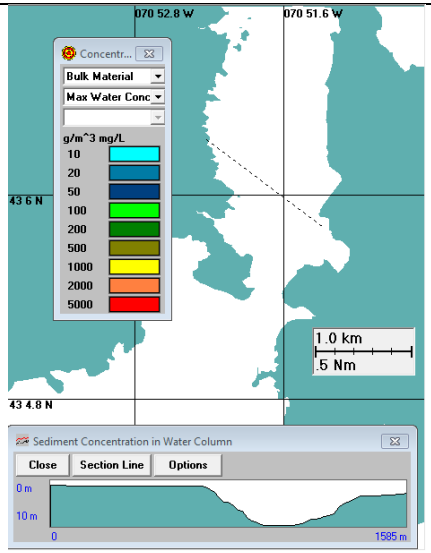	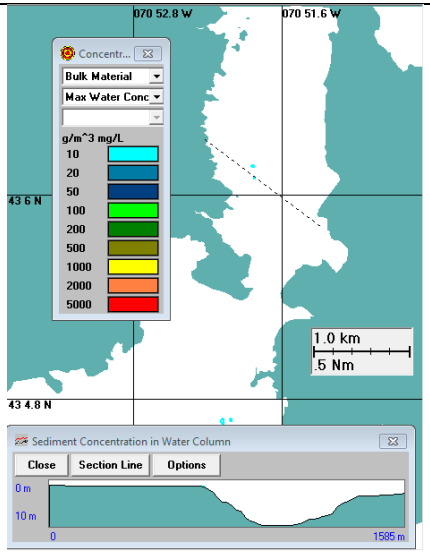	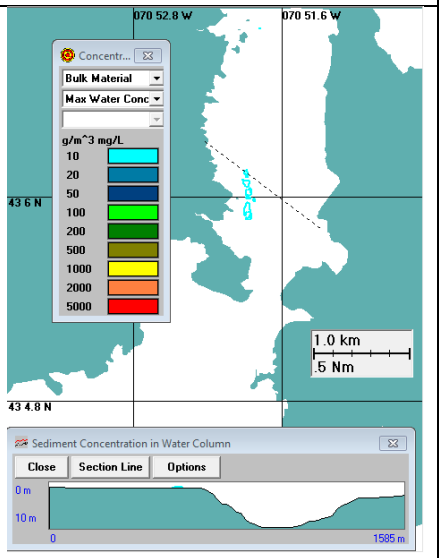
Hour 37	**Hour 38**	**Hour 39**	**Hour 40**
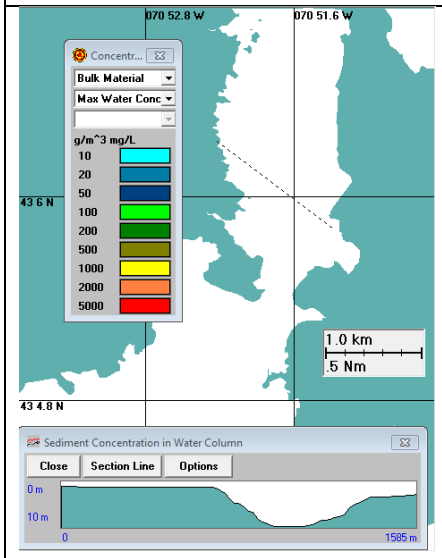	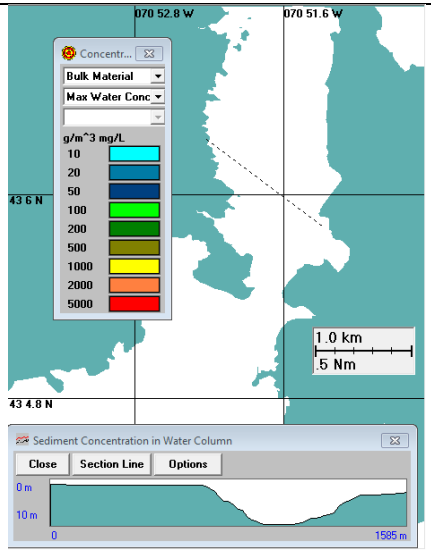	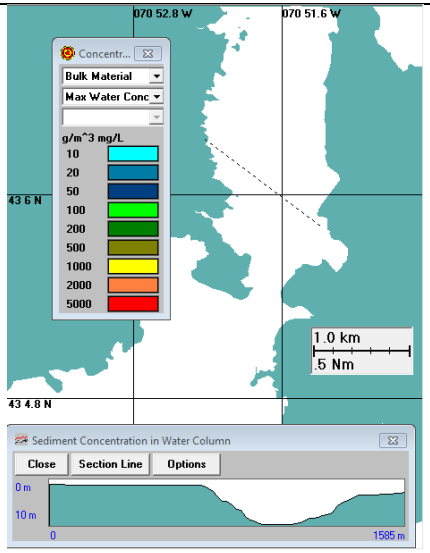	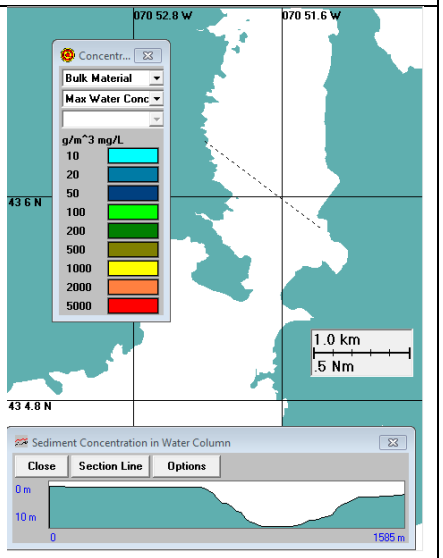

Hour 41	Hour 42	Hour 43	Hour 44
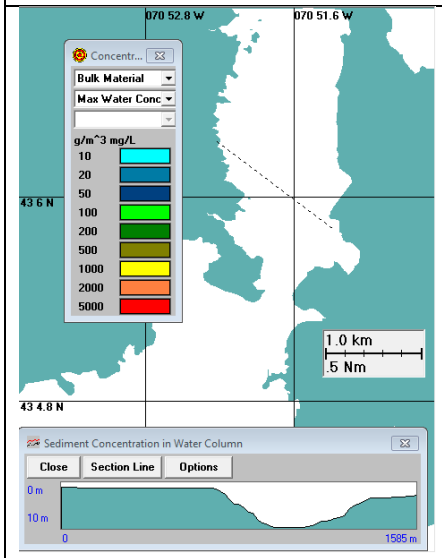	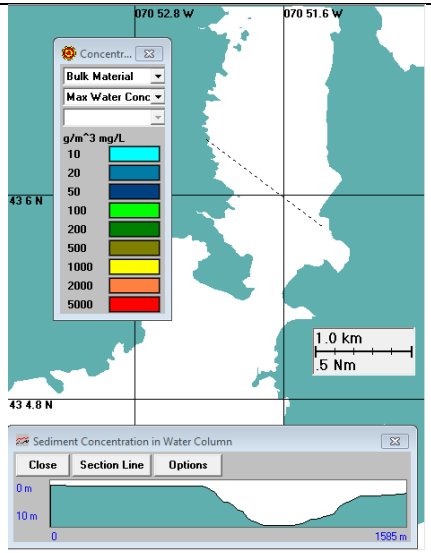	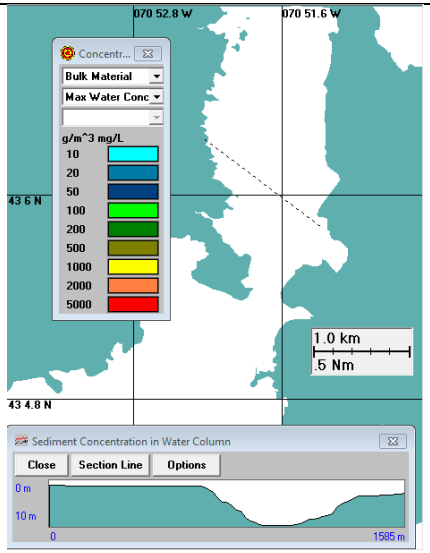	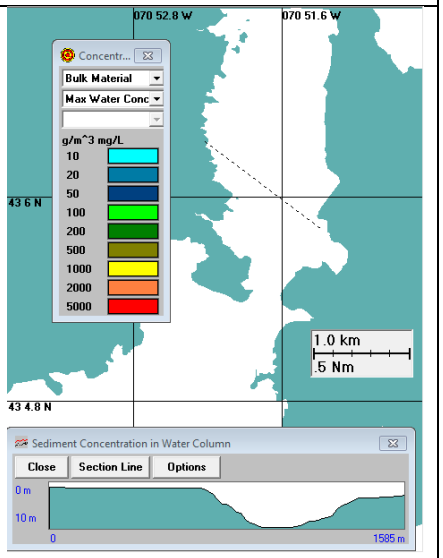
Hour 45	**Hour 46**	**Hour 47**	**Hour 48**
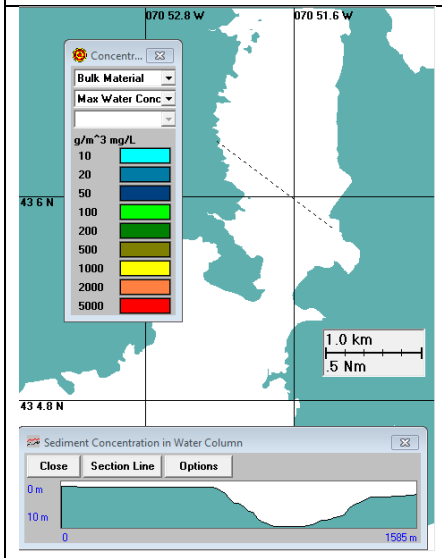	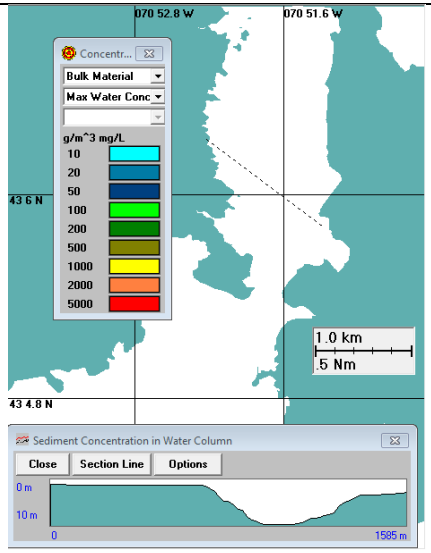	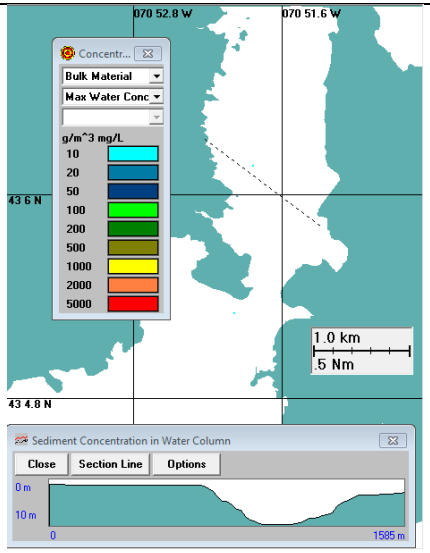	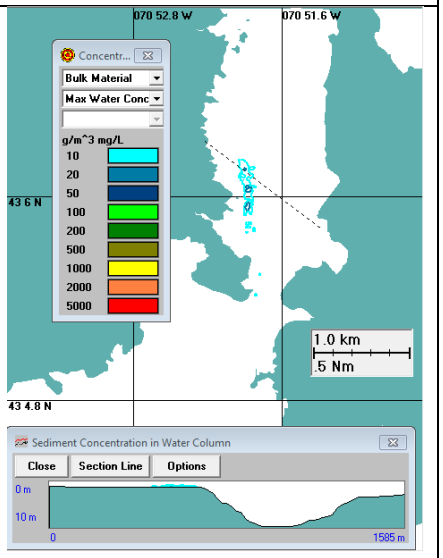

Hour 49	Hour 50	Hour 51	Hour 52
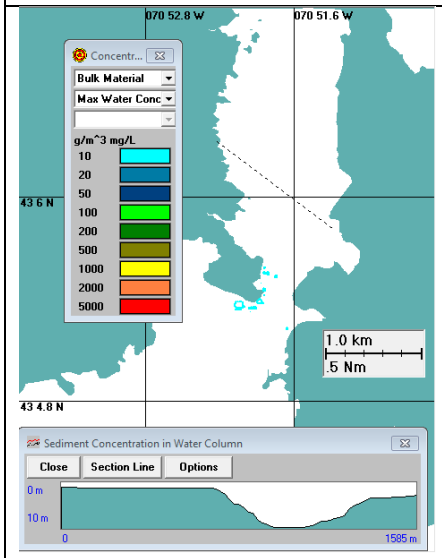	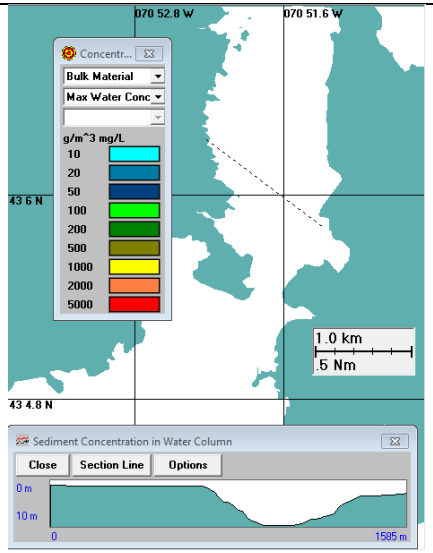	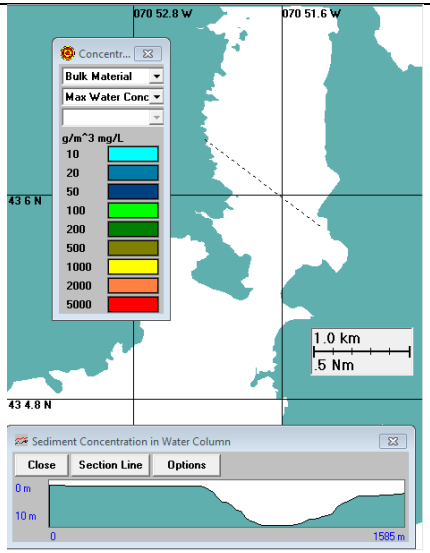	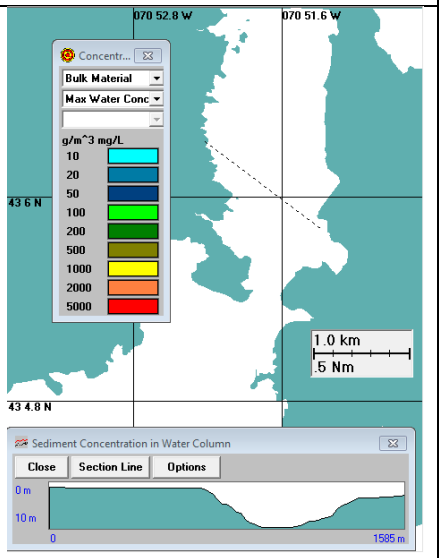
Hour 53	**Hour 54**	**Hour 55**	**Hour 56**
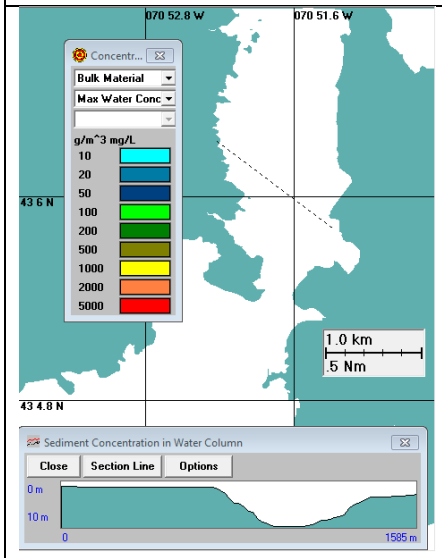	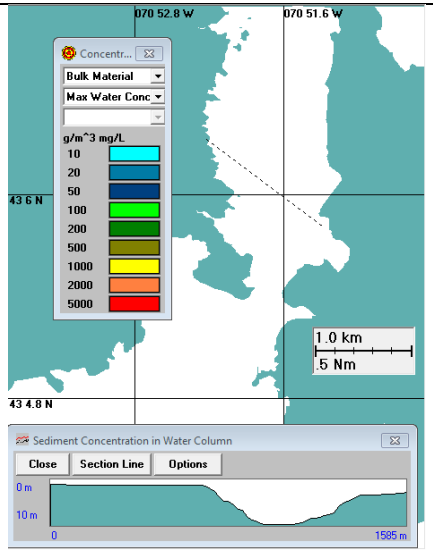	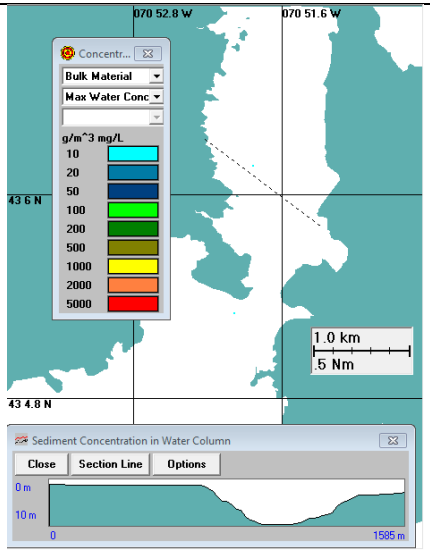	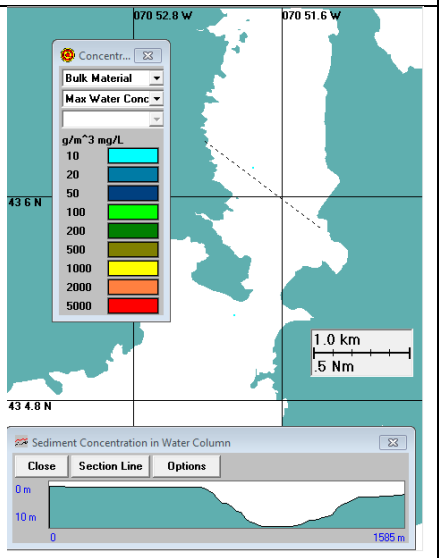

Hour 57	Hour 58	Hour 59	Hour 60
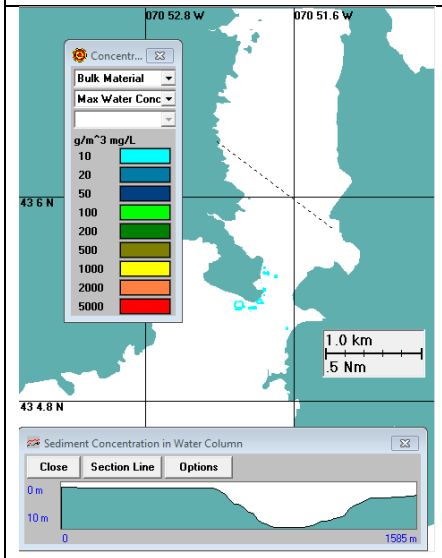	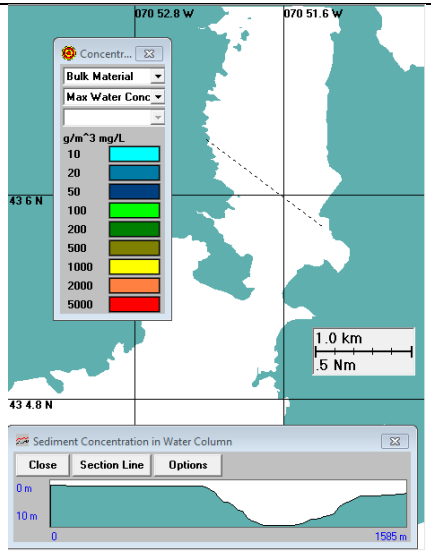	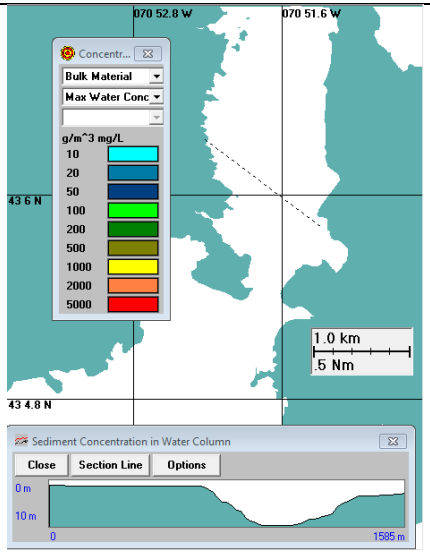	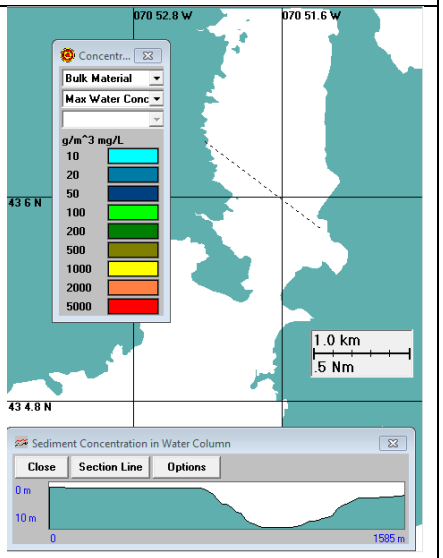
Hour 61	**Hour 62**	**Hour 63**	**Hour 64**